MODELING, SIMULATION AND VERIFICATION OF IMPACT DYNAMICS

Vol. 3, State of the Art of Impact Testing

By:

D. H. Robbins

Date:

July 24, 1973

Report Status:

Draft Report

1. Report No.	2. Government Accession No.	3. Recipient's Catalog No.

4. Title and Subtitle	5. Report Date
Modeling, Simulation and Verification of Impact Dynamics - Vol.3, State of the Art of Impact Testing	16 July 1973
	6. Performing Organization Code
7. Author(s) Robbins, D. H.	8. Performing Organization Report No. UM-HSRI-BI-73-4-3
9. Performing Organization Name and Address Highway Safety Research Institue and Department of Applied Mechanics and Engineering Science The University of Michigan Ann Arbor, Michigan 48105	10. Work Unit No. 11. Contract or Grant No. DOT-HS-031-2-121
12. Sponsoring Agency Name and Address National Highway Traffic Safety Administration U.S. Department of Transportation Nassif Building, 7th and E Streets, S.W. Washington, D.C. 20590	13. Type of Report and Period Covered Final Report June 28, 1973-July 27, 1973 14. Sponsoring Agency Code
15. Supplementary Notes	

16. Abstract

To determine the state of the art of impact testing as related to mathematical crashworthiness modeling, the following six questions were posed: 1. What techniques are used to obtain test specimens? 2. What techniques are used for physically simulating crash loading? 3. What techniques are used for retrieving structural crash response data from physical tests? 4. How are state variables controlled and the data retrieved from a test? 5. What is the confidence level of physical simulation techniques as a realistic indication of the crash event? and, 6. How does one verify the predictions of a crashworthiness mathematical model using test procedures?

The approach used on the first five questions has been to combine similar test methods, data acquisition procedures, and data analysis procedures to present the state of the art of impact testing in the compact package necessary for developing an overview. The question which arose in estimating the confidence level of physical simulation techniques was "How does one compare the results of two impact events whether they be experiment, computer prediction, or real world crash?" To answer this question it was found necessary to study digital and analog filtering equipment and procedures.

The three main parts of the report cover impact test techniques, verification of crashworthiness analyses by test, and filtering techniques. A concluding part summarizes the recommendations.

17. Key Words	18. Distribution Statement

19. Security Classif.(of this report)	20. Security Classif.(of this page)	21. No. of Pages	22. Price

Form DOT F 1700.7 (8-69)

The opinions, findings, and conclusions expressed in this publication are those of the author and not necessarily those of the National Highway Traffic Safety Administration.

TABLE OF CONTENTS

TABLE OF CONTENTS
(Continued)

FIGURES

FIGURES
(Continued)

TABLES

ACKNOWLEDGMENTS

This [illegible] was supported jointly by the staffs of the Biosciences Division of the Highway Safety Research Institute and the Department of Applied Mechanics and Engineering Science, both at the University of Michigan. The author would like to thank Mr. Robert Krauss of NHTSA for his support, Dr. H.C. Wang of HSRI for gathering much of the background material necessary for this study, and Dr. J.H. McElhaney of HSRI for guidance in the subjects of instrumentation and filtering.

1.0 INTRODUCTION

Task 4 of the study, "Modeling, Simulation and Verification of Impact Dynamics," posed five questions directly and one question indirectly to define the state of the art of crashworthiness testing. These are:

1. What techniques are used to obtain test specimens?
2. What techniques are used for physically simulating crash loading?
3. What techniques are used for retrieving structural crash response data from physical tests?
4. How are state variable controlled and the data retrieved from a test?
5. What is the confidence level of physical simulation techniques as a realistic indication of the crash event?
6. How does one verify the predictions of a crashworthiness mathematical model using test procedures?

The first five of these items are discussed in Part 2 of this report, "State of the Art of Impact Testing." The approach used has been to combine similar testing methods, data acquisition procedures, and data analysis procedures and present the state of the art of impact testing in the compact package necessary for developing an overview.

Several questions arose when the subject of confidence level of physical simulation techniques was considered. The primary one was a basic question, "How does one compare the results of two impact events, whether they be experiment, computer prediction or real world crash?" The answer to this question is basic to developing quantitative measures of confidence in test results. Its answer is also basic to verification of crashworthiness computer models by test, the subject of Question 6 above. As part of the attempt to answer this question, it was found necessary to study how real data

is altered either by a data gathering/processing system or by computational processes in a computer program.

The chapter on physical test techniques is therefore supplemented by two additional chapters designed to probe further the state of the art of physical testing. Part 3 shows the relationship between mathematical crashworthiness modeling and physical testing and also where the relationship needs to be strengthened. Part 4 reports the results of a preliminary study of filtering and signal comparision. Recommendations and conclusions reached elsewhere in the report are summarized in Part 5. This report has been prepared simultaneously with References 1, 2, and 3 to form the total report for NHTSA Contract No. DOT-HS-031-2-481, "Modeling, Simulation and Verification and Impact Dynamics."

2.0 STATE OF THE ART OF IMPACT TESTING

The primary objective of Task 4 is to identify the state-of-the-art of impact testing including:

1. Techniques for obtaining test specimens;
2. Techniques for physically simulating crash loading;
3. Techniques for retrieving structural crash response data from physical tests;
4. Control of state variables in the test and data retrieval systems relative to the state variables.
5. Confidence level of physical simulation techniques as a realistic indication of the crash event; and,
6. Assessment of the economics of the various forms of crash testing and other empirical structural crash simulation techniques.

Two approaches might be proposed for conducting a study such as this. The first is to obtain detailed information about every test facility, testing technique, and all related hardware which is in use at the present time. This obviously would be an immense task and easily be beyond the scope of the entire budget for this project. The result would be several large volumes of information in the form of a compendium which could serve as a reference document.

The second approach is to lump similar testing methods, data acquisition procedures, and data analysis procedures together and present the state-of-the art of impact testing in a compact package which is more suitable for developing an overview. This second approach has been adopted for the current project. The key is a table entitled "Review of Impact Test Procedures" which follows [illegible] discussion of the methods used in its formulation.

2.1 WHAT TESTING IS DONE?

A very broad range of test procedures have been evaluated to answer the question, "What Testing is Done?" Any test procedure designed to duplicate a potential dynamic structural crash event is included. Thus static tests designed to reproduce structural damage which may occur in a crash should be considered. This breadth is justified because of the relevance and use of both static and dynamic test procedures in the gathering of input data for use with mathematical crashworthiness models.

Seven classes of testing techniques relating to crashworthiness assessment have been evaluated including:

1. impact sleds such as those used in industry (Ford, GM, Chrysler, American Motors, Eaton, etc.), research organizations (HSRI, WSU, Calspan, Southwest Research Institute, Dynamic Science, Transportation Research Center, etc.), and the government (Air Force, Army and Navy installations). Three classes of sleds are included in the tabulation: deceleration, acceleration, and impact with rebound.
2. flat, pole and angle barriers. All barriers are lumped together because of the general similarity of propulsion and data acquisition techniques.
3. SAE test procedures (J857a, J850a, J972, J996, J374, J367, and J980). These cover rollover tests, barrier tests, inverted vehicle drop tests, car roof crush tests, door system crush tests, and bumper evaluation tests. Some are dynamic and some static but all involve vehicle structural failure. As far as is known, these are the only [illegible]

because of their specific use. These are MVSS 214 (Side Door Strength - Passenger Cars), MVSS 215 (Exterior Protection - Passenger Cars), and MVSS 216 (Roof Crush Resistance - Passenger Cars).

4. Motor Vehicle Safety Standards. Only one additional motor vehicle safety standard has been included in this review -- MVSS 208. The testing procedures are similar to those mentioned previously but the data retrieval and analysis procedures are very specific.
5. Vehicle crushers. Although a vehicle crusher is a subset of static test techniques, it has been included in this list because of its importance in obtaining input data for certain mathematical crashworthiness models.
6. Dynamic Testing Machines. These are standard laboratory devices or machines with the capability of applying dynamic loads. They are included to compare their potential for load magnitude, load rate, and specimen size with the other procedures. The facility at HSRI is included as a specific example.
7. Static Testing Machines. These are standard laboratory devices for applying loads and deformations to structures and materials in a highly controlled, but very slow, manner. They are included as a class for comparison with the other types of procedures particularly relative to load and specimen size capabilities.

2.2 Evaluation Scheme for Each Testing Procedure

Each one of these techniques has been rated with respect to ten items as follows:

1. Testing [illegible]
2. [illegible] vehicle;
3. [illegible];

4. Method of loading (e.g. specimen accelerated to a test velocity, specimen loaded statically between platens, etc.);
5. Range of loads;
6. Equipment used for data gathering and retrieval;
7. Techniques of data analysis;
8. Estimated test cost;
9. Typical test programs;
10. Confidence level of physical simulation technique.

Although the various classes of testing techniques have been discussed previously it remains to provide a description of the tabulation relative to other items such as test cost and confidence level. The classification of test cost is a simple 1, 2, or 3 rating:

1 = cost less than $50.

2 = cost between $50 and $1000.

3 = cost greater than $1000.

The idea is to classify tests costs as: 1. minimal - requiring only a few man-hours and inexpensive test fixtures and test pieces; 2. moderate requiring more than one person to accomplish the test and probably more than one day total elapsed time as well as relatively expensive test fixtures and specimens; and, 3. expensive requiring major management decisions as to man-hours to be expended and hardware to be used.

The remaining item is to classify the confidence level of physical simulation techniques as a realistic indication of crash events. In order to accomplish this it is necessary to define what is meant by "physical simulation techniques" and "crash events" as well as to develop a measure of "confidence." Physical simulation techniques and crash events have been defined in the broadest sense to include seven types of physical simulation

techniques and all types of crash events regardless of direction and velocity of impact.

Three items can be proposed [illegible] of the confidence level one may develop for a particular test procedure: 1. the acceleration of the occupant compartment in the test as compared with real crash events; 2. equivalence of damage produced in the test and in reality; and, 3. frequency of simulated crash event in the real world of crash events. It is difficult to attach numerical rating schemes to these three items.

It may be argued that the spectrum of simulation techniques and crash eventswhich has been selected is too broad. Occupant compartment acceleration has been selected because crashworthiness design is ultimately related to occupant protection; equivalence of test damage for obvious reasons; and, frequency of the crash event being simulated in order to allow test procedures as diverse as a full-scale barrier crash and a roof drop test to be evaluated within the same framework. The fact that accident type frequency is included rather than merely a statement of accident type adds a dimension to the evaluation -- that being the likelihood that the physically simulated event might represent a real case.

A variety of techniques may be proposed to compare occupant compartment accelerations. The simple, but somewhat arbitrary three point rating system which has been selected is:

1. Test does not produce acceleration of the occupant compartment;
2. Test produces a pulse shape with the basic features of the actual pulse (similar hills and valleys), and reproduces magnitude within 30%
3. All aspects of pulse shape and phase are very similar in detail, and magnitudes do not vary by more than 10% at any point in time.

A far superior procedure would be to perform an analytical waveform comparison of the two pulses to isolate the degree of distortion, phase shifts, and amplitude differences which may exist. The effects of occupant compartment acceleration differences on occupant protection could then be quantitatively evaluated using any one of several man motion models developed at HSRI or elsewhere. Pulse shape differences have been studied as part of the evaluation of analog and digital filtering procedures included in Part 4.

The equivalence of the damage produced offers visible evidence of the similarity of the crash events and the resulting energy absorption patterns. The arbitrary three point rating scale which has been selected is:

1. Dissimilar patterns of damage (buckling modes, regions of large deformation or collapse, locations of plastic yielding, etc., are different).
2. Generally similar damage patterns without faithful reproduction of all details (buckling modes, locations of material yielding, and deformation are the same but details of the extent of deformation may vary).
3. Similar damage patterns including detail.

The frequency of the crash event itself is also included in the rating scheme. This allows assessment of the payoff of a proposed test procedure with respect to the overall collection of accident types. Sample data describing accident frequency as a function of direction have been obtained from HSRI Accident Data Banks and are based on data gathered in Washtenaw County, Michigan during the period 1968-1970 and include 9840 accidents.

TABLE 1 REVIEW OF IMPACT TEST PROCEDURES (Page 1 of 10)

Testing Technique	Type of Test Specimens	Static or Dynamic	Method of Loading	Range of Loads	Data Gathering Equipment	Techniques of Data Analysis	Test Cost	Typical Test Programs	Confidence Level
1. Deceleration type impact sled (many installations including General Motors, U.S. Air Force, HSRI, WSU, etc.)	Wide range including: a. small seat plus animal, human volunteer or dummy test subject. b. complete automobile body buck including occupants. c. Structural elements located between moving sled mass and deceleration barrier.	Dynamic	Sled is accelerated to a test velocity using a long-stroke hydraulic piston and decelerated in a variety of ways including programmable hydraulic piston, inversion tubes, water brakes, and energy absorbing crushable material. A typical problem is initial positioning of the test object because of the acceleration phase.	Loading is usually specified as a G-level, (up to 120 G's known), a pulse shape (triangles, squares, sines, and a few others resembling barrier pulses), and a duration (up to 200 ms known). Usually each installation is limited in pulse shape capability.	a. The complete range of acceleration, velocity, position, and force measurement transducers most often hard-wired to the recording system. b. Photographic coverage is extensive with both real time and high speed photography up to 10,000 frames per second. c. Electronic signals are usually recorded on FM tape for later data analysis.	a. On-line computation of acceleration resultants. b. On-line or post-process filter procedures. c. On-line or post-process time-scaled plots of measured parameters. d. Photometric analysis of motion pictures and computation of velocities and accelerations from position data. e. Post process procedures may involve large A-D conversions, computer programs, and output graphical procedures.	2 and sometimes 3.	a. Development and evaluation of occupant restraint systems. b. Human impact tolerance testing c. Component impact tolerance testing. d. Structural crush measurement under dynamic load. e. Most experiments requiring application of dynamic loads can be adopted to an impact sled environment.	3 (rare), 3 (possible), 1 (possible but multidimensional accelerations not generally possible.

TABLE 1 REVIEW OF IMPACT TEST PROCEDURES (Page 2 of 10)

Testing Technique	Type of Test Specimens	Static or Dynamic	Method of Loading	Range of Loads	Data Gathering Equipment	Techniques of Data Analysis	Test Cost	Typical Test Programs	Confidence Level
2. Acceleration type impact sled (Installations at [illegible] U. S. auto companies, independent research agencies (Calspan, Ohio Transportation Research Center, etc.) and various government agencies).	Same as 1.	Dynamic	Sled is initially at rest. An accumulated energy source, usually hydraulic or a falling weight, propels the sled to the rear simulating a frontal impact. The positioning problems of the first technique is eliminated.	Same as 1. The pulse shape is often determined by the shape of a hydraulic metering pin. Design for any but simple pulses is difficult.	Same as 1.	Same as 1.	2 and sometimes 3.	Same as 1.	Same as 1.
3. Impact Sled with Rebound (a few installations most often based on an MTS shock programmer. A large system exists at HSRI.)	Same as 1.	Dynamic	Sled is accelerated to a velocity up to 40 mph and impacts a programmable decelerator which stores energy resulting in a rebound up to 30 mph. The result is an impact simulation of 75 mph. in a small space.	Same as 1. The pulse shape is determined by the characteristics of the shock programmer. At HSRI it produces a square wave with a maximum of 75 G's and a stroke of 36".	Same as 1.	Same as 1.	2 and sometimes 3.	Same as 1.	Same as 1.

TABLE 1 REVIEW OF IMPACT TEST PROCEDURES (Page 3 of 10)

Testing Technique	Type of Test Specimens	Static or Dynamic	Method of Loading	Range of Loads	Data Gathering Equipment	Techniques of Data Analysis	Test Cost	Typical Test Programs	Confidence Level
4. Full-scale barrier crash facilities (available at auto companies, independent organizations (HSRI, MSU, Calspan, Dynamic Science, etc.))	Most often fully instrumented vehicles. Occupants may or may not be included.	Dynamic	Vehicle is accelerated up to speed by a single or tandem automobile engines and towed into the barrier. A towing vehicle is sometimes used. Some facilities are capable of towing more than one vehicle to represent vehicle-vehicle impact. Speed control is often difficult.	The target may be a rigid flat barrier, a rigid pole barrier, an angle barrier, another vehicle, the ground if a ramp is used to simulate rollover, or other desired barriers. Loading is not controlled, it is a result of the kinetic energy of the vehicle making velocity control especially important.	Same as 1. Telemetry of transducer data to the data gathering is often preferred to hard-wired umbilical cable. The barrier is usually instrumented to record the dynamic impact load.	Same as 1.	3	a. Vehicle crashworthiness development. b. Compliance testing.	3, 3, 1 or 2.

TABLE 1 REVIEW OF IMPACT TEST PROCEDURES (Page 4 of 10)

Testing Technique	Type of Test Specimens	Static or Dynamic	Method of Loading	Range of Loads	Data Gathering Equipment	Techniques of Data Analysis	Test Cost	Typical Test Programs	Confidence Level
5. Static crusher testing of vehicles (Two known to be operational at General Motors and Pioneer Engineering. Others are under construction at automobile companies. Data has been obtained on the Pioneer crusher).	Motor vehicles as well as structural components and parts.	Static	Test structure is fastened to a rigid test bed. A horizontal, hydraulically operated platen crushes the test structure at a controlled rate to the desired degree of deformation.	300,000 lb. maximum capicity.	a. Deformation potentiometers and strain gage load cells. b. Direct recording using a Honeywell visicorder (960C)	Plotting of the force-deformation characteristics of the structure and/or its components.	2 or 3	a. Determination of static force-deformation properties of a total vehicle or its components. b. Determination of static force deformation properties of structural components to use as input data for analytical structural crashworthiness models.	1, 3 (possible) 1 (unidirectional crush direction only.
6. SAE J 857 (a) roll-over tests without collision.	Motor vehicles often including dummy passengers.	Dynamic	a. Ground level roll-over. Vehicle is towed at desired speed and then put into broadslide or rollover is initiated by a ramp. b. Hill rollover. Vehicle is pushed sideways down steep (~60°) hill. c. In J 857 a, a curved ramp guide rack system has been substituted for consistency of results.	Load is not controlled. It is a function of the kinetic energy of the vehicle before the test.	a. Triaxial accelerometers to monitor vehicle and occupant dynamics. b. Transducers on belt restraint systems to measure dynamic force. c. Real time and high speed coverage of event including on-board cameras to monitor vehicle interior.	Same as 1 plus additional measurements of vehicle structural deformation.	3	a. Evaluation of vehicle structural and occupant injury potential in a rollover. b. Mechanisms of accidental door unlatching.	3, 3, 2

TABLE 1 REVIEW OF IMPACT TEST PROCEDURES (Page 5 of 10)

Testing Technique	Type of Test Specimens	Static or Dynamic	Method of Loading	Range of Loads	Data Gathering Equipment	Techniques of Data Analysis	Test Cost	Typical Test Program	Confidence Level
7. SAE J 850 (a) Barrier Collision Tests	Motor vehicles often including dummy passengers.	Dynamic	Vehicle is towed into a barrier. Barrier is constructed from reinforced concrete, at least 10 ft. wide, 5 ft. high and 2 ft. thick with 200,000 lb. of earth fill behind barrier. Barrier facing is 3/4 inch plywood.	Loading is not controlled. It is a result of the kinetic energy of the vehicle. The major control variable is therefore impact velocity which must be rigidly controlled. 30 mph is recommended.	Same as 4.	Same as 4.	3	a. Vehicle crashworthiness development. b. Occupant restraint system development. c. Compliance testing.	3, 3, 1
8. SAE J 972. Moving Barrier Collision Tests.	Fully instrumented automobile often with test dummy occupants.	Dynamic	A flat faced moving barrier weighing 4000 lb. is towed into the rear of the stationary vehicle. The vehicle reacts as it would on a roadway and the moving barrier is braked to a stop.	Loading is not controlled. It is a result of the kinetic energy of the moving barrier which is most often towed at 20 mph. The major control variable is impact velocity which must be rigidly controlled	Same as 4.	Same as 4.	3	Same as 7.	3, 3, 2.

TABLE 1 REVIEW OF IMPACT TEST PROCEDURES (Page 6 of 10)

Testing Technique	Type of Test Specimens	Static or Dynamic	Method of Loading	Range of Loads	Data Gathering Equipment	Techniques of Data Analysis	Test Cost	Typical Test Programs	Confidence Level
9. SAE J 996. Inverted Vehicle Drop Test Procedure.	Automobile	Dynamic	Vehicle is inverted and lifted to desired height. A quick release mechanism drops the vehicle onto its roof on a 4 in bituminous or 6 in reinforced cement concrete pad with a compacted gravel base.	The load depends on vehicle deformation properties, vehicle weight, and drop height. The vehicle is ballasted to its curb weight.	The test as specified in J 966 is essentially uninstrumented.	A measurement is made of the distance from the design H-point of the vehicle (front seat rearmost position) to the crushed interior of the roof structure.	3 (Primary cost is the vehicle. The test procedure itself would be 2.	a. Simulation of possible deformation in a roll-over. b. Comparison between vehicle models and various roof and roll bar designs.	3, 3, 2
10. SAE J 374. Passenger Car Roof Crush Test Procedure (Similar to MVSS 216 - Roof Crush resistance-passenger cars).	Automobile body containing all components which may affect load or deformation.	Static	Vehicle body is rigidly attached to test stand. Platen applies load to vehicle roof structure at a vehicle pitch angle of 5° and a roll angle of 25°.	The range shall be sufficient to determine force-deformation characteristics of vehicle roof-structure.	a. Force transducer in loading platen. b. Displacement transducer to measure platen travel.	Electronic or hard plotting of the force-deformation characteristics of the roof structure.	2 or 3	The static analog of the rollover and roof drop tests. Provides a uniform laboratory technique to assess roof crush properties.	1, 2, 2

TABLE 1 REVIEW OF IMPACT TEST PROCEDURES (Page 7 of 10)

Testing Technique	Type of Test Specimens	Static or Dynamic	Method of Loading	Range of Loads	Data Gathering Equipment	Techniques of Data Analysis	Test Cost	Typical Test Programs	Confidence Level
11. SAE J 367. Passenger Car Door System Crush Test Procedure. (This is similar with a few changes in detail to MVSS 214 Side Door Strength - Passenger Cars)	Automobile body and chassis frame with all standard door system components which may affect load or deflection. Body may be used for more than one test if frame, floor, and sill on opposite side are essentially undistorted.	Static	Vehicle body is rigidly attached to test stand. A 12 in. diameter, 24 in. high penetrator applies load to the midpoint of the door with its bottom located 4 inches above the highest surface of the body sill.	Load is sufficient to allow a 24 in. travel of the loading ram to penetrate the vehicle.	Same as 10.	Electronic or hand plotting of the force-deformation characteristics of the door structure.	2 or 3	This is a static test to assess door crashworthiness properties and penetrability. It is intended to offer a uniform laboratory method to evaluate the capability of car door systems to resist a concentrated lateral load.	1, 2, 2
12. SAE J 980 a Bumper Evaluation Test Procedure (A similar procedure is included in MVSS 215 - Exterior Protection - Passenger Cars).	Automobile loaded with the equivalent of one passenger. The car is in neutral without brakes set. (In MVSS 215, the vehicle is at unloaded curb weight.	Dynamic	Load is applied by a pendulum, the contact surface of which is 24 in. wide, 18 in. high, and 2 in. thick. The weight of the pendulum is 4000 lbs. with an arm of 132 in. The striker may be located to strike front and rear bumpers centrally or at an angle, usually 30° with respect to vehicle direction. In MVSS 215 the pendulum mass = vehicle mass. Its shape is more bumper-like. Front and rear impacts are 5 mph and corners are 3mph.	The pendulum is intended to simulate low speed impacts such as may occur in parking maneuvers. The control variable is the angle from which the pendulum drops thus allowing precise control of impact energy.	Not specified in the procedure. No instrumentation is needed to assess vehicle damage but the usual transducer and photographic equipment can be used for additional detail.	Not specified	2	Assessment of the bumper system as a protecter against damage affecting the performance of front and rear external lamps and other components during low-speed impacts, as in vehicle parking maneuvers.	2, 2, 1 or 2

TABLE 1 REVIEW OF IMPACT TEST PROCEDURES (Page 8 of 10)

Testing Technique	Type of Test Specimens	Static or Dynamic	Method of Loading	Range of Loads	Data Gathering Equipment	Techniques of Data Analysis	Test Cost	Typical Test Programs	Confidence Level
13. MVSS 208. Occupant Crash Protection. (Frontal, lateral and rollover test procedures as specified in Docket 69-7; Notice No. 9).	Automobile loaded with instrumented dummy passengers.	Dynamic	a. Front barrier (Same as 7).	a. Up to 30 mph impact velocity.	a. Same as 7 specifically to record dummy head triaxial, chest triaxial, and femur loads.	a. Computations of resultant accelerations of triaxial accelerometer packs and filtering as specified in SAE J 211.	3	Compliance to the specifications included in the standard.	3, 3, 1
			b. Lateral Moving Barrier Similar to SAE J 972 with dimensions 78 in. wide, 60 in. high, and 5 in. above the ground.). Barrier moves in to side of vehicle at 20 mph with centerline passing through driver's seating reference point.	b. 20 mph.	b. Same as a.	b. Same as a.	3	Same	3, 3, 2
			c. Rollover test. Vehicle sits on tilted platform. Platform is decelerated from 30 mph to 0 in 3 ft.	c. Vehicle is dumped onto road surface at 30 mph.	c. Same as a.	c. Same as a.	3	Same	3, 3, 2.

TABLE 1 REVIEW OF IMPACT TEST PROCEDURES (Page 9 of 10)

Testing Technique	Type of Test Specimens	Static or Dynamic	Method of Loading	Range of Loads	Data Gathering Equipment	Techniques of Data Analysis	Test Cost	Typical Test Programs	Confidence Level
14. HSRI Biomaterials Laboratory Plastechon High Speed Testing Facility.	Structures as large as 22 in. wide and 48 in. in the direction of load application or as small as desired.	Dynamic (Minimum of 20 in./min up to maximum of 30,000 in./min.	Hydraulically operated ram applies loads at rates up to 10,000 in./min., ram speed is constant regardless of load.	Maximum of 10,000 lb.	Load cells to record ram load. Optical tracking, linear potentiometers, high speed motion pictures and other procedures have been used to study motion. Signals have been recorded on oscilloscope or on tape.	Cross plots of a force quantity and a motion or strain quantity are produced normally.	1 to 2.	a. Material properties of bone, brain, dura mater, and other biological materials. b. Belt material dynamic strength properties. c. Energy absorbing foams and other materials. d. Automobile shock absorber response. e. Structural component tests.	1, 3 possible on components, 1 or 2.
15. Dynamic testing machines (although a few standard designs are available, many installations are custom. The most prominent suppliers are MTS Systems Corporation and Gilmore Industries.)	Structures up to 24 in. wide and 60 in. high. Specimen size depends on test frame. Non-standard sizes are common.	Dynamic (Up to 50,000 in./min. with MTS PS 819 system).	Hydraulically operated ram applies loads.	Gilmore advertises loads up to 100,000 lb. for dynamic testing whereas MTS limits itself to 6000 lbs. Usually the trade-off is speed vs loads.	Same as 14	Same as 14.	1 to 2.	Normally the same as 14.	Same as 14.

TABLE 1 REVIEW OF IMPACT TEST PROCEDURES (Page 10 of 10)

Testing Technique	Type of Test Specimens	Static or Dynamic	Method of Loading	Range of Loads	Data Gathering Equipment	Techniques of Data Analysis	Test Cost	Typical Test Programs	Confidence Level
15. Static testing machines. Many sizes, types and varieties are available ranging in size from table top units to large units equal in size to a small building. Companies specializing in standard units are Instron Corp., Riehle Testing Machines, Baldwin-Southwark, Tinius-Olsen, etc.	Most often tests are conducted on small components or material property test specimen. However large specimens such as automobile bodies (see items 5, 10, 11) and completed Saturn rocket cases are routinely loaded in special design load frames.	Very slow (< 0.001 in/min) up to about 10 in/min.	Hydraulically operated rams or electrically operated screws.	Up to 4,000,000 lb. Most standard laboratory units do not exceed 300,000 lbs. Instron machines are limited to 20,000 lb.	The complete range of force, motion and strain measuring techniques are used regularly.	Same as 14.	1 to 2.	Structural or material static strength tests.	Same as 14.

A simple two point scheme has been selected as an accident frequency indicator:

1. Test procedure reflects the most common direction of impact (frontal). Relationship of damage and injury caused by a test barrier crash to the real accident environment is not yet established.

TABLE 2. ACCIDENT TYPE PROBABILITY

direction of impact	probability
front	39%
right front oblique	15.8%
left front oblique	14.2%
right lateral	5.4%
left lateral	4.9%
right rear oblique	2.4%
left rear oblique	2.4%
rearand	2.3%

2. Test procedure reflects an uncommon accident type.

The last column in Table 1 contains a rating of confidence. In each case three numbers are given. The first results from the three point rating of occupant compartment acceleration, the second from the damage pattern rating scheme, and the last from the accident frequency indicator.

2.3 Conclusions and Observations

The following represents a collection of conclusions and observations as they relate to the six items included under the statement of Task 4.

1. The test specimens used in most of the procedures are large ranging from fully equipped automobiles to major sub-structural components. This might seem to make scale model testing attractive. For a complete vehicle this would be very expensive as the same metal forming techniques would be necessary to construct a scale model as are used to fabricate a full size vehicle. Scaled test specimens may

be useful in some component testing as has already been demonstrated in the case of bumpers. At the present time, however, it appears that the primary source of vehicle crashworthiness test specimens will be the assembly line or the prototype shop.

2. To physically simulate crash loadings it is necessary to possess a large energy source. This may be an accumulated energy source capable of programmed delivery (Hy-Ge impact sleds and dynamic testing machines), a towing assembly usually powered by gasoline engines capable of imparting a velocity to a test specimen, screw or hydraulic powered platens in the case of static test machines, gravity loading applied as an energy source through the mechanism of a falling weight, and any other technique of imparting loads or motions to an object.
3. Techniques for retrieving structural crash response data from the tests spans the range of electromechanical motion, velocity, acceleration, and force transducers as well as optical recording techniques. The standard is to record the dynamic data on FM tape for later processing. The event itself usually lasts less than 1/2 second with a frequency content ranging from about 3 cps up to at most 10,000 cps -- this last occurring rarely. Motion picture cameras are operated most frequently at 500 fps, 1000 fps, and sometimes 2000 fps or more.
4. Control of state variables is highly important and a particular problem in the full scale crash tests. Most experienced impact sled crews are able to control impact velocity and the deceleration pulse with high accuracy. An effective velocity control procedure for barrier test sites has been a problem in the past. The best

technique is to run the vehicle through a velocity window prior to impact such that the test can be aborted if velocity is not within tolerances. Some information on velocity is necessary as the test vehicle is being accelerated and stabilized at test speed and this must be fed back to the towing control. Static and dynamic test machines, properly maintained and operated, have a high level of control available on load and deformation rates.

5. The confidence level of a physical simulation technique as a realistic indicator of the crash event can only be estimated roughly at best. It is certainly possible to compare the final damaged state of tested vehicles with accident-damaged vehicles. A precise comparison of the deceleration pulses is not yet possible. The greatest problem may be that inherent in a statement made previously. "Relationship of potential damage and injury caused by a test barrier crash to the real accident environment is not yet established." Beyond this, only a miniscule percentage of real world accidents are similar to a flat, pole, or angle barrier test. Real world accidents may be even less relatable to the other testing procedures.

6. Crashworthiness testing is expensive. All full scale tests will cost a bare minimum of $1000. It may be possible to conduct some of the SAE tests for less than $1000. The static tests, the uninstrumented tests, and the tests using static and dynamic test machines are generally the least expensive.

3.0 THE NEED FOR PHYSICAL TESTING IN THE USE AND VERIFICATION OF MATHEMATICAL CRASHWORTHINESS MODELS

Physical testing is intimately involved with modeling procedures. First, physical data is required as input to the computer programs. Second, the output generated should be comparable with feasible physical measurements wherever possible. The following three studies have been made:

1. Definition of the physical input data requirements for representative models evaluated during this project;
2. Determination of the types of output data which are produced by the models either by direct computation or by post-process procedures; and,
3. Determination of the availability and accuracy of experimental techniques to provide input data for model execution and to provide data for comparison with model output as well as estimation of the effects of experimental inaccuracies on the ability to conduct verifications.

3.1 COMPARISON BETWEEN MODELING CONCEPTS

A series of comparisons of input required and output produced has been made between five mathematical crashworthiness models (See Tables 2-6). The mechanism used for these comparisons is a series of tables described in the text which follows. The models are those developed by Emori (Ref. 4), IBM (CSMP, Ref. 5), Battelle (FMCCM, Ref. 6), Calspan (Shieh, Ref. 7), and Philco-Ford (Young, Ref. 8 and Melosh, Ref. 9). These five models have been selected to approximate the five levels of model sophistication outlined by McIvor (Ref. 2), The format used in these tables can be applied to other existing models as well as help in defining models for future development and use.

The INPUT table includes four columns with the following headings:

1. Input quantity,
2. Source of data,
3. Techniques for determination, and
4. Accuracy of technique.

The reader of this table will be able to determine the ease and accuracy of preparing a data set for any of the models considered. For any input data quantity, the source can be an experimental number, a hypothesis, a guess, or one in a series of parameter variations. Possible techniques for determining the various quantities are listed as well as estimations of their accuracy. If experience of the model user is believed to be an important factor in conducting a successful exercise of the model, this is also indicated.

The OUTPUT table covers two pages for each model and has the following headings:

1. Output quantity,
2. Mode,
3. Computational technique,
4. Presentation,
5. Computational accuracy,
6. Probable accuracy of results,
7. Related experimental variables,
8. Technique of measurement,
9. Accuracy of measurement, and,
10. Potential for verification.

If a particular output quantity is produced automatically, optionally, or only using special post-processing methods, this fact is indicated under "mode." The heading "computational technique" refers to whether the

quantity is computed directly as a solution to the problem (e.g., a dependent variable in a system of equations) and also to the numerical analysis techniques used. The "presentation" of output may be tables, hard-line graphs, printer plots, CRT displays, etc. The "computational accuracy" of the numerical procedures used in producing the output is also estimated while "probable accuracy of results" refers to the level of confidence the user may have in his results based on the input data.

The second OUTPUT sheet considers the relation between model output and experimentally measured data. If physical data can be obtained which is related to output quantities, this is indicated under "related experimental variables." The "technique of measurement" and "accuracy of measurement" for the physical quantities is also indicated.

The user of these tables has at his disposal a list of output variables, a list of related experimental quantities, and accuracy estimates on both of these. The last column considers the "potential for verification" for all the output quantities. Besides being a mechanism for isolating research and development needs with respect to refined experimental measurement and data analysis procedures as well as advanced post-processing of model output, this last column give the model user an idea of the applicability of a particular simulation to the problem at hand. In other words, it helps him to answer the following question, "Can the model estimate improved performance trends, explain observed performance with accuracy, provide the accuracy and reproducibility necessary in a compliance procedure, or serve as an explicit tool in optimizing a design?"

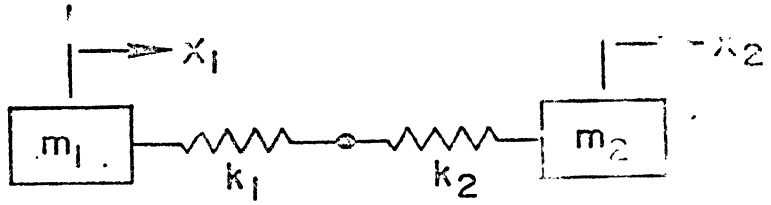

INPUT QUANTITY	SOURCE OF DATA	TECHNIQUE FOR DETERMINATION	ACCURACY OF TECHNIQUE
m_1, m_2 masses of colliding vehicles	Experimental	Weight measurement	Within 1%
α_1, α_2 acceleration of intact portion of colliding vehicles, or impact force.	Experimental	Accelerometers mounted on vehicle structure or force transducers on impact barrier.	Accelerometers - Depends on filter technique, mounting locations in vehicle, and structural integrity of vehicle. The average of several locations is best. Force transducers - Depend on filter technique. Can be within 1%.
$x_1(0)$, $x_2(0)$ - Initial displacement of vehicles	Experimental	Location measurement	Within 0.1%
$\dot{x}_1(0)$, $\dot{x}_2(0)$ - Initial vehicle velocity	Experimental	Velocity pickup	Within 1%
K_1, K_2 - Linear spring force-crush characteristics of vehicles	Experimental	Plot acceleration of vehicle (accelerometer data) versus vehicle crush (high speed movie analysis). Fit linear curve to resulting plots.	Does not allow dynamic interaction between various vehicle parts. Rough fit to data.

TABLE 2. EMORI MODEL (Sheet 1 of 3)

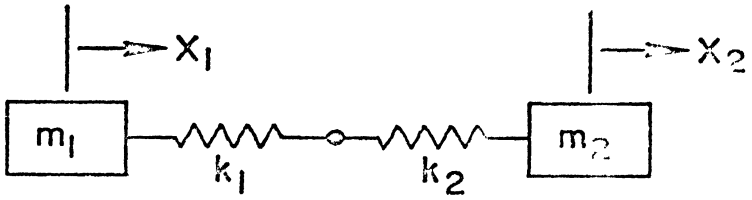

OUTPUT QUANTITY	MODE	COMPUTATIONAL TECHNIQUE	PRESENTATION	COMPUTATIONAL ACCURACY	PROBABLE ACCURACY OF RESULTS
$x_1(t)$, $x_2(t)$ - displacement of vehicles	Unknown (Possible hand calculation)	Direct Computation	Line Graphics	Exact	Highly dependent on the accuracy of k_1, k_2. It can be no more accurate than those quantities. The model is a fit of an energy-absorbing linear spring to vehicle crush data. Emori found that (k/m) does not appear to vary much between selected older vehicles.

TABLE 2. EMORI MODEL (Sheet 2 of 3)

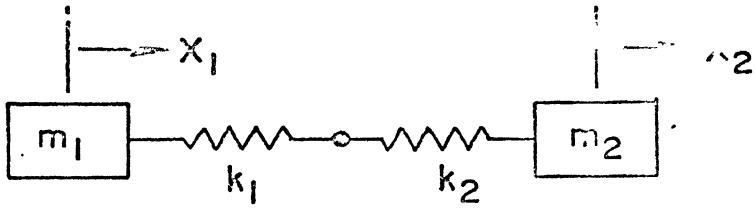

OUTPUT QUANTITY	RELATED EXPERIMENTAL VARIABLES	TECHNIQUE OF MEASUREMENT	ACCURACY OF MEASUREMENT	POTENTIAL FOR VERIFICATION
$x_1(t)$, $x_2(t)$ - displacement of vehicle	Same	High speed motion pictures	Probably 5%	Good. The major problem is locating a target on the intact portion of the vehicle.

TABLE 2. EMORI MODEL (Sheet 3 of 3)

INPUT QUANTITY	SOURCE OF DATA	TECHNIQUE FOR DETERMINATION	ACCURACY OF TECHNIQUE
Differential equations of motion in terms of generalized coordinates and time derivatives	Analysis of physical problem	not applicable	not applicable
Physical constants in equations	Experiments or hypothesis	not applicable	not applicable
Initial conditions on generalized coordinates	Experiments or hypothesis	not applicable	not applicable
Selection of solution procedure and its accuracy	Experience with physical system and its behavior	not applicable	not applicable
Selection of output variables and tabular or print-plot presentation	Depends on purpose of simulation	not applicable	not applicable

TABLE 3. APPLICATION OF CSMP (Sheet 1 of 2)

OUTPUT QUANTITY	MODE	COMPUTATIONAL TECHNIQUE	PRESENTATION	COMPUTATIONAL ACCURACY	PROBABLE ACCURACY OF RESULTS
Any computed variable versus independent variable	Optional	Direct or post-process computation depending on system of equations.	Tabular or printer plot	Depends on match of one of six integration procedures to the physical problem. They are: 1. Milne predictor-corrector 2. Runge-Kutta 3. Adams 2nd order integration 4. Simpson's rule 5. Trapezoidal integration 6. Rectangular integraiton	Depends on match of physical problem and solution procedure

TABLE 3. APPLICATION OF CSMP (Sheet 2 of 2)

INPUT QUANTITY	SOURCE OF DATA	TECHNIQUE FOR DETERMINATION	ACCURACY OF TECHNIQUE
Vehicle component masses. Four for each of two vehicles. For front collisions M_1=body, chassis M_2=engine, transmission M_3=front cross-structure & suspension M_4=bumper mass.	Vehicle specifications or hypothesis	Weight measurements of specific components.	For well-defined components, weight is easily specified within 1%. For components which have less well-defined boundaries such as the body and the torque box in a car with unit body construction, it is difficult to estimate the accuracy.
Energy-absorbing connections between the components. For front collision, typical connections are: EA1=engine-body EA2=front structure-body EA3=bumper-body EA4=front structure-engine EA5=bumper-front structure EA6=bumper-engine EA7=bumper-barrier	Experiment or hypothesis	Determination of force-deflection curves requires force measurements and the displacement of two points. It may be relatively easy to obtain displacements between engine and bumper but difficult to measure a force. For deforming structures such as torque box and sheet metal, it will be difficult even to specify a point for measurement. Motion of points will be measured using high speed motion pictures. Force measurements can be made using strain gages, force links and accelerometers	Specification of force-deformation properties is difficult. Their accuracy is generally unknown except for a few well-defined frame and bumper tests. Possibly the most acceptable technique at the present state of the art is to perform a static crush test on the vehicle and estimate the dynamic properties of the individual energy absorber either by component test or based on experience with the model.
Integration step size & output requirements	Computer model user	User experience with model	Depends on user experience with the model or particular physical problem particularly in the selection of an integration time step.

TABLE 4. BATTELLE MODEL (Sheet 1 of 4)

OUTPUT QUANTITY	MODE	COMPUTATIONAL TECHNIQUE	PRESENTATION	COMPUTATIONAL ACCURACY	PROBABLE ACCURACY OF RESULTS
Mass position, velocity and acceleration	Automatic	Independent variables (position) and solution of the equations of motion	Tables and/ or Calcomp plot versus time or other variables.	Depends on error Control built in program and the time integration step. May break down in the case of high frequency oscillations.	The dynamics problem and the solution procedure are straight forward. For a well-defined set of input data, the accuracy could be within 10% on accelerations and better for velocity and position.
Force, deflection, and deflection rate of energy absorbers.	Automatic	Necessary quantities in equations of motion.	Tables and/ or Calcomp plots versus time or other variables	Depends on error control built in program and the time integration step.	For a well-defined set of input data, the accuracy could be within 10% on force, deflection, and deflection rate.

TABLE 4. BATTELLE MODEL (Sheet 2 of 4)

OUTPUT QUANTITY	RELATED EXPERIMENTAL VARIABLES	TECHNIQUE OF MEASUREMENT	ACCURACY OF MEASUREMENT	POTENTIAL FOR VERIFICATION
Mass position, velocity, and acceleration	Same	Position--high speed motion pictures. Velocity-Differentiation of high speed motion picture data. Acceleration-Accelerometer and/or force links, strain gages.	Position can be determined within 1/2 inch for a rigid body using two cameras. The targeting is difficult for many of the components. It is difficult to choose a target position on masses which may deform. Acceleration of a rigid mass can be measured within 5%. A problem here is the collinearity of the model. Because the masses may translate in three directions and have three additional rotational directions, it is difficult to estimate accuracy. Further extensive problems arise if the mass is deformable.	For reasonably well-defined masses such as the bumper, engine, and occupant compartment, it may be possible to design a verification experiment using current test procedures.

TABLE 4. BATTELLE MODEL (Sheet 3 of 4)

OUTPUT QUANTITY	RELATED EXPERIMENTAL VARIABLES	TECHNIQUE OF MEASUREMENT	ACCURACY OF MEASUREMENT	POTENTIAL FOR VERIFICATION
Force, deflection, and deflection rate of energy absorbers	Force exerted on masses by interconnecting components and relative motion between masses.	Force will be difficult to measure in the deforming energy-absorbers. In some cases, strain gages and force links may be used. Indirect measurement may be possible by measuring the effect of the force on a mass element using accelerometers	For well-defined energy-absorbing elements, such as a viscous shock absorber in series with a bumper, force and deflection measurements should be accurate within 5%. For deformable masses with questionable targeting and complex geometry, accuracy is difficult to judge.	In most cases verification will be difficult at best. Probably the greatest potential is for verification of the impact force exerted on the barrier and the resulting deceleration of the occupant compartment. Fortunately, these are probably the two most important variables although occupant compartment motion is limited to one direction.

TABLE 4. BATTELLE MODEL (Sheet 4 of 4)

INPUT QUANTITY	SOURCE OF DATA	TECHNIQUE FOR DETERMINATION	ACCURACY OF TECHNIQUE
System Geometry a. Beam lengths b. Number of beam members. c. Degrees of freedom d. Angular orientation of beam member	Data is obtained from existing truss hardware which has been fabricated in the laboratory as part of crashworthiness structural concept development projects at Calspan	Length measurements and idealization of 3-D physical framework to two dimensional frame.	Good for well defined trusses which remain two-dimensional during deformation.
Mass properties The number and location of mass points.	Experimental	Weight measurements	Masses are lumped and applied where desired to the truss. They should be chosen to simulate rotational inertia. Their selection strongly affects the hinge formation. The technique can be accurate when used by persons highly experienced with the model and the related physical problem.
Computational specifications such as initial time, integration time steps, printout specifications etc.	Computer user	Intuition of physical event or past experience with model	These quantities, especially as they relate to the integration time step, influence the accuracy and the cost strongly. An experienced user is required to make the optimum trade off between accuracy and cost based on a thorough understanding of the physics of the problem.

TABLE 5. SHIEH MODEL (Sheet 1 of 5)

INPUT QUANTITY	SOURCE OF DATA	TECHNIQUE FOR DETERMINATION	ACCURACY OF TECHNIQUE
Bending and extensional stiffness vectors	Experiment or hypothesis	If Young's modulus, cross-sectional area, and moment of inertia for a beam are known, these vectors may be computed. Otherwise, an engineering estimate must be made.	Accuracy is especially good for long, uniform beam elements. For short beams, or beams with non-uniform cross section, the accuracy depends largely on the skill of the user.
Plastic moments and axial yield force	Experiment or hypothesis	If Young's modulus, cross-sectional area, and yield stress are known, these quantitites may be computed.	Physical measurement is probably more accurate than calculation in most cases. To account for strain rate effects, these quantities are often altered to "tune" the model predictions.
Location of contact between vehicle and barrier, initial displacement, external forcing functions	Experiment or hypothesis	These quantities drive the model and may be hypothesized or determined from photogrammy, by distance measurements or by force transducers.	Can be exact.

TABLE 5. SHIEH MODEL (Sheet 2 of 5)

OUTPUT QUANTITY	MODE	COMPUTATIONAL TECHNIQUE	PRESENTATION	COMPUTATIONAL ACCURACY	PROBABLE ACCURACY OF RESULTS
Time	Automatic	Independent Variable	Tabular	Exact	-
Displacement, velocity, and acceleration of joints	Automatic	From solution of the equations of motions	Tabular	Strongly dependent on integration specifications	Strongly dependent on input data.
Internal forces and bending moments	Automatic	From solution of equations of motion	Tabular	Depends on integration specification	Strongly dependent on input data.

TABLE 5. SHIEH MODEL (Sheet 3 of 5)

OUTPUT QUANTITY	RELATED EXPERIMENTAL VARIABLES	TECHNIQUE OF MEASUREMENT	ACCURACY OF MEASUREMENT	POTENTIAL FOR VERIFICATION
Time	Time	Time pulse generator on tape or high speed motion picture	<0.01%	Time establishes a base against which all other variables are plotted. Its high accuracy is a basic requirement. It should be stored at 1 msec intervals in the experiment.
Displacement, velocity, and acceleration of joints.	Same	1. Displacement from motion pictures. 2. Velocity from analysis of motion pictures or velocity. 3. Acceleration from film analysis or accelerometers.	1. Can be within 1/2 inch as a function of time. 2. Velocity can be measured within 0.1 ft/sec. with a pickup. Estimates or film analysis are not easily obtained but may be within 1 ft/sec. 3. Acceleration may be measured from film within 30% accuracy. Accelerometer accuracy is difficult to assess because of placement problems.	The problems with photometric techniques are targeting and camera placement for three-dimensional viewing of the joints at all points in time. Also, accurate film analysis techniques are only now being developed. At the present state of the experimental art, the ability to predict is at least as high as the ability to measure. Reliable electronic measurement procedures are also not available. The model could be verified for idealized structure but probably not now against a full-scale vehicle test.

TABLE 5. SHIEH MODEL (Sheet 4 of 5)

OUTPUT QUANTITY	RELATED EXPERIMENTAL VARIABLES	TECHNIQUE OF MEASUREMENT	ACCURACY OF MEASUREMENT	POTENTIAL FOR VERIFICATION
Internal forces and bending moments	Same	Possibly strain gages	<1%	If data gathering techniques can be developed, there is some potential for verifying these predictions. The hinge moments will be especially difficult to assess except for ideal geometries. Idealized structures could possibly be used to verify these predictions.

TABLE 5. SHIEH MODEL (Sheet 5 of 5)

INPUT QUANTITY	SOURCE OF DATA	TECHNIQUE FOR DETERMINATION	ACCURACY OF TECHNIQUE
Joint Data a. coordinates b. degrees of freedom	A three-dimensional mesh of points is selected representing a studied estimate of the structure's load-carrying characteristics.	At the present state of the art, the user is required to be highly skilled in finite-element mechanics and, at the same time, very knowledgable in real crash mechanics.	Potentially good accuracy for well-defined frame structures. Not yet successfuly verified for full-scale vehicle structures.
Member parameters a. Joints to which the two ends of the member are connected b. Code names relating material, buckling etc.	Based on the mesh of points selected above.	User experience in selecting an appropriate arrangement of frame elements to represent the expected structural behavior.	Potentially good accuracy for well-defined frame structures. Not yet successfully verified for full-scale vehicle structures.
Member section properties a. cross-section area. b. controid location c. moments of inertia d. shear center e. torsion constant	If a well-defined frame is simulated, the input can come directly from physical measurements. Otherwise, engineering estimates must be made based on experience with finite element procedures.	Length, weight, moment of inertia, and other mass-geometric measurements or past experience with finite element modeling procedures.	When physical measurements provide the data, accuracy can be within 1%
Material Tables a. uniaxial stress-strain tabular input	Experiment or hypothesis	Static and dynamic tensile tests.	Experimental procedures are highly accurate (1%)

TABLE 6. CRASH PROGRAM (Sheet 1 of 4)

INPUT QUANTITY	SOURCE OF DATA	TECHNIQUE FOR DETERMINATION	ACCURACY OF TECHNIQUE
Lumped mass parameters	Data is obtained by distributing the weight of the structure as lumped masses at the joints.	Weight measurements of well-defined components and engineering judgment as to the most satisfactory distribution of the weight	Can be accurate for a fine grid of joints. The most appropriate distribution for vehicle dynamics has not yet been established
Initial conditions a. displacements b. velocities c. accelerations d. forces	Experiment or hypothesis	Optical position and velocity measurements. Transducer measurement of acceleration and force.	Can be accurate within 1%
Control and integration Parameters	Computer user	Intuition of physical event or past experience with model	These quantities, especially as they relate to automatic error control, influence the accuracy and the cost strongly. Accuracy is often related to the experience of the user who is required to make the optimum trade-off between accuracy and cost based on a thorough understanding of the physics of the problem.

TABLE 6. CRASH PROGRAM (Sheet 2 of 4)

OUTPUT QUANTITY	RELATED EXPERIMENTAL VARIABLES	TECHNIQUE OF MEASUREMENT	ACCURACY OF MEASUREMENT	POTENTIAL FOR VERIFICATION
Joint position, velocity, and acceleration	Position, velocity, and acceleration of related points on structure. This fact points to desirability of selecting a grid which consists of "observable" points.	Optical measurement of position with data processing and differentiation to produce velocities and accelerations	Three-dimensional measurement of the motion of a point in space is a state of the art procedure with 5% accuracy if the point is viewable from two different high-speed cameras with sufficient frame rate. Velocity and acceleration are far less accurate because of the numerical differentiation process.	Difficult and expensive to instrument. Time-consuming to reduce the data. However, if crashworthiness models are to be widely accepted as an engineering tool, experimental procedures must be developed to accomplish this goal. It is probable that this can be accomplished for only a few carefully selected points on the structure. Further development is required for the computer data-processing tools used to handle the large amount of data which is generated.
Stress at selected points in members	Stress at a point	Strain gages, photoelastic coating, stress-sensitive coating.	For surface points, strain gages offer the greatest potential for accuracy. Measurement of stress internal to a structural member is probably beyond the current state of the art	It is possible that strain gages can be used in stress-determinations at key points on the structure. Some limitation is inherent because of mass effects, the use of umbilical cables for many channels, and blocking the view of optical procedures.

TABLE 6. CRASH PROGRAM (Sheet 3 of 4)

OUTPUT QUANTITY	MODE	COMPUTATIONAL TECHNIQUE	PRESENTATION	COMPUTATIONAL ACCURACY	PROBABLE ACCURACY OF RESULTS
Joint position, velocity and acceleration	Automatic	From solution of the equations of motion	Tabular	Strongly dependent on error control parameters on the time integration	Highly dependent on input data. It should be possible at the present state of the art to predict these quantities within 10 for well-defined frame structures. The accuracy possible for a whole-vehicle simulation is not yet established.
Stress at selected points in members	Automatic	From solution of the equations of motion.	Tabular	Strongly dependent on error control parameters on the time integration.	Highly dependent on input data. It should be possible at the present state of the art to predict these quantities within 10 for well-defined frame structures. When the structural elements used in the simulation are not directly related to hardware, it is difficult to attach meaning to the accuracy of stress at selected points in the members.

TABLE 6. CRASH PROGRAM (Sheet 4 of 4)

3.2 VERIFICATION OF THE ACCURACY OF CRASHWORTHINESS MODEL PREDICTIONS CURRENT STATE OF THE ART.

In this part of the report, the content of the tables presented in section 3.1 are evaluated in order to establish the current state of the art of the verifiability of crashworthiness model predictions. The five models which have been selected for this study approximate the five simulation levels described by McIvor (Ref. 2). Hence, they represent the complete range of sophistication found in current crashworthiness models. The Emori model represents Level 1 and consists of one mass and one spring describing each vehicle. CSMP can be used to implement Level 1 models and possibly Level 2 models consisting of lumped masses and the associated interconnected spring elements. The Battelle model can be classified someplace between Levels 2 and 3 as it uses only a few lumped masses and generalized resistances representing specific vehicle components. However, rather general representations of component force-deformation behavior can be included. The Shieh model might be used to represent total vehicle behavior at Level 3. However, if a single component is simulated, the Shieh model would be satisfactory as a Level 4 module. The very general finite element model of Melosh should be satisfactory as a Level 5 module.

There are two problems in the verification of the Emori model - one with input data and the other with experimental technique. The structural crush properties of the vehicle are based on fitting a curve to a collection of crush data obtained in full scale tests and comprise one of the two major sets of input data quantities. A verification experiment involves measurement of vehicle motion or displacement of the vehicle relative to a barrier or another vehicle. Targeting a collapsing structure (hopefully the occupant compartment does not deform extensively and maintains straight line motion) and measuring the resulting motion can result in a gross verification at best.

The Battelle model reveals more detailed problems in verification. Again it is difficult to obtain force-deformation data for the energy absorbing links. The force is difficult to obtain and the deformation even more so especially when the energy-absorbing member consists of a geometrically complex link between two deforming masses. It was estimated that mass deflection, velocity, and acceleration, force in energy-absorbing links, as well as link deflection could be predicted within 10% at best. Using a model at the level of sophistication of the Battelle model, it is possible to obtain input data for a well-defined arrangement of masses and links and to design a verification experiment. Force measurements will be very difficult to obtain in the verification experiment except for impact force exerted on a barrier and deceleration of an occupant compartment on the other end. Fortunately, those are probably the two most critical quantities. At the present state of the art it should be possible to establish agreement between predictions and tests involving simplified structures within a band representing 10-25% of the signal maximum amplitude for a few of the key variables if careful control is exerted over the processing of both the test and computer-generated data.

The Shieh model represents an increase in the sophistication of input data requirements as a structural definition is attached to the linkage between the mass points. For a verification test using a structure which develops well-defined hinges it should be possible to reduce the band of uncertainty between prediction and experiment to 10%. Processing of the photometric data appears to be the procedure with the greatest possibility for error because of its relatively undeveloped state of the art. It does not appear to be possible at this time without further study to estimate the accuracy with which the Shieh model can reproduce the results of a full-scale unmodified vehicle crash test.

Most of the comments made concerning the Shieh model are also applicable, to the Melosh model. One additional comment relates to the highly sophisticated finite element representation of structure necessary as input data. The user of the Melosh model must have extensive experience with finite element procedures in order to select a representation with the most likely chance for accurate reproduction of structural response. It is possible that this problem may be reduced with the implementation in the model of state-of-the-art software for aiding the user in setting up his input structural gridwork. Again, it does not appear to be possible at this time without further study to estimate the accuracy with which the Melosh model can reproduce the results of a full-scale unmodified vehicle crash test. In other applications, finite element models have been used to predict structural response with high accuracy.

Three additional items should be mentioned which can have a major influence on the accuracy of crashworthiness model predictions. These all relate to the user himself. First, it is necessary for the computer user to have experience in using numerical integration procedures and also to have first-hand knowledge of the specific program which is using these procedures. Second, it is necessary for the engineer user to have experience with the model input physical parameters and their measurement. Third, it usually requires a competent computer-user-engineer experienced with the particular model to interpret the output beyond a superficial overview. These three properties seldom occur in any one individual emphasizing the teamwork necessary in the development, operation, verification, and application of crashworthiness mathematical models.

3.3 RECOMMENDATIONS TO ADVANCE THE STATE OF THE ART OF MATHEMATICAL CRASHWORTHINESS MODEL VERIFIABILITY

Seven recommendations conclude Part 3 of this report based on the preceding tables and discussions. Their intent is to advance the state of the art

of mathematical crashworthiness model verifiability.

1. Guidelines for model verification experiments should be developed which include the following steps:
   a. Provision of model output variables which relate directly to measurable physical quantities.
   b. Estimation of the potential accuracy of the prediction based on the accuracy of the input data.
   c. Estimation of filter properties of the data gathering and processing system to determine modification of the real physical signal;
   d. Estimation of filter properties of model computational procedures to determine modification of the signal described by the equations of motion;
   e. Definition of a realistic band of agreement between experimental results and model predictions before the fact based on the four preceding steps.
2. Crashworthiness mathematical model computer programs should be required to possess the following three features:
   a. Preprocessor subprograms for aiding in preparation of input data (e.g., the finite element grid or the structuring of crash test data in the appropriate format);
   b. Postprocessors to present the output as variables compatible with experimentally obtained data.
   c. User-oriented documentation containing model analysis, explanation of program function, and detailed user instructions.

All three of these features require considerable research effort. Feature "a" is a discipline in its initial state of development which has been forced because of the input requirements of large scale computer programs. Feature

"b" has been largely neglected in development of computer programs because of the typical structuring of research groups as either analytical or experimental. Feature "c" is another discipline in its infancy for which guidelines should be developed.

3. Techniques should be developed for estimating the overall properties (transfer function) of a system of filters in series to aid in quantifying the verifiability of a model before the fact and the level of agreement between model predictions and experimental results after the fact.
4. A body of data on the force-deformation properties of vehicles and their components should be compiled as an aid to crashworthiness modelers and model users.
5. Research should be conducted to upgrade three-dimensional optical position measurement techniques and the associated computer software required to process the data.
6. Research efforts should be initiated to develop new techniques of force measurement within structures.
7. Research should be initiated to develop techniques for verification of advanced finite element models.

4.0 THE ROLE OF THE FILTER IN CRASHWORTHINESS ANALYSES AND EXPERIMENTS

The design and conduct of a meaningful verification experiment to determine the extent to which a crashworthiness analytical model predicts real structural resonse is an extremely difficult problem. Many of the complexities relate to a subject area which will require considerably more research before assessment of model verification can be totally quantitative rather than a qualitative measurement. The subject is the role of the filter in crashworthiness analyses and experiments.

Three types of studies must be conducted to gain understanding in this subject area: 1. a study of the transfer functions of analytical, numerical, and electronic filtering procedures; 2. the ability to quantitatively measure the similarity of two time-dependent curves which may have been produced using different filtering procedures (On one hand the filtering procedures may yield the digital output from a computer model. On the other hand, they may be related to electronic filtering used in data gathering, storage, and analysis); and, 3. development of logical procedures to estimate model verifiability while the physical model is being chosen as well as to measure verification after computer output has been generated (This will be based on model properties, availability of input and output, and the accuracy as well as detail of comparison experiments). A study of this nature will yield an aid to the experimental designer, the mathematical modeler, the hardware designer from the viewpoint that he can assess the suitability of a particular model as a design tool, the sponsor of coupled experimental and analytical research projects, and the developer of compliance procedures.

The following text attempts to survey briefly the types of filtering processes which may be related to crashworthiness modeling and experimentation.

The work accomplished represents an initial attempt at defining the scope of the first two studies outlined above. Demonstrations of the performance of specific filters are included. In addition, means for rating filter performance and comparing signals are proposed. This work serves as a basis for the third type of study mentioned above and included in a section of this report covering recommendations.

4.1 COLLECTION AND TABULATION OF FILTERING TECHNIQUES

Filters have been grouped according to the following categories: 1. digital filters; 2. smoothing operations; 3. integration and differentiation procedures; 4. active electronic filters; 5. analog-to-digital and digital-to-analog converters; 6. transducers (particularly for measurement of force and acceleration); 7. filters occurring because of data transmission over a distance; 8. signal conditioning equipment; 9. data recording equipment such as FM tape recorders; 10. data playback equipment including the galvanometers in light-beam oscillographs; and, 11. specifications and standards developed to control filtering procedures. Assessment of the properties of all filters included in each of these classes of filters is a large task well beyond the scope of this project. In fact, entire books have been written about filters in some of the categories. Rather, the objective is to show where filtering will occur in crashworthiness analyses and experiments and to demonstrate the extent to which real structural behavior may be masked.

4.1.1 Digital Filters

The idea of a digital filter is that it passes all frequencies, f, such that $|f| < f_c$ without change and deletes all frequencies greater than f_c where f_c is called the cut-off frequency. In mathematical form a filter is described by

$$S(f)=G(f)H(f) \tag{1}$$

where

G(f) is the input function

S(f) is the output function, and

H(f) is the transfer function for the filter

For an ideal filter,

$$H(f)=\begin{cases}1, & |f|<fc\\ 0, & |f|>fc\end{cases} \tag{2}$$

Because digital filters are most commonly applied in the time domain, an inverse Fourier transform formulation is used.

$$s(t)=\int_{-\infty}^{\infty}F(f)e^{2\pi ift}df$$
$$=\int_{-\infty}^{\infty}G(f)H(f)e^{2\pi ift}df=g(t)*h(t) \tag{3}$$

where g(t) is the input function or data in the time domain and h(t) is called the weight function. As seen in Equation 2, the ideal transfer function has a jump discontinuity which will cause Gibb's phenomenon. In order to avoid this, H(f) must be approximated by a continuous function defined as follows

$$H(f)=\begin{cases}1 & 0\leq f\leq fc\\ \text{monotonic decreasing} & fc<f<f_\tau\\ 0 & f\geq f_\tau\\ H(-f) & f<0\end{cases} \tag{4}$$

where f_τ is called the termination frequency. The monotonic decreasing function used in this formulation describes the rolloff properties of the filter.

A digital filter is based on a discrete date set. The output of Equation 3 can be restated as

$$f_m=\sum_{n=-N}^{N}h_n g_{m+n} \tag{5}$$

where

f_m is the output value of data item "m."

h_n is the weight function (defined below)

g_{m+n} is the input value of data item "m+n."

N is the number of weights chosen by the user.

Essentially this process reflects the fact that input data around the point "g_n" are necessary to describe functional behavior in order to form a basis for the application of the filter properties contained in the function "h." This discretized form of the weight function is determined by

$$h_n = \frac{1}{f_s} h\left(-\frac{n}{f_s}\right) \tag{6}$$

where f_s is the sampling frequency. In terms of the transfer function H(f),

$$h(t)=k(t) \cdot \frac{\sin \pi (f_\tau+fc)t}{\pi t} \tag{7}$$

$$k(t)=\int_{-\frac{f_\tau - fc}{2}}^{\frac{f_\tau - fc}{2}} K(f)e^{2\pi ift}df \tag{8}$$

$$H(f)=\int_{f-\frac{f_\tau+fc}{2}}^{f+\frac{f_\tau+fc}{2}} K(Z)dZ \tag{9}$$

A more general and complete description has been given by Anders (Ref.10).

In order to use the digital filter given in Equation 5, a set of equally spaced data, g_n, is required which must satisfy the following three conditions: 1. it arises from a function g(t) defining a generalized function; 2. it is band limited; and, 3. the desired signal spectrum and the unwanted spectrum of g(t) are disjoint. Besides satisfying these conditions, editing of g_n may be necessary because of missing or "wild points" in the set. The most common practice is to replace each missing or wild value using a linear interpolation between the nearest data values on each side of the missing value.

In addition to a data set several control parameters must be specified including:

1. The largest frequency, f_α , which is present in the data. This is commonly found by visually determining the shortest period in the data.

2. The sampling frequency, f_s, which must be at least $\geq f_\alpha$.

3. The cut-off frequency, f_c, which is chosen to be at least as great as the highest frequency of interest present in the data.

4 The termination frequency, f_τ . This should be chosen such that either no frequencies present in the data are in the interval (f_c, f_τ), or frequencies appearing in (f_c, f_τ) have no significant amplitude.

5. The number of weights, 2N + 1 of the filter. Guidlines on weight selection must be developed on an individual basis for each type of filter.

Among the many digital filters which have been located in the open literature, several have been examined including the Ormsby filter (Reference 10), the Martin-Graham filter (Reference 10), the Kaiser filter (Reference 11), the Blackman filter (Reference 12), the Schulz filter (Reference 13), and the Robinson filter (Reference 14). In addition a general formulation of the processes involved in digital filtering is contained in a book by Morrison (Reference 15). This subject is of great current research interest as evidenced by publications emanating from organizations such as Bell Laboratories. A session at the April 1973 meeting of the Acoustical Society of America was devoted to related topics. It is recommended that a more detailed evaluation of this subject be conducted than is possible under the current contract to establish the level of masking of structural dynamic resonse which may occur in both analytical procedures and in the difficult area of structural dynamic measurements.

The Martin-Graham filter (Reference 10) has been used to process output data from both crashworthiness and human motion mathematical models developed

under NHTSA contract. The transfer function for this filter is given by

$$H(f) = \begin{cases} 1 & f \leq fc \\ 0 & f \geq f\tau \\ 1/2\left[1+\cos\frac{\pi(f-fc)}{f\tau-fc}\right] & fc<f<f\tau \\ 1/2\left[1+\cos\frac{\pi(f+fc)}{f\tau-fc}\right] & -f\tau<\omega<-fc \end{cases} \qquad (10)$$

A plot of the output-input ratio as a function of frequency is shown as Figure 1.

4.1.2 Smoothing Operations on Digitized Data

Smoothing operations are often performed on a set of data $g(n\Delta t)$ where n is the number of a particular member of the set and Δt is the time increment between members. The simplest form of smoothing is carried out by the data user when he plots each point on a graph and then fits a line through the points. There is no control on the mathematical properties of the smoothing procedure when this technique is used. Mathematically sophisticated techniques are also in use which remove unwanted information, often of a random nature, from the discrete set. It is obvious that smoothing operations and digital filters possess the same fundamental mathematical properties given in the previous section of this report.

The artificial separation of smoothing operations from digital filters in the present discussion reflects common problems usually considered separately in dynamic measurements. Digital filtering is most often applied to remove unwanted frequency content from a signal which often originated as an analog electrical signal before digitization and data processing. Smoothing is usually related to removal of random observational errors introduced in a data preparation process where a human is an integral part of the data-gathering system or where substantial random noise may be superimposed on the signal. A "smooth" plot of the resulting data is generally more palatable to the project supervisor and to the sponsor.

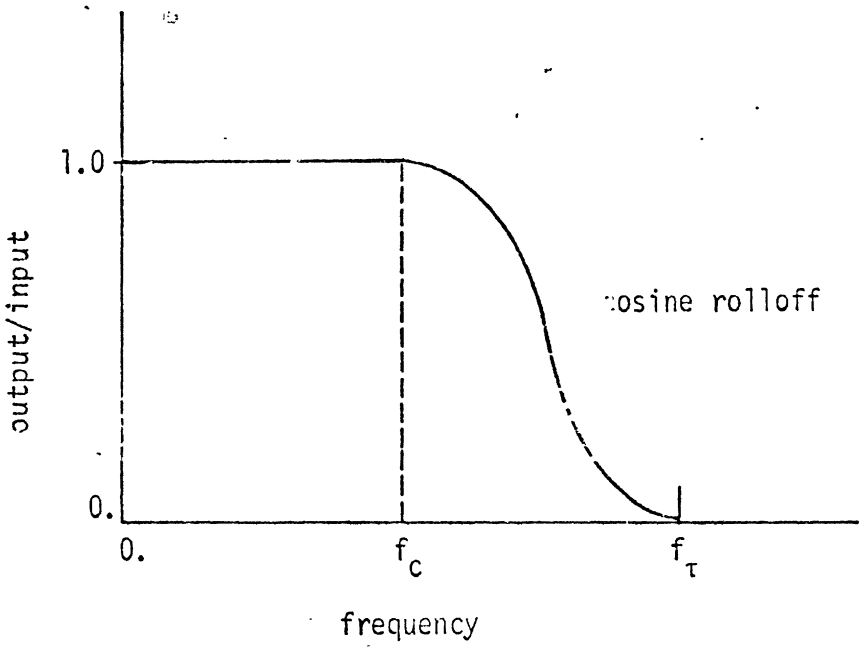

Figure 1. Characteristics of Martin-Graham Digital Filter

Several typical techniques for data smoothing have been reviewed briefly. One popular technique for smoothing a sequence of data uses a least-squares polynomial over the range (Reference 16). Examples of smoothing formula are:

1. 1st degree, 3-point formulae,

$$f_1 = \frac{1}{6}(5g_1 + 2g_2 - g_3)$$
$$f_i = \frac{1}{3}(g_{i-1} + g_i + g_{i+1}), \quad i = 2, 3, \cdots, n-1 \qquad (11)$$
$$f_n = \frac{1}{6}(-g_{n-2} + 2g_{n-1} + 5g_n)$$

2. 1st degree, 5-point formulae,

$$f_1 = \frac{1}{5}(3g_1 + 2g_2 + g_3 - g_5)$$
$$f_2 = \frac{1}{10}(4g_1 + 3g_2 + 2g_3 + g_4)$$
$$f_i = \frac{1}{5}(g_{i-2} + g_{i-1} + g_i + g_{i+1} + g_{i+2}), \quad i = 3, 4, \cdots, n-2$$
$$f_{n-1} = \frac{1}{10}(g_{n-3} + 2g_{n-2} + 3g_{n-1} + 4g_n) \qquad (12)$$
$$f_n = \frac{1}{5}(-g_{n-4} + g_{n-2} + 2g_{n-1} + 3g_n)$$

3. 3rd degree, 5-point formulae,

$$f_1 = \frac{1}{70}(69g_1 + 4g_2 - 6g_3 + 4g_4 - g_5)$$
$$f_2 = \frac{1}{35}(2g_1 + 27g_2 + 12g_3 - 8g_4 + 2g_5)$$
$$f_i = \frac{1}{35}(-3g_{i-2} + 12g_{i-1} + 17g_i + 12g_{i+1} - 3g_{i+2})$$
$$\text{for } i = 3, 4, \cdots, n-2$$
$$f_{n-2} = \cdots \text{, etc.} \qquad (13)$$

The first two sets of formulae use a straight line to approximate function behavior in the three or five point range of interest. The third uses a third-degree polynomial and should provide a better fit in most cases. A simple version is in use at HSRI for the analysis of high speed photographic data gathered during impact sled tests (Reference 17). The filtering properties of these three smoothing operations are compared by an example in the next section of this report. Several standard software packages are available in most computer systems. Two typical routines will be mentioned which are contained in the IBM System/360 Scientific Subroutine Package (Reference 18). The first is subroutine SMO which calculates the smoothed or filtered series given a time series A1, A2,..., A_n, a selection integer L, and a weighting series W1, W2,..., Wm. The smoothed data are given by

$$R_i = \sum_{j=1}^{m} A_p \, Wj \qquad (14)$$

$$p = jL - L + k$$

$$k = i - IL + 1$$

$$i = IL \text{ to } IH$$

$$IL = \frac{L(m-1)}{2} + 1$$

$$IH = n - \frac{L(m-1)}{2}$$

and L = a given selection integer. (For example, L = 4 applies weights to every 4th item of the time series).

m = number of weights, an odd integer.

h = number of items in the time series.

Equation (14) is a restatement of Equation (5) with the weights supplied by the program user. The subroutine EXSMO provide triple exponential smoothing yielding a smoothed series S1, S2, ..., S_{nx}, given a time series X1, X2, ...,

X_{nx} and a smoothing constant α. The subroutine has two stages for i=1,2,..., NX, starting with initial A,B,C either given by the user or provided automatically by the subroutine. The first stage is to find S_i for one period ahead.

$$Si = A + B + 0.5C \tag{15}$$

The second stage is to update A,B,C

$$\begin{aligned} A &= X_i + (1-\alpha)^3 (S_i - X_i) \\ B &= B + C - 1.5(\alpha)^2 (2-\alpha)(S_i - X_i) \\ C &= C - (\alpha)^3 (S_i - X_i) \end{aligned} \tag{16}$$

where α = a smoothing constant specified by the user ($0<\alpha<1$).

A final representative smoothing technique, which has been applied to automotive safety research involving photogrammetric analysis, uses the Gaussian distribution function to establish a weighting procedure (Reference 19) This method is based on the fact that, given a continuous integrable function g(t) normalized to satisfy the requirement

$$\int_{-\infty}^{\infty} g(t)dt = 1$$

for any continuous integrable function f(t)

then $$\lim_{\sigma \to 0} \frac{1}{\sigma} \int_{-\infty}^{\infty} f(\tau)\, g\left(\frac{t-\tau}{\sigma}\right) d\tau = f(t)$$

$$f(t) \approx \frac{\Delta T}{\sigma} \sum_{n=0}^{N} g\left(\frac{t - n\Delta T}{\sigma}\right) f(n\Delta T) \tag{17}$$

or

$$\begin{aligned} f^{(i)}(t) &\approx \frac{\Delta T}{\sigma} \sum_{n=0}^{N} \frac{d^i}{dt^i}\left[g\left(\frac{t - n\Delta T}{\sigma}\right)\right] f(n\Delta T) \\ &= \frac{\Delta T}{\sigma^{i+1}} \sum_{n=0}^{N} g^{(i)}\left(\frac{t - n\Delta T}{\sigma}\right) f(n\Delta T) \end{aligned} \tag{18}$$

The function g(t) can be chosen as the Gaussian distribution function

$$g(t) = \frac{1}{\sigma\sqrt{2\pi}} e^{-\frac{t^2}{2\sigma^2}} \qquad (19)$$

This technique can be used to evaluate derivatives of f(t). For example, if $f(n\Delta t)$ is the displacement, it can be smoothed by Equation 17. Velocity and acceleration can be computed using Equation 18. The values of σ and N depend on the sampling rate and the convergence of

$$g^{(i)}\left(\frac{n\Delta t}{\sigma}\right)$$

The effect of smoothing procedures can be illustrated by a frequency versus input/output ratio graph in the same manner as other filtering procedures. Figure 2 shows the characteristics of the three least-squares procedures as applied to sine waves. The sampling frequency is held fixed at approximately 5000 samples/second while frequency is increased. In other words a sample is taken every .2 millisecond. Thus each half cycle of a 600 cps sine wave is described by about four data points. It should be noted that the first degree, three point and the third-degree five point formulae do not degrade a 600 cps signal component more than 20%. However, the first-degree, five-point method is unsuited to handle a 600 cps signal unless a smaller time step is used. This appears logical in that all 5 points on a half-cycle are included in computing the fit. The third-degree technique introduces curvature allowing a better fit to the data even for the same number of points. Great care must be taken in choosing sample size and cut off frequency. Guidelines should be prepared for the application of these procedures to crashworthiness test data reduction.

4.1.3 Integration and Differentiation Procedures

A large variety of integration procedures are in use, each of which has its own filter properties. Many of these are available as package subroutines

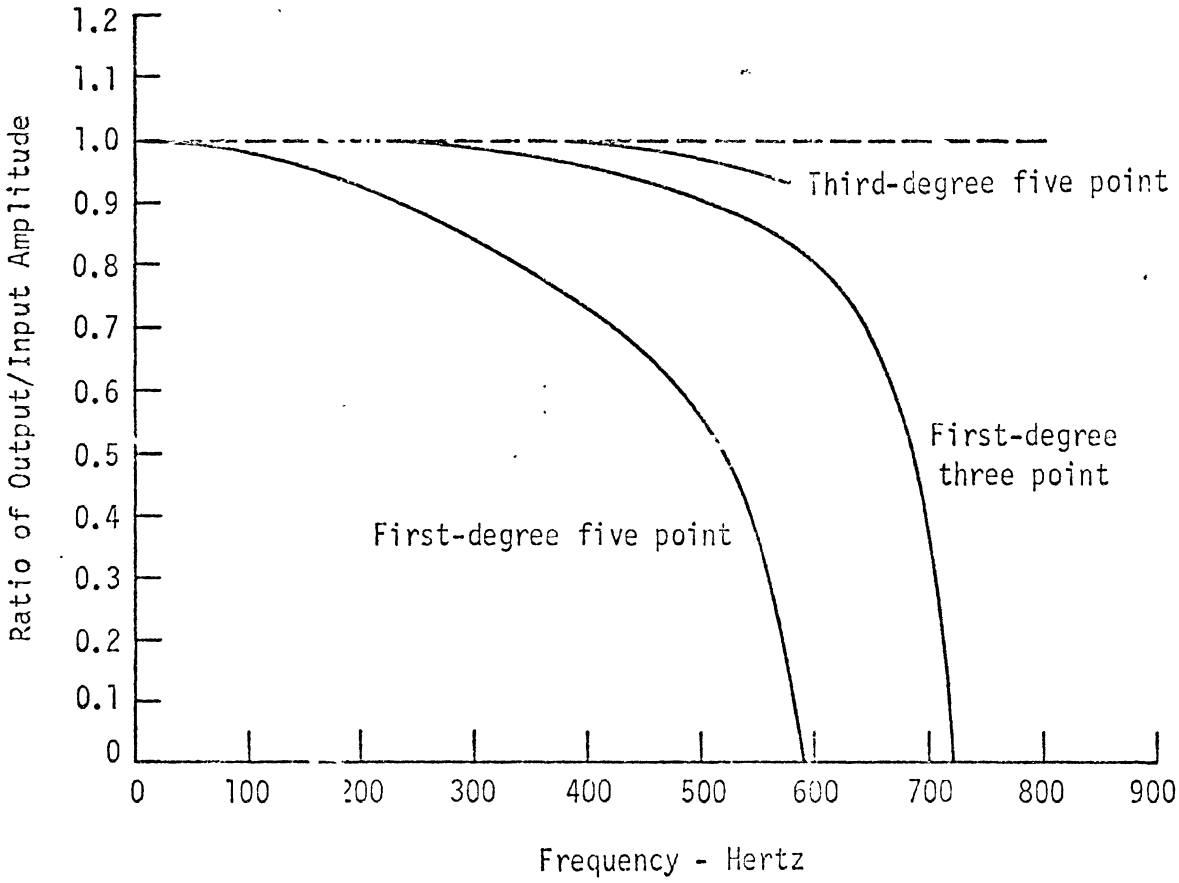

Figure 1. Filter Performance of Smoothing Procedures

in digital computer libraries such as IBM-SSP (Reference 18). Similar integration procedures have been developed by research organizations (for example, NHTSA contractors such as HSRI and Calspan) for use in specialized computer programs. Numerical differentiation procedures are not so common as they tend to propagate errors in experimental or computed data and must be used with great care. A study should be conducted to determine the suitability of obtaining acceleration data for a rigid body based on position measurements taken on the object using high-speed motion pictures. This procedure is usually coupled with smoothing procedures which also act as filters.

A limited number of integration procedures will be discussed including DHPCG, RK1, QC2, QSF, and QTFE (all from the IBM-SSP Reference 18), DINT developed by Calspan (Reference 20 which is used in crashworthiness models, and the package developed at HSRI for use with mathematical crash victim simulators. (Reference 21).

In DHPCG, the evaluation is done by means of Hamming's Modified predictor-corrector method. It is a fourth order method using four preceeding points for computation of a new vector of the dependent variables. A fourth order Runge-Kutta method suggested by Ralston is used for adjustment of the initial increment and for computation of starting values. This subroutine automatically adjusts the increment during the computation by halving or doubling. References 22 and 23 by Ralston describe the analytical features.

The subroutine RK1 integrates a given function using the Runge-Kutta technique and produces the final computed value of the integral. The ordinary differential equation

$$\frac{dy}{dx} = f(x,y)$$

with initial condition $y(x_0) = y_0$ is solved numerically using a fourth-order

Runge-Kutta integration process. This is a single-step method in which the value of y at $x = x_n$ is used to compute $y_{n+1} = y(x_n + 1)$ and earlier values y_{n-1}, y_{n-2}, etc. are not used. The relevant formulas are

$$y_{n+1} = y_n + \frac{1}{6}\left(k_0 + 2k_1 + 2k_2 + k_3\right)$$

where for step size h,

$$k_0 = h\, f(x_n, y_n)$$
$$k_1 = h f\left(x_n + \frac{h}{2}, y_n = \frac{k_0}{2}\right)$$
$$k_2 = h f\left(x_n + \frac{h}{2}, y_n = \frac{k_1}{2}\right)$$
$$k_3 = h f\left(x_n + h, y_n = k_2\right)$$

The method is described in Reference 18,

Subroutines such as QC2, QC3, ..., QC10, DQG4, DQG8, DQG12, DQG16, DQG24, and DQG32 perform the integration of a given function by Gaussian quadrature formulas.

To compute

$$y = \int_a^b f(x)\,dx$$

Gaussian quadrature formulas with n = 2,3,..., 10 (or n = 4,8,12,16,24,32) points are used. Transforming the range x=a...b into t=-1...1 by

$$t = \frac{2x - (a+b)}{b-a}, \quad x = \frac{b-a}{2}t + \frac{b+a}{2}$$

the result is

$$y = \frac{b-a}{2}\int_{-1}^{1} \phi(t)\,dt, \quad \phi(t) = f\left(\frac{b-a}{2}, \frac{b+a}{2}\right)$$

Using

$$\int_{-1}^{1} \phi(t)\,dt = \sum_{k=1}^{n}\left[A_k^{(n)}\ \phi^{(n)}(t_k)\right], \quad n = 2, 3, \ldots$$

with coefficients $A_k^{(n)}$ and nodes $t_k^{(n)}$ (note that $t_k^{(n)}$ are the roots of Legendre polynomials of degree n), the result is the approximations

$$y_n = (b-a)\sum_{k=1}^{n}\left\{\frac{A_k^{(n)}}{2} f\left[(b-a)\frac{t_k^{(n)}}{2} + \frac{b+a}{2}\right]\right\} \quad , n = 2, 3, \cdots$$

which are exact whenever f(x) is a polynomial up to the degree 2n-1.

The $A_k^{(n)}$ and $t_k^{(n)}$ are symmetric with respect to t = 0

$$A_k^{(n)} = A_{n-k+1}^{(n)} \quad ; \quad t_k^{(n)} = -t_{n-k+1}^{(n)}$$

This method is described in Reference 24.

Subroutine QSF performs the integration of an equidistantly tabulated function by Simpson's rule. To compute the vector of integral values

$$\left.\begin{aligned} z_i = z(x_i) &= \int_a^{x_i} y(x)dx \\ \text{with } x_i &= a + (i-1)h \end{aligned}\right\} \; i = 1, 2, \cdots, n$$

for a table of function values y_i(i-1,2,...,n), given at equidistant points x_i=a+(i-1)h(i=1,2,...,n), Simpson's rule together with Newton's 3/8 rule or a combination of these two rules is used. Local truncation error is of the order h^5 in all cases with more than three points in the given table. Only z_2 has a truncation error of the order h^4 if there are only three points in the given table. No action takes place if the table consists of less than three sample points.

The function to be integrated is assumed to be continuous and differentiable (three or four times, depending on the rule used).

Formulas used in this subroutine (z_j are integral values, y_j function values) are

$$z_j = z_{j-1} + \frac{h}{3}\left(1.25\, y_{j-1} + 2\, y_j - 0.25\, y_{j+1}\right)$$

$$z_j = z_{j-2} + \frac{h}{3}\left(y_{j-2} + 4y_{j-1} + y_j\right) \qquad \text{(Simpson's rule)}$$

$$z_j = z_{j-3} + \frac{3}{8}\left(y_{j-3} + 3y_{j-2} + 3y_{j-1} + y_j\right)$$

(Newton's 3/8 rule)

$$z_j = z_{j-5} + \frac{h}{3}\left(y_{j-5} + 3.875\,y_{j-4} + 2.625\,y_{j-3} + 2.625\,y_{j-2} + 3.875\,y_{j-1} + y_j\right)$$

Sometimes Simpson's rule is used in the following form

$$z_j = z_{j+2} - \frac{h}{3}\left(y_j + 4y_{j+1} + y_{j+2}\right)$$

The local truncation errors of the first four formulae are respectively

$$R_1 = \frac{1}{24}h^4 y'''(\xi_1) \quad (\xi_1 \in [x_{j-1}, x_{j+1}])$$

$$R_2 = -\frac{1}{90}h^5 y''''(\xi_2) \quad (\xi_2 \in [x_{j-2}, x_j])$$

$$R_3 = -\frac{3}{80}h^5 y''''(\xi_3) \quad (\xi_3 \in [x_{j-3}, x_j])$$

$$R_4 = -\frac{1}{144}h^5 y''''(\xi_4) \quad (\xi_4 \in [x_{j-5}, x_j])$$

However, these truncation errors may accumulate. This method is discussed in References 18 and 25.

Likewise, the subroutine QTFE performs the integration of an equidistantly tabulated function by trapezoidal rule. To compute the vector of integral values

$$\left.\begin{aligned} z_i = z(x_i) &= \int_a^{x_i} y(x)\,dx \\ \text{with } x_i &= a + (i-1)h \end{aligned}\right\} i = 1,2,3,\ldots,n)$$

for a table of function values $y_i (i = 1,2,\ldots,n)$, given at equidistant points $x_i = a + (i-1)\cdot h$ $(i = 1,2,\ldots,n)$, the trapezoidal rule is used. It is assumed that the function to be integrated is continuous and can be differentiated

at least twice. Starting with the integral value $z_1 = 0$, successive integral values $z_i (i = 2,3,\ldots,n)$ are computed, using the trapezoidal rule in the following form

$$z_i = z_{i-1} + \frac{h}{2}(y_i + y_{i-1}) \quad , \quad i = 2, 3, \cdots, n$$

with a given increment h of argument values. As local truncation error at each step is

$$R_i = -\frac{1}{12} h^3 y''(\xi_i) \quad , \quad \xi_i \in [x_{i-1}, x_i]$$

the global truncation error R in z_n appears as follows

$$R = -\frac{1}{12}(n-1) h^3 y''(\xi) \quad , \quad \xi \in [x_1, x_n]$$

or

$$R = -\frac{l}{12} h^2 y''(\xi)$$

where l is the length of the whole integration interval. See Reference 18

The DINT subroutine developed by Calspan (Reference 20) is a variable step integrator which returns to the calling program whenever an estimate of the variable at a specified time interval is achieved. The integration procedure is based on a four parameter Runge-Kutta technique which has been modified to handle exponential behavior in each variable. The option is available to use a least square procedure to estimate the parameters. Step size is controlled by ordered tests on acceleration of one human body segment (magnitude and change). A failure of the tests causes the step size to be halved unless it is already less than some specified value in which case it is not changed. After a specified number of successful steps at a particular time increment, step size is doubled.

The HSRI integration procedures are based on HPCG with some simplifications and some extensions. The basic Milne-Hamming integration procedure is used although some updating is eliminated resulting in a much faster routine without great loss in accuracy. Upon selection of an appropriate switch, the classical Adams-Monlton procedure may be used in cases where great solution stability is needed. Three starting methods are available based on the expected volatility of the solution. These are a Ralston-Runge-Kutta method, a classical Runge-Kutta method, and a final method which uses the Euler method for the second point, the trapezoidal method for the third point, and Simpson's rule for the fourth point, all combined with a regular predictor-corrector to establish convergence at each level. See Reference 21 for extensive details and operational characteristics.

4.1.4 Active Electronic Filters

Active Electronic filters consist of an electronic circuit specifically designed to remove a certain range of frequencies from an analog electronic signal. Usually they are designed to remove low frequencies (high pass filters), high frequencies (low pass filter), or some band of frequencies (band reject filters).

Three of the most common types are Bessel, Butterworth, or Tchebyscheff filters based on their response characteristics. (See Reference 26). Low-pass Butterworth filters have excellent gain accuracy in the lower portion of the pass band and reasonably well-behaved phase-shift characteristics. They provide the flattest possible amplitude response obtainable without having gain-ripple in the pass band. The attenuation rate beyond the passband is set by the number of poles-for N poles the rolloff is N X 6 dB/Octave. They are recommended for low-pass filtering of signals that are to be processed by analog to digital converters or other data acquisition equipment and for

general purpose low-pass filtering. The characteristics of typical Butterworth filters are shown in Figure 3. In the figure cutoff frequency fc is defined as the frequency at which the attenuation is - 3dB. In general, the cutoff frequency should be well above the maximum signal frequency for best gain accuracy in the pass band.

The Bessel filter provides excellent phase-shift linearity, but the amplitude cutoff is not as sharp as Butterworth or Tchebyscheff filters. Bessel filters, as a group, are also referred to as a type of "linear phase" filter. These filters will pass rectangular pulses with a minimum of distortion and with a delay time that is linearly proportional to the phase-shift characteristic. That is, the time delay through the filter is almost constant with frequency and is equal to the slope of the filter phase characteristic. The overshoot to a step input is essentially zero for Bessel filters, where Tchebyscheff filters may exhibit more that 25% overshoot. Because of these characteristics Bessel filters are sometimes used to provide time delays. Bessel filters are also used for low-pass filtering of rectangular waveforms in pulse-width modulation systems, voltage-to-frequency converters, and similar circuits. "Running-average" filters often require a Bessel-type response. Gain and phase Response curves for Bessel filters are shown in Figure 4.

Since phase shift is the parameter of interest for a Bessel filter, the cutoff frequency f_c is defined in terms of phase shift. The frequency at which the phase shift is one-half the maximum phase shift is defined as the cutoff frequency f_c. The maximum phase shift depends directly upon the order (no. of poles) of the filter. For a Bessel filter of N poles and phase-shift $\theta(f)$,

$$\theta(f_c) = \frac{\theta(f)_{max}}{2} = \frac{N\pi/2}{2} \text{ rad.} = \frac{N\pi}{4} \text{ rad.}$$

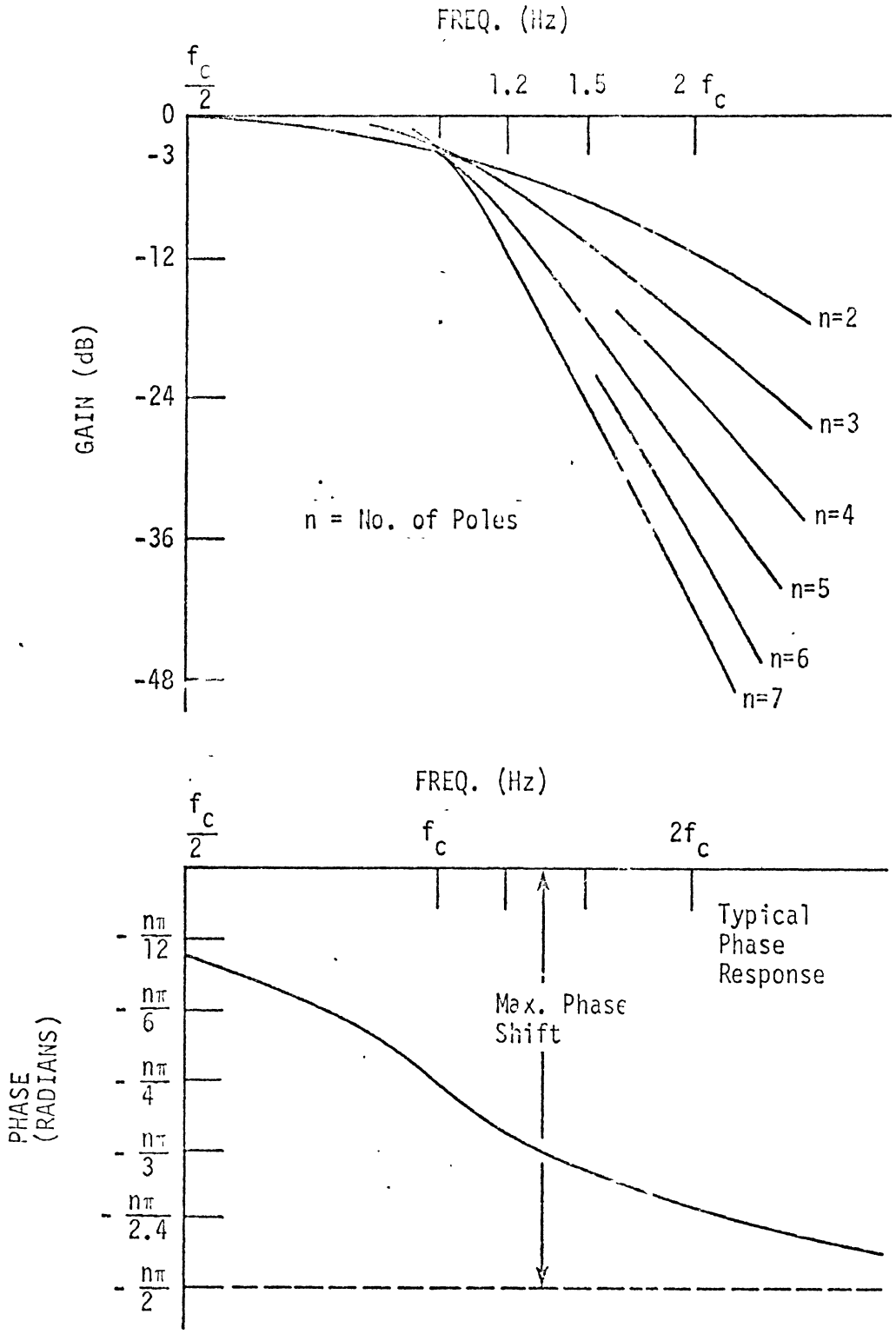

Figure 3. Low-Pass Butterworth Response

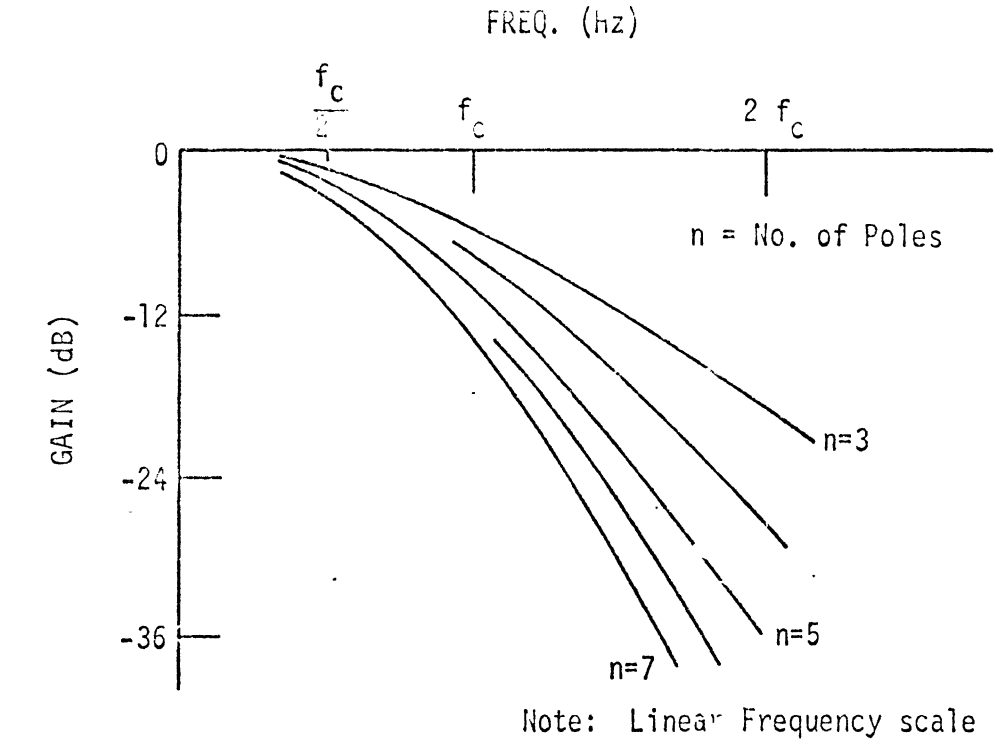

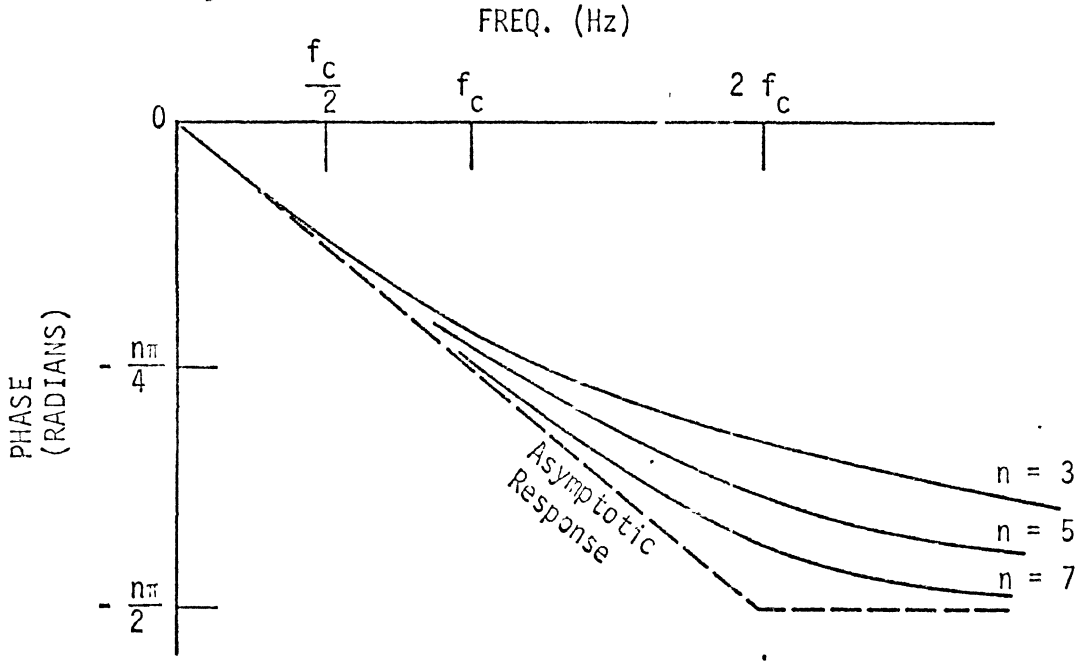

Figure 4. Bessel Linear Phase Response

Thus the phase shift at cutoff frequency f_c for a 5-pole Bessel filter would be 3/4 - radians. The phase shift at cutoff (f_c) is often referred to as the "phase constant" or "delay at cutoff". For accurate delay (phase constant), f_c should be about twice as high as the maximum signal frequency.

Tchebyscheff filters offer a maximum attenuation rate beyond cutoff, which is achieved at the expense of pass band ripple as shown in the response curves (Figure 5). Higher attenuation rates outside the pass band are accompanied by correspondingly greater pass band ripple. The step response of such filters is lightly damped in comparison to Butterworth or Bessel filters and will exhibit considerable overshoot and ringing. Tchebyscheff filters are excellent for many audio applications and others where ripple in the pass band is not important, but where sharp cutoff is required. In general, Tchebyscheff filters should not be used where good transient response is important. Cutoff frequency f_c is defined as the frequency at which the gain curve first departs from the specified maximum ripple band.

Over 100 companies manufacture active electronic filters for one or another application. Most of these are listed in Reference 27.

4.1.5 Analog to Digital and Digital to Analog Converters

Much time is spent preparing data from large-scale experiments such as crash impact tests for review by the test engineer and presentation in reports. The preparation of graphs, reduction of data, reading of strip recordings of analog data, etc., is made easier when the power and speed of a digital computer and its associated output hardware is employed. This may be done either by having the analog signal fed directly to a computer on line, by preprocessing the data onto digital magnetic or paper tape for later computer processing, or by connecting to a remote teletype terminal.

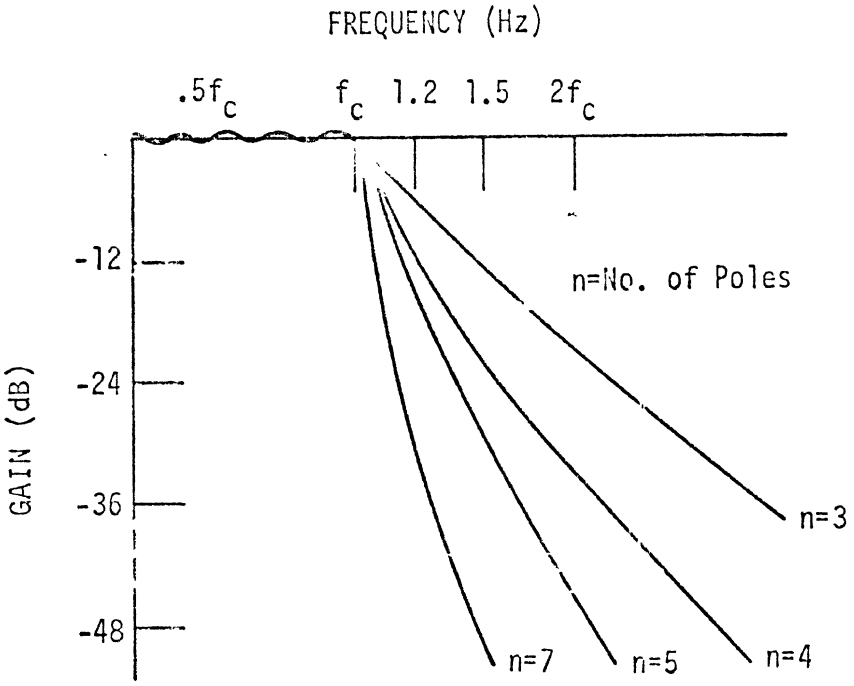

Figure 5. Tchebycheff Response

In all these cases, an analog to digital (A/D) converter is required which: 1. receives an analog signal; 2. samples it at a set rate; and, 3. outputs the signal as binary coded data. As such, an A/D converter has many of the same filter properties as the smoothing operations mentioned earlier in this report which also involve discrete sets of data points. Many companies produce A/D conversion hardware or components. One system which has been developed specifically for crash impact studies is the Thomas Instrumentation Recording Analog Digitizer Model 1720. The specifications of the Thomas system will be given as an example of relevant A/D converter properties. The AC power requirement is 120 AC volts and 100 watts. The amplitude accuracy is $\pm$ 1% of full scale and the accuracy of the sample rate is $\pm$0.1% of the selected rate. This system allows 512 different sample rates ranging from 0.1 milliseconds to 12.8 seconds. The input impedance is 100K ohms and the range of the analog signal is +10 volts.

The standard current output interface of the Thomas system is compatible with an ASR33 teletype. As such it has built-in logic to provide blocks of 64 characters bracketed by carriage return/line feed. The discrete output is coded as 8 bit binary values transmitted in two characters to allow for high density and high-speed output. Yet, it permits the detection of output errors by means of even parity checks.

Often times in data analysis or the preparation of graphic output displays it is necessary to reconstruct an analog signal from the digital form (digital to analog or D/A conversion). In the simplest procedure (a zero-order converter), the signal is reconstructed as a series of steps between sampling points. For a sinusoidal signal the error at the peak is

$$e_p = 1 - \cos \frac{\pi}{(T/\tau)}$$

and the instantaneous error midway between two sample points is

$$e_b = \sin \frac{\pi}{(T/\tau)}$$

where T is the waveform period and τ is the sample period. These errors can be plotted (Figure 6).

In a first-order D/A converter, the signal is reconstructed a set of linear sigments joining sample points. This procedure greatly reduces the error (Figure 7). A second-order D/A converter fits three data points with a quadratic equation further improving the results (Figure 8). Further improvements are inherent as the order is increased. For a fourth-order converter

$$e_b = -\sin \frac{\pi}{T/\tau} + \frac{1}{16}\left[10 \sin \frac{2\pi}{T/\tau} - \sin \frac{4\pi}{T/\tau}\right]$$

$$e_p = 1 - \frac{1}{8}\left[9 \cos \frac{\pi}{T/\tau} - \cos \frac{3\pi}{T/\tau}\right]$$

The error in reconstruction is less than 0.3% for only 10 samples/cycle as shown in Figure 9. Further details on reconstruction errors in digital to analog conversion are found in Reference 28.

4.1.6 Transducers (Accelerometers, Force Measurement, etc.)

The purpose of transducers in crashworthiness testing is to monitor physical quantities such as linear acceleration and velocity, angular acceleration and velocity, force, etc. Over one-hundred companies manufacture transducer hardware which could be used in these applications. Most types of these transducers use one of the following principles to produce a signal: 1. wire-wound or piezoresistive strain gages; 2. piezoelectric crystal; or, 3. capacitance. In the case of accelerometers, a sprung mass is used to load the strain gages, the crystal, or the material in the capacitor gap. In the case of force transducers, the applied load activates similar types of sensing elements in the various types of transducers. Their filter properties will be discussed briefly only as applied to accelerometers.

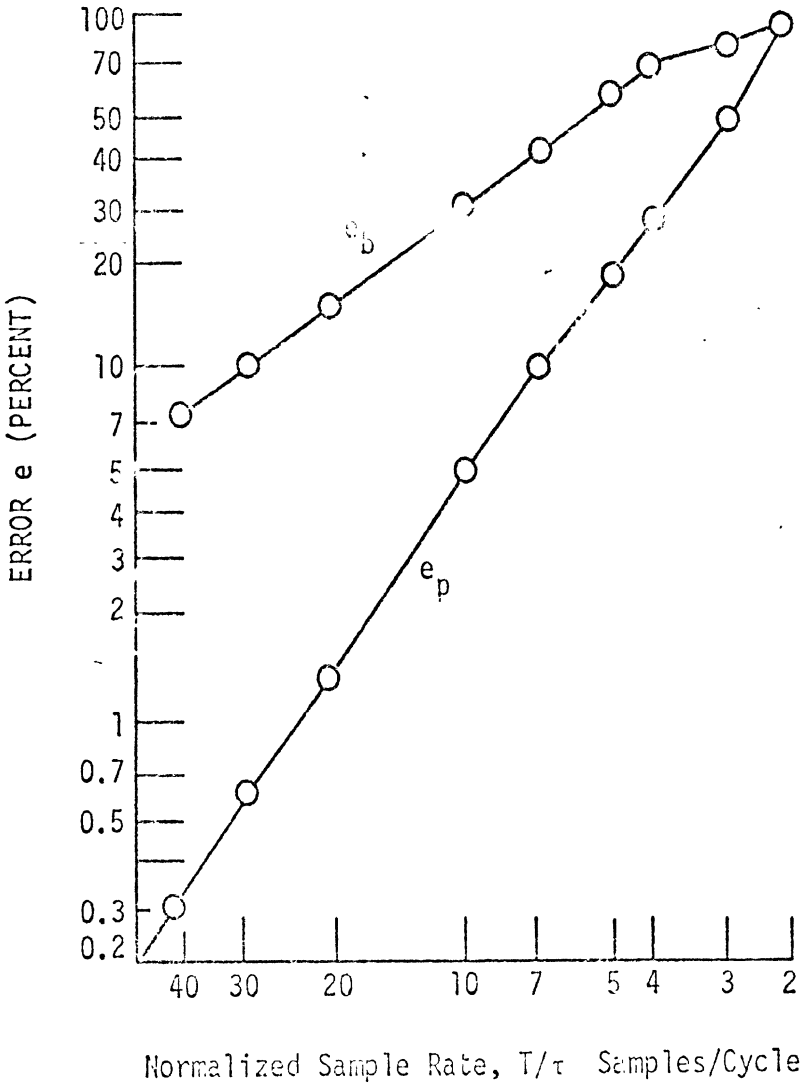

Figure 6. Errors Inherent in a Zero-Order Digital to Analog Converter.

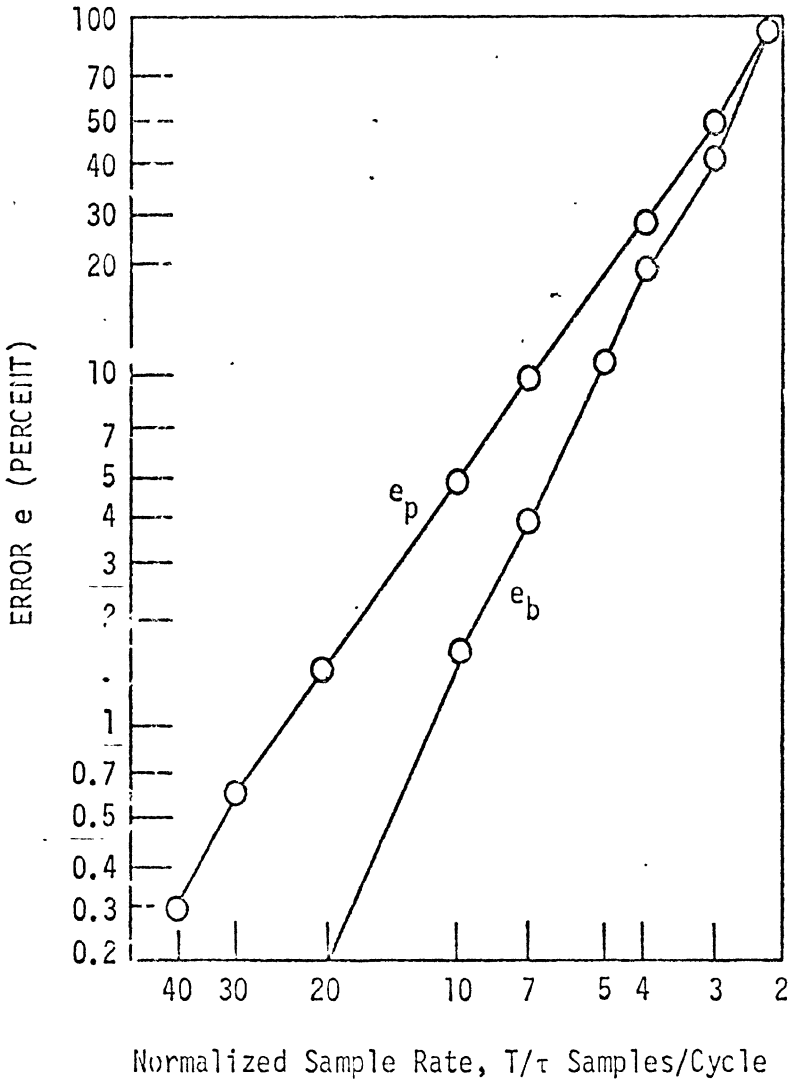

Figure 7. Errors Inherent in a First-Order Digital to Analog Converent

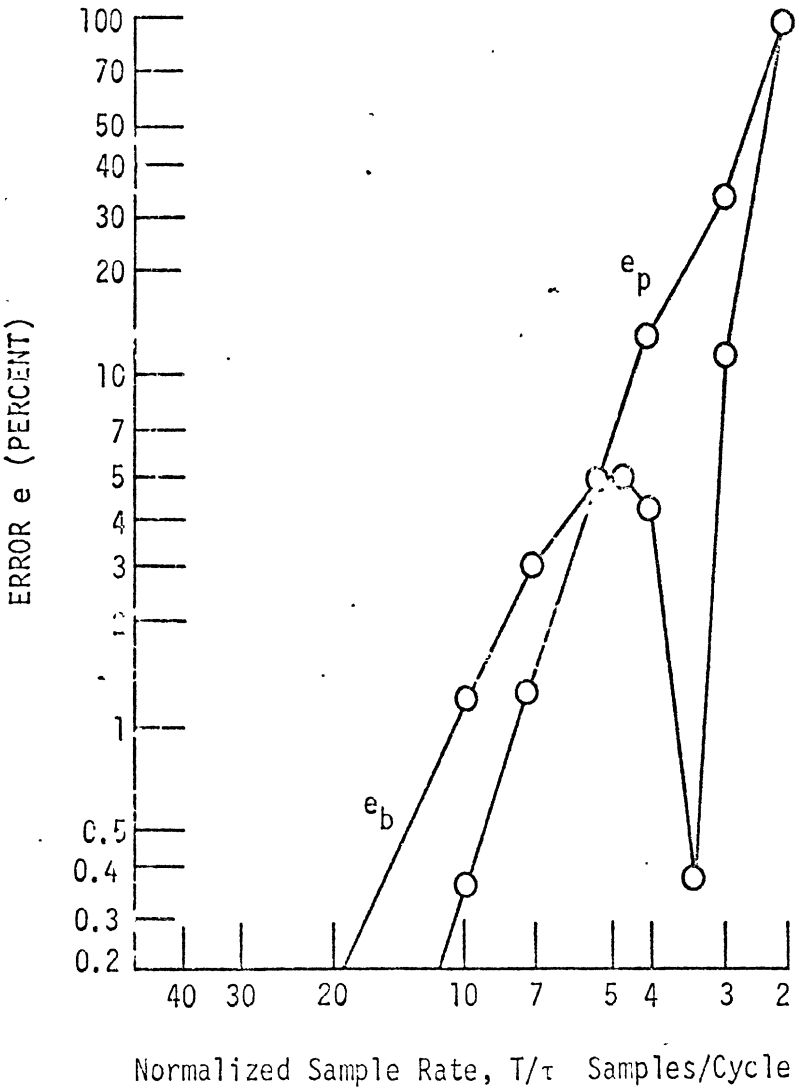

Figure 8. Errors Inherent in a Second-Order Digital to Analog Computer

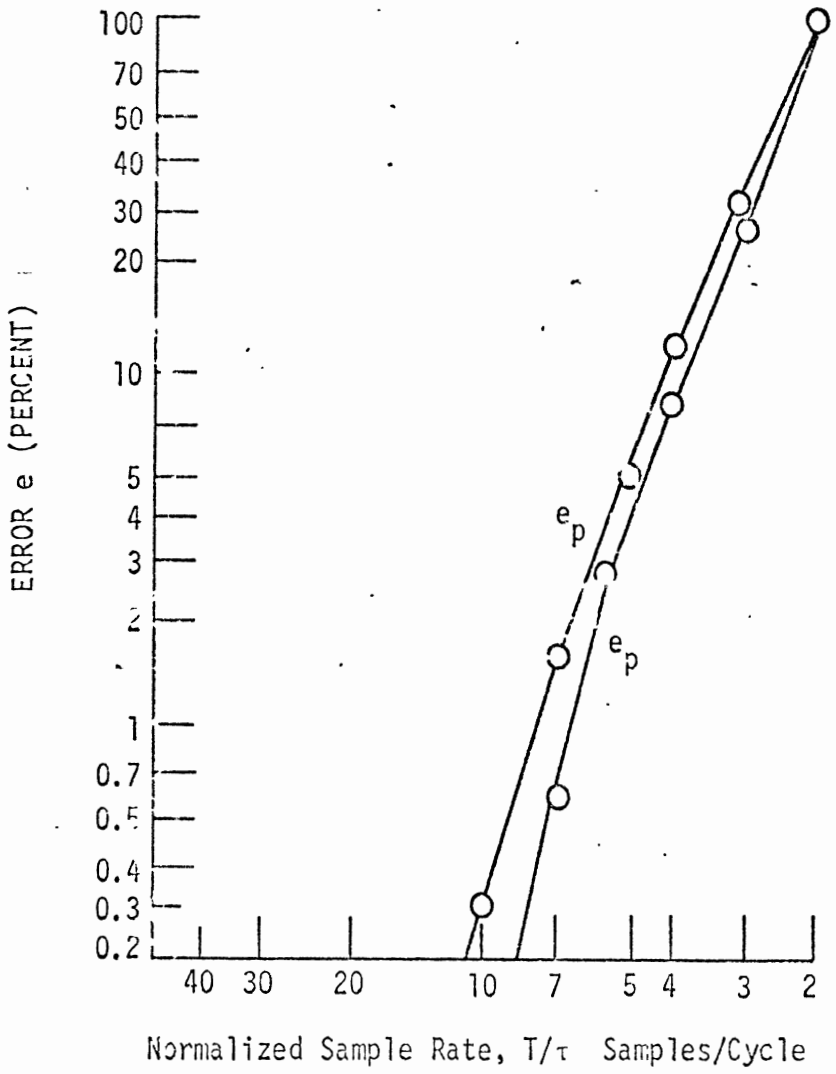

Figure 9. Errors Inherent in a Third-Order Digital to Analog Converter

The four criteria for judging the filter properties of accelerometers (and the other transducers) are low frequency response, high frequency response, output signal level, and phase shift properties. Low frequency response of strain gage or capacitance sensing elements is excellent and they may be considered flat to DC for most practical purposes. Crystal or piezoelectric elements are not generally suited for very low frequency measurements. Most are unsuitable for signals less than 2-20 hertz without substantial loss in amplitude.

High frequency response is one of the main attributes of piezoelectric accelerometers because of the higher natural frequency. However, modern piezoresistive strain gage and capacitive accelerometers can compete favorably in ranges suitable for vehicle crash testing (e.g. an accelerometer with a range of 250 G's can have a response from 0 to 2000 hertz $\pm$ 5%). The wire strain gage elements are distinctly limited in high frequency response.

Piezoelectric, piezoresistive, and capacitive elements are most often comparable when output signal is considered. A typical 250 G accelerometer might have an output of 10/millivolts/G. Again, wire strain gage accelerometers do not have this capability.

The output phase shift as a function of frequency is a major consideration in the selection of accelerometers. If the mass is damped to 0.7, linear phase shift is possible. Many piezoresistive and wire strain gage accelerometers can be supplied with these properties. Piezoelectric accelerometers are usually undamped resulting in zero phase shift over the practical frequency range. Great care shoudd be taken to purchase hardware with known linear or zero phase shift characteristics. If this is not possible, the phase shift as a function of frequency should be specified in order to allow comparison of data gathered at various test laboratories. Temperature variations can cause significant changes in damping coefficient and thus in linearity of phase response.

Specific properties of typical accelerometers are illustrated in a series of figures (10-15). The response of an oil-damped piezoresistive accelerometer is shown in Figure 10. It should be noted that the response is flat in the low frequency range but that temperature has a considerable effect on the high frequency range. The range of the affect on the linear phase response is illustrated in Figure 11. Without stating specific errors the effect of linear phase shift is shown in Figure 12. It should be noted that zero phase shift will yield a curve with the same shape and amplitude, but displaced in time. A piezoelectric accelerometer depends on the generation of a charge to cause a signal. As release of charge is a transient phenomenon, response to low frequency excitation is inherently limited. Figure 13 can be used in a discussion of low frequency response. The output voltage from the accelerometer will not remain constant since charge is dissipated when current flows through the circuit. An external capacitance, C_E, helps to reduce the rate of decay. Low-frequency response is determined by the value of the product R_L C_T (circuit time constant), in which R_L is the load impedance and C_T is total system capacitance. It should be noted however that a great increase in C_E reduces transducer sensitivity. Figure 14 shows a typical plot of output and phase shift as a function of frequency. The theoretical low-frequency response of a piezoelectric accelerometer with external capacitance using a charge amplifier is shown in Figure 15 where f is the frequency in hertz, R is the load impedance in ohms, and C is the total capacitance in farads. References 29, 30 and 31 contain further details.

4.1.7 Data Transmission

The fact that the transducer and the recording system are not in the same location leads to an additional set of filtering properties - those of data transmission. Three types will be mentioned: 1. Cable losses; 2. tribo-

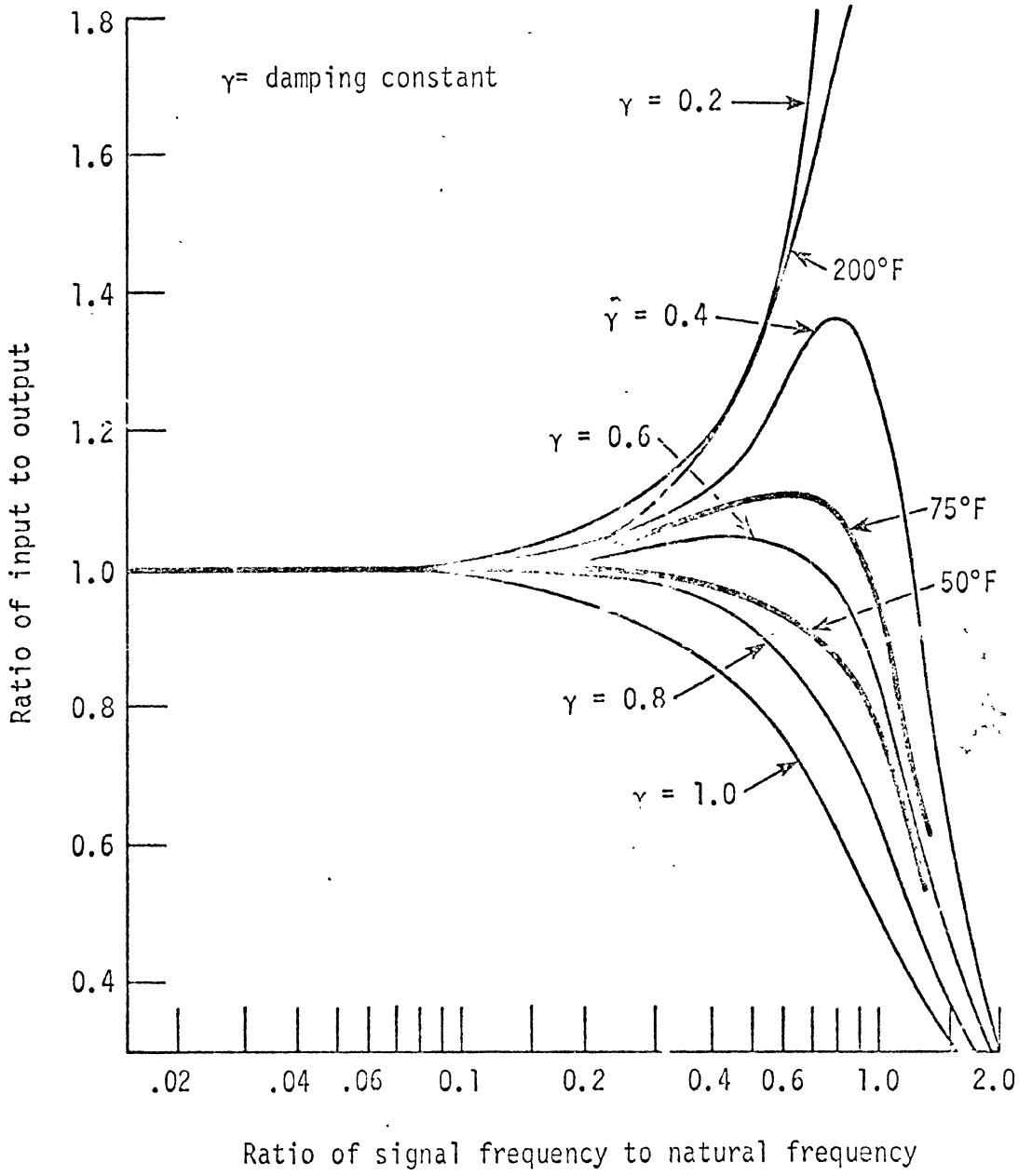

Figure 10. Frequency Response Characteristics of an Oil-Damped Piezoresistive Accelerometer.

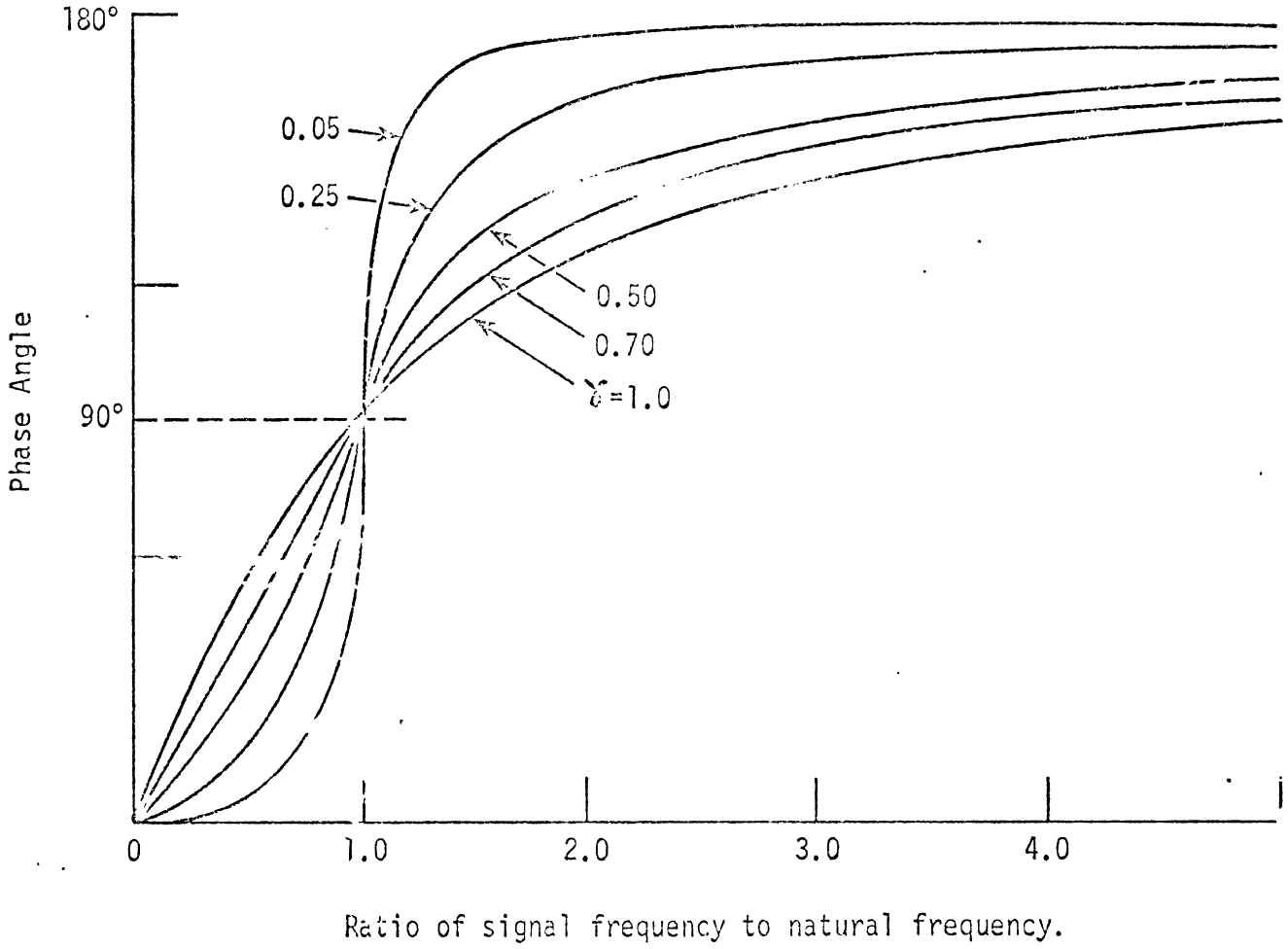

Figure 11. Phase Shift as a Function of Frequency Ratio and Damping Factor.

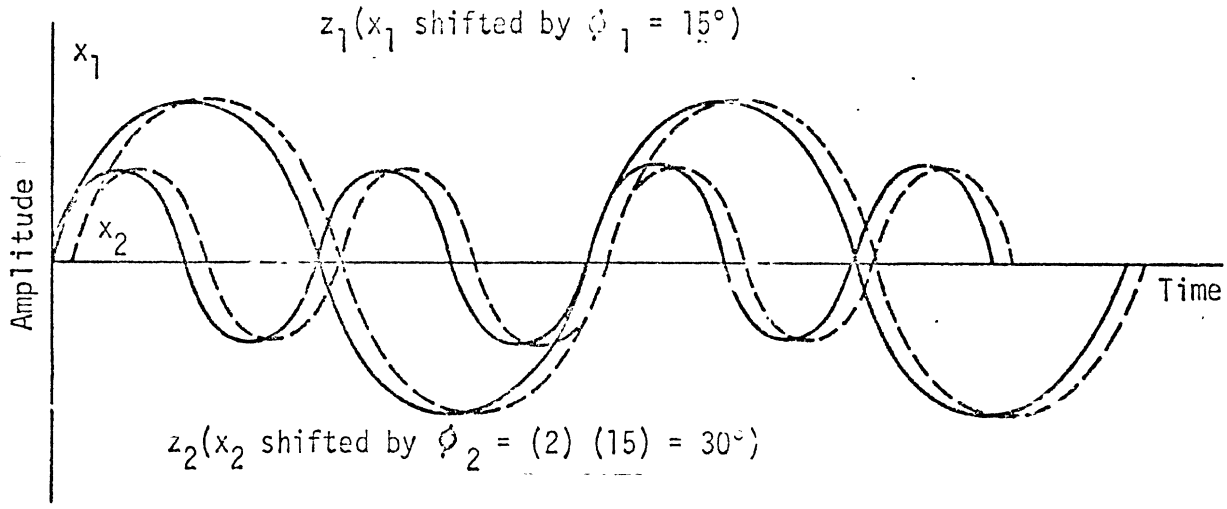

Figure 12. Effect of Linear Phase Shift

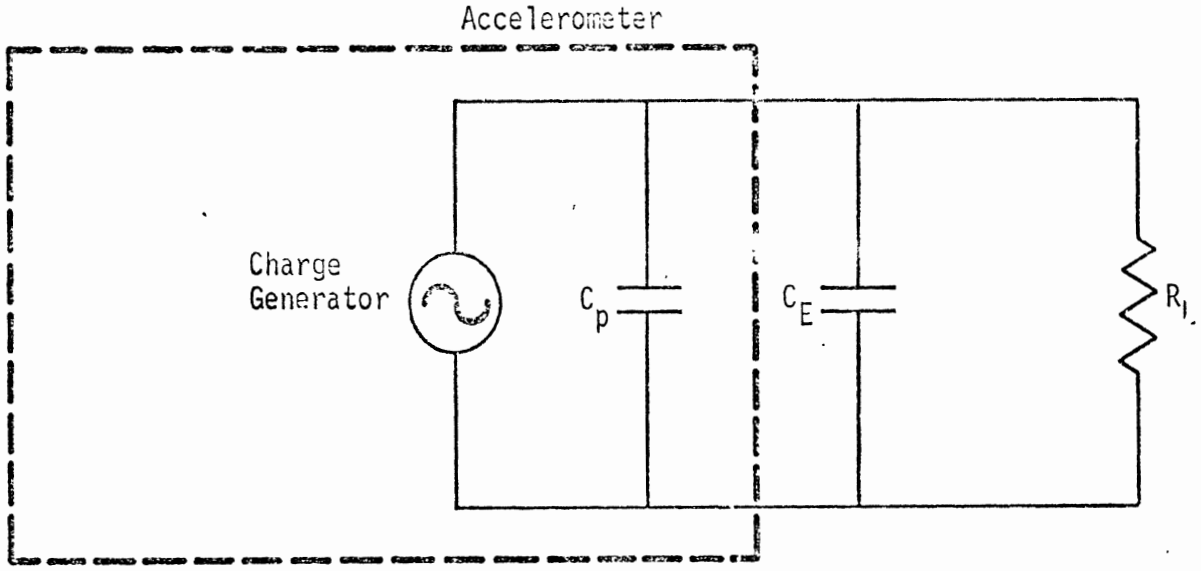

Figure 13. Piezoelectric Accelerometer, External Capacitance, and Load Impedance.

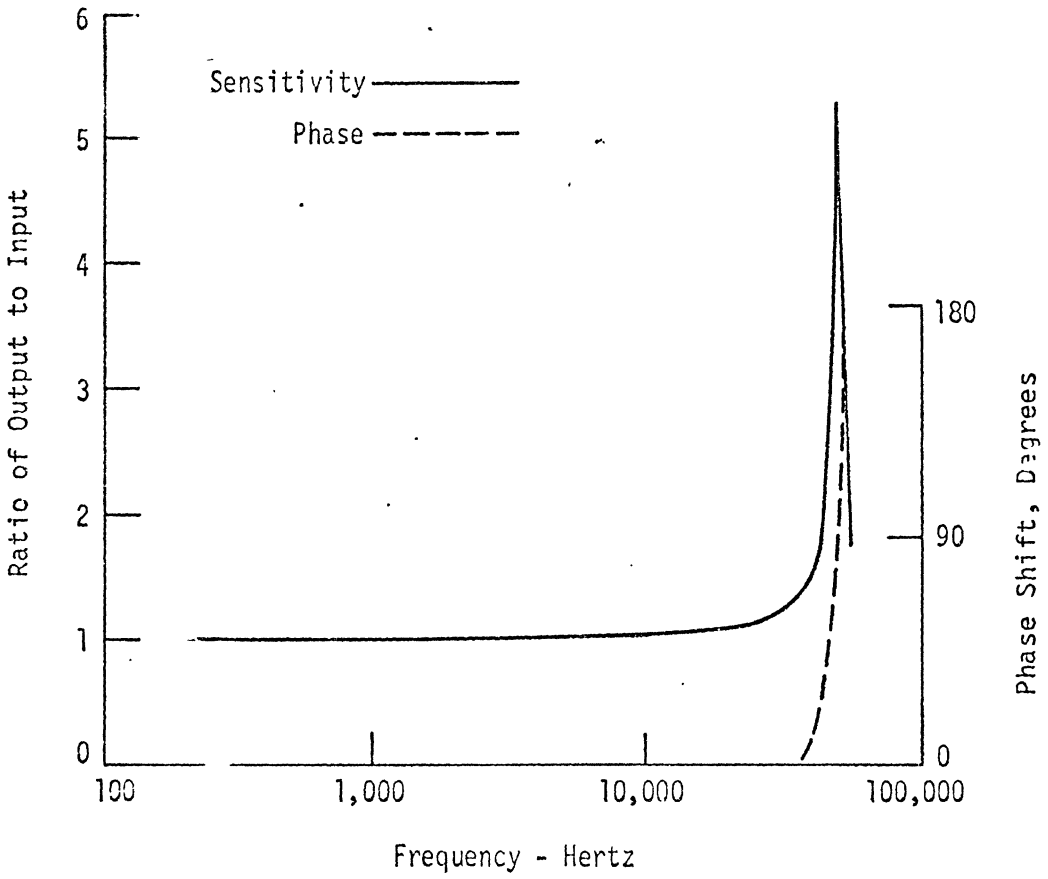

Figure 14. Sensitivity and Phase Properties of a Typical Piezoelectric Accelerometer.

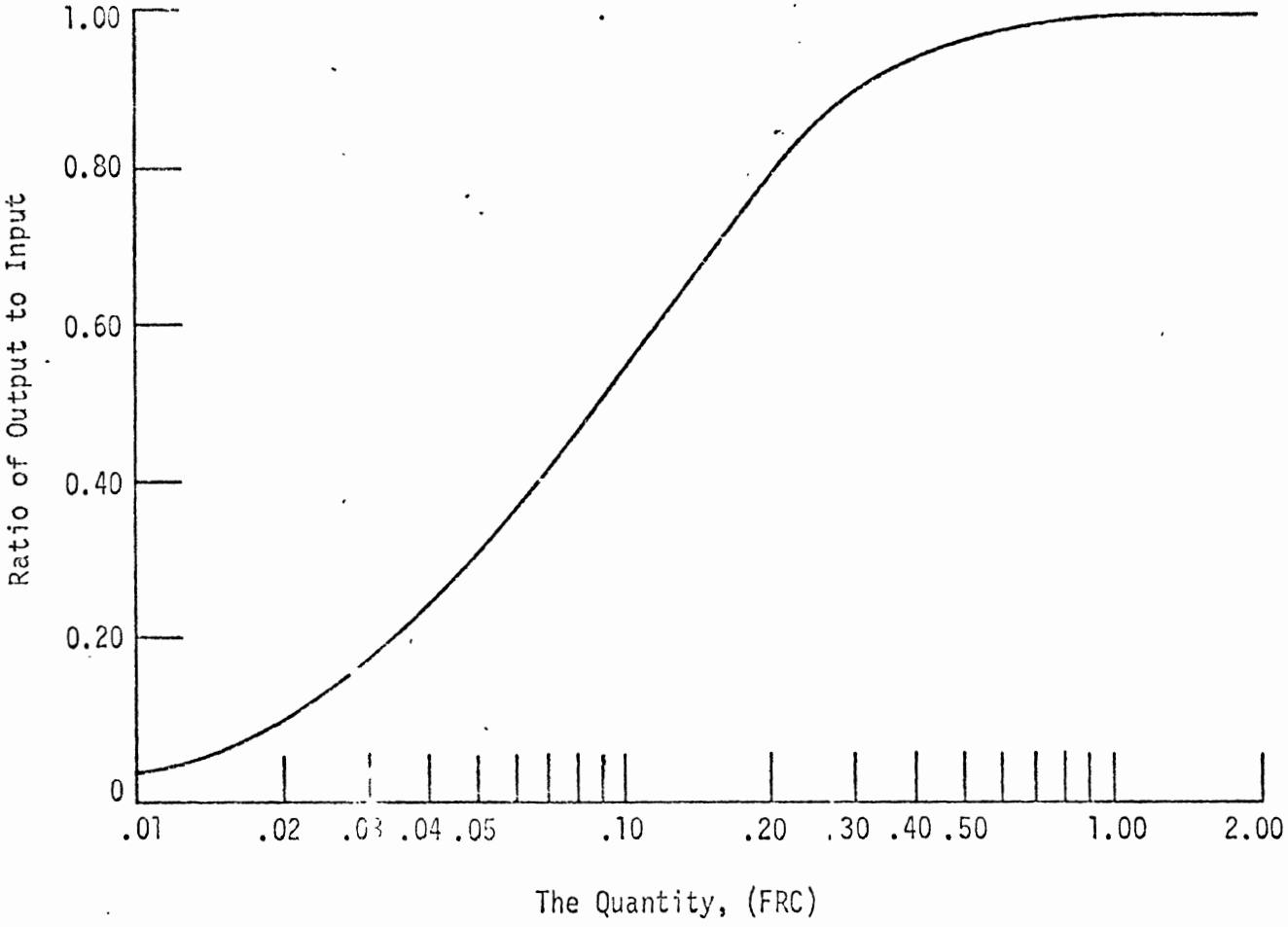

Figure 15. Low-frequency Response versus Loading for Piezoelectric Accelerometer.

electricity; and, 3. the effects of telemetering data.

The cable attaching the transducer to the recording system acts as a capacitor. The amount of capacitance varies almost directly with the length of the connecting cable. Therefore, accelerometer voltage output will vary inversely with cable length, and with variation in cable capacitance (not the case if a charge amplifier is used). Common accelerometer cables have capacitances between 20 and 30 picofarads per foot.

In the case of a crash impact test, the accelerometer cables are subjected to severe shock. Noise is often observed to be present in such cases which is related to the cable itself. Apparently this is generated between the cable conductor and its dielectric. Cable noise can result from friction. Also, momentary separations of the dielectric and the conductor can cause a change in the capacitance, and thus, a change in signal level (triboelectricity). In tests such as these, low-noise cables should be used.

An alternative to the use of umbilical cables in crash tests is telemetry The signal from the transducer is usually broadcast from the test vehicle using an FM transmitter. If signals are combined for transmission and recording by multiplexing, each signal has a different frequency response potential based on the carrier frequency used for each channel.

4.1.8 Signal Conditioning

A great variety of electronic signal conditioning devices can be placed between the transmission line or receiver and the data recording equipment. These include attenuators, [illegible] all of which possess varying filter characteristics. The purposes of these devices are two-fold: 1. provide an appropriate signal level to drive the recording device; and, 2. match the impedance of the signal source to that of the recording device.

Occasionally a transducer will produce a signal level too great to be handled by the recording system. An attenuator is added to the circuit to reduce the signal level. This is usually accomplished by adding shunt capacitance.

Many common transducers such as accelerometers are designed to be offered a much higher impedance than is offered by most recording devices. In this case it is necessary to insert a cathode- follower or charge-type preamplifier between the transducer and the recorder. For higher impedance loads a voltage-type preamplifier is used. A typical device shows an impedance of 1000 X 10^6 ohms to the transducer and gives 10 volts to a 10 Kohm or higher load. For lower impedance loads a current-type preamplifier is used. A typical device shows similar impedances and output voltages, only into a 1000 ohm or less load.

Although not generally recommended, low pass filters are sometimes added to the circuit before the signal is recorded. These active electronic filters have been discussed previously.

Many of the companies which produce transducers also provide signal conditioning equipment to be used with their products. A typical example can be provided by the Endevco Model 4640 VBR system amplifier for use as a signal conditioner and amplifier for prezoresistive accelerometers.

It features a wide frequency response (0.2 to 5000 Hz). The source impedance is 5000 ohm, maximum, the resistive load is 2500 ohm maximum, the output voltage is ± 10 volts maximum, etc. The frequency response is ± 2% from 0.2 to 5000 hertz with a standard filter included in the circuit. At the low end, the signal is down 3db at 0.03 hertz with a 6db/octave rolloff, at the high end, the active, 2-pole, Butterworth filter is down 3dB at 20 kHz with a 12db/octave rolloff. The phase response of this device is shown in Figure 16 indicating the necessity of taking it into account in certain higher frequency applications.

4.1.9 Data Recording and Playback

A conditioned signal can take one of several routes. It can be recorded for later playback or it can be recorded as a permanent visual record. Both techniques are in common use in the gathering of crashworthiness test data. A summary of a few of the important properties will be given for each of the following record and/or playback systems: 1. direct record tape recorder; 2. FM tape recorder; 3. digital tape recorder; 4. light beam oscillograph; 5. heat pen strip chart recorder; and, 6. ink pen strip chart recorder. Each of these devices has a variety of signal manipulating electronic or electro-mechanical circuits which act as filters.

Direct recording is the process most commonly used to record audio signals. Although it has very high frequency response, it is distinctly limited in the lower range. Signals with a frequency of 250 Khz can be recorded but care must be taken to find a system which can handle signals less than 50 hz. Direct recording is not commonly used in structural crashworthiness testing.

Probably the most commonly used technique is the eight or nine track FM tape recorder. The response is very appropriate for most crashworthiness

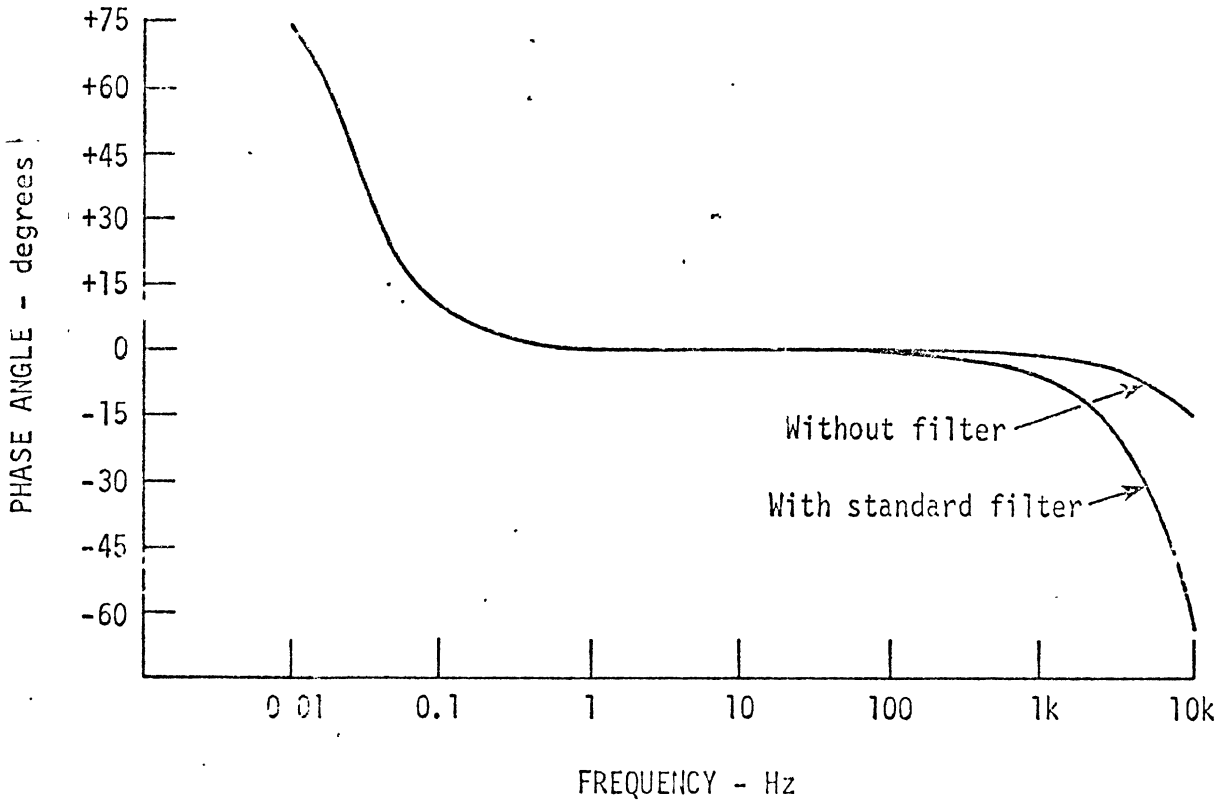

Figure 16. Typical Phase Shift Characteristics of Endevco Model 4640 Signal Conditioner.

testing and can range from 0.2 to 10,000 hz with little error. The tape signal can then be played back to a recorder producing a visual record or it can be digitized for sophisticated computer processing.

A procedure becoming increasingly common is the use of digital tape recording and other digital procedures. Digital tape recording results in a tape which can be processed by a computer, or in some large installations, the digitized signal can be processed directly by the computer while the test proceeds. There are several limitations to frequency response which might be considered but which can be solved.

The primary limitation is the sampling rate of the analog to digital converter. As the signal must be discretized, the same rules apply as have been discussed earlier in the section on digital filters. Sampling rates as high as 100 Khz are available. This corresponds to a signal of about 20 Khz being discernible. The digitizing system being used in the HSRI impact sled laboratory can sample at 5 Khz to minimally handle a 1000 hz signal.

A second limitation is related to the mechanics of the tape recorder itself. The analog to digital converter samples the analog signal and most commonly produces an eight-bit binary code for the signal. This is equivalent to almost a three digit number, adequate for most purposes. Each eight-bit group or word is strung across the tape. The words are then strung along the length of the tape for later playback onto a digital computer and analysis. Digital tapes are usually limited to 1000 BPI (bits/inch). If maximum tape speed is 120 in/sec, 120,000 bits can be recorded in a real time second. This corresponds to 15,000 words per second approximating a 3000 hz filter. The basic assumption is that the analog signal is digitized and fed to the recorder continuously using all channels. Digital

tape hardware is thus rather severely limited frequency-wise when compared with real time FM recorders when used as a real-time device.

Although limited to 20 khz by the analog to digital converter, digital tape systems are capable of [illegible] and complex data when coupled with permanent magnetic storage in a small computer. In this case, the digitized signal from one or many channels is fed to the permanent storage. Each channel may have a response of 20 khz if it is required. As the storage is filled, the tape is filled at a slower rate. The data words from several channels can be fed in sequence thus using a single tape to handle as many channels as desired. This extremely flexible system (which could eventually eliminate tape entirely in favor of a portable magnetic storage disc pack) is probably the best and most flexible available today especially for tests where complex data analysis is required.

The last three types of devices to be discussed produce a visual record These are the light beam oscillograph, the heat pen strip chart, and the ink pen strip chart They are listed in order of decreasing frequency response - 0-20 khz for the light beam oscillograph, 0-150 hz for heat pen strip charts, and less than 5 hz for ink pen strip charts. The frequency response is limited by the mass of the electromechanical system. Galvanometers for light beam oscillographs involve small motions of an extremely light-weight mirror reflecting a beam onto a moving strip of light-sensitive paper. The stylus of the heat pen is heavier and produces its trace on heat sensitive paper. The heaviest and slowest is the standard ink pen. The advantages of these systems are the permanence of the record, especially in the case of the ink pen. The disadvantage is the inability to reproduce or analyze the data in any other form once the record is completed. Most

often these devices are connected to the playback of a tape recorder which is run at slow speed so as not to exceed the frequency capacity of the strip recorder. Often times the tape output is filtered before the permanent record is produced.

Galvanometers in light beam oscillographs serve as very effective filters and are designed with that function in mind. The cutoff frequencies and rolloff of a group of Honeywell galvonometers is shown in Figure 17 (See Reference 32). The damping characteristics of the electro-mechanical elements are ideally chosen to yield a linear phase shift. The transient distortion ideally available with CEC galvanometers with 0.64 damping and which results in linear phase distortion is shown in Figure 18 (See Reference 33).

4.1.10 Specifications

The survey of specifications has been limited to SAE J211a (Reference 34) which is widely used as a guideline in restraint system and vehicle crashworthiness testing. Its aim is "to achieve uniformity in instrumentation practice and in reporting test results, without imposing undue restructions on the performance characteristics of the individual elements in an instrumentation or data analysis system."

Several classes of low-pass filters are defined by the specifications given in Figure 19 and Table 7. The only properties of filters which are included

TABLE 7. FREQUENCY RESPONSE VALUES

Channel Class	L Hz	a dB	H Hz	b dB	N Hz	c dB	d dB/ octave	d dB/ octave	g dB
1000	0.1	+1/2,-1/2	1000	+1/2,-1	1600	+1,-4	-6	-24	-30
600	0.1	+1/2,-1/2	600	+1/2,-1	1000	+1,-4	-6	-24	-30
180	0.1	+1/2,-1/2	180	+1/2,-1	300	+1,-4	-6	-24	-30
60	0.1	+1/2,-1/2	60	+1/2,-1	100	+1,-4	-6	-24	-30

in this recommended practice apply to frequency response. Details are not included with regard to signal phase distortion or other types of distortion.

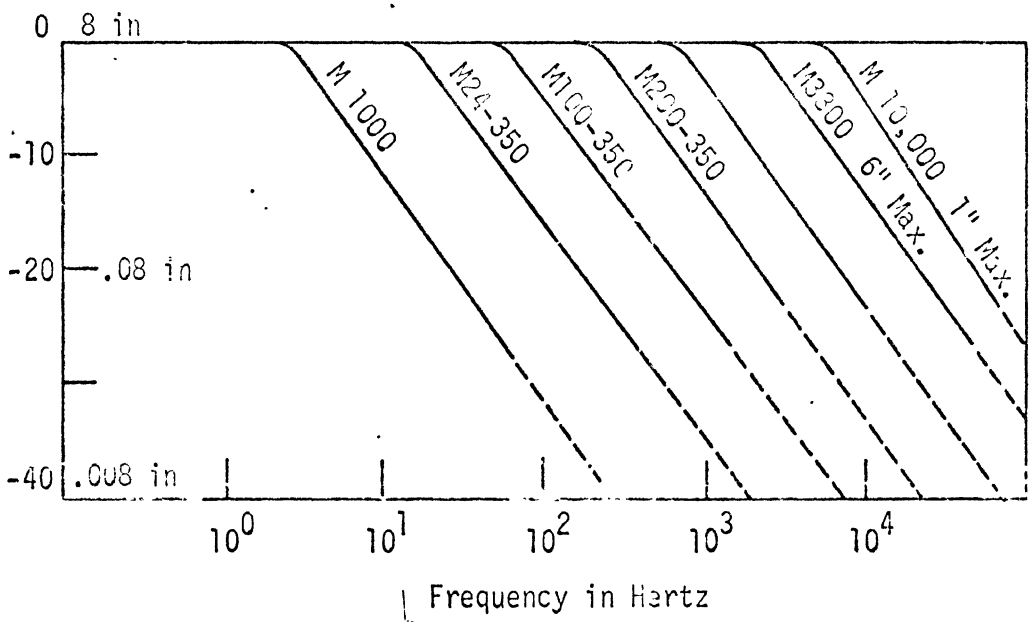

Figure 17. Filter Properties of a Group of Galvanometers

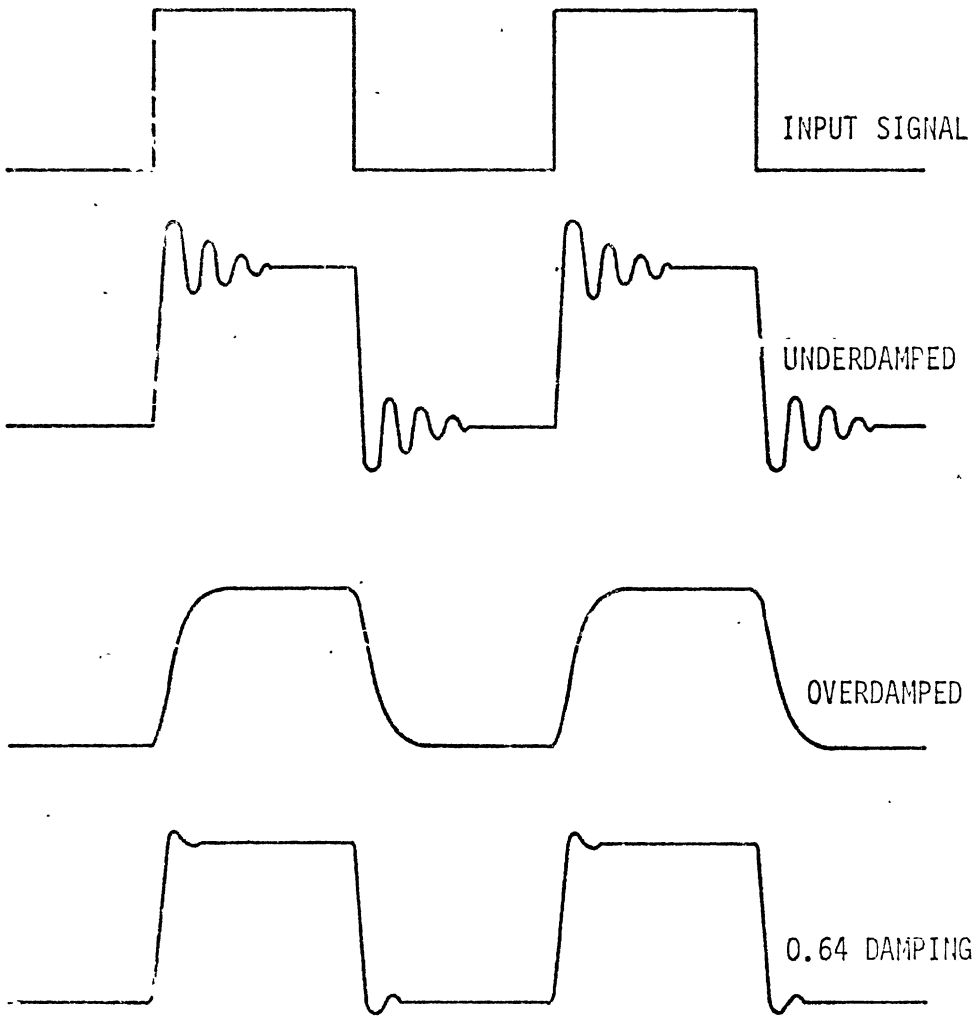

Figure 18. Transient Distortion Using Galvanometers

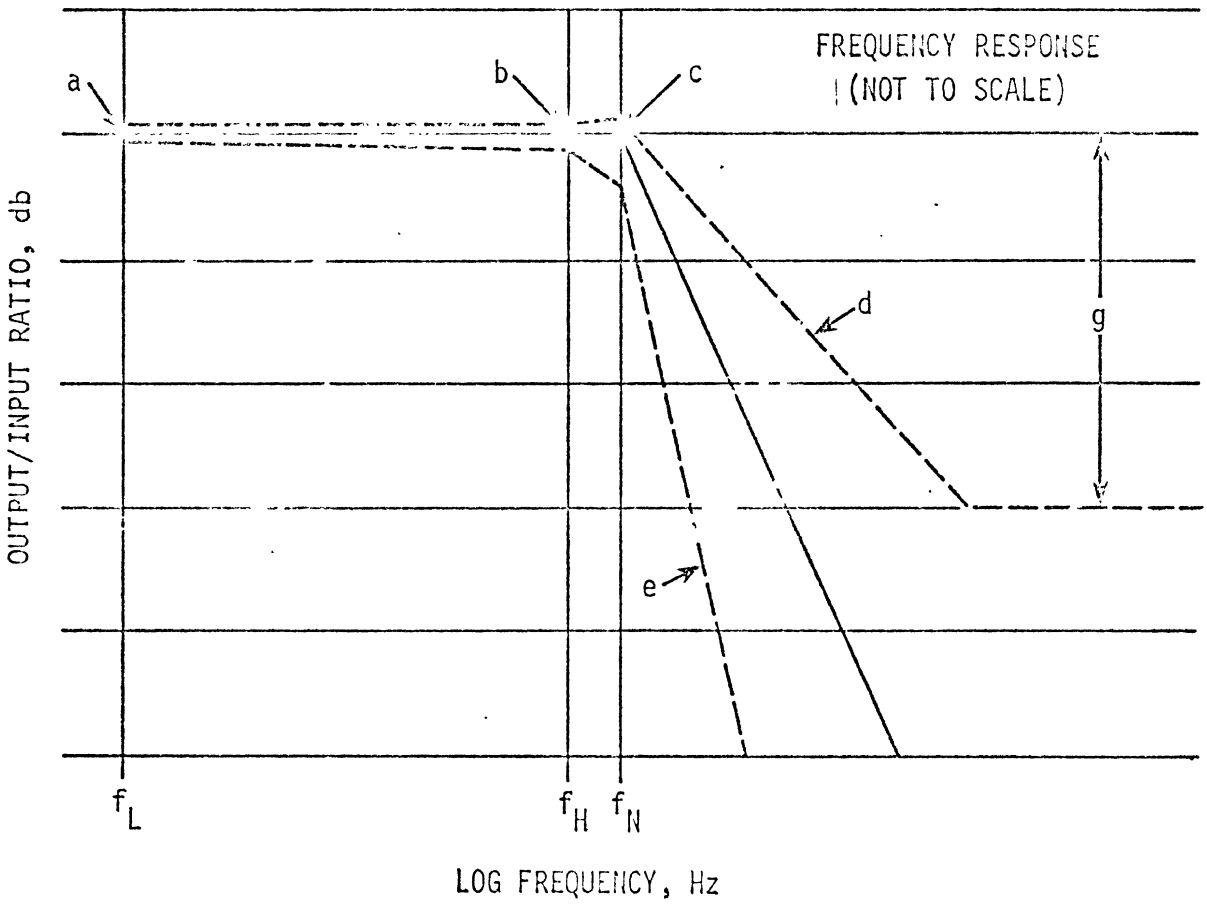

Figure 19. SAE J211a Filter Specifications

Some examples of the implications of SAE J211a are given in Section 4.3 of this report which follows.

4.2 COMPARISON OF SIGNALS

A variety of techniques may be employed to compare signals. The two signals which are to be compared may result from an analytical procedure and an experiment. Another application would be to define filter properties using an input and an output signal.

The simplest technique which is most often used in comparisons of crash test data involves visual comparison of the two signals. A simple, but arbitrary, three point rating system could be used in this type of an analysis:

1. The signals are dissimilar;
2. The signals agree in their basic features (similar hills and valleys), and their magnitudes are within 30%;
3. All aspects of pulse shape and phase are very similar in detail, and magnitudes do not vary by more than 10% at any point in time.

A rating of 2 on the above scale is often considered to reflect good agreement between two sets of crash test data. A rating of 3 stretches the state of the art in both crashworthiness testing and safety development testing involving dummies.

A potentially superior procedure which eliminates user visual judgement is to perform an analytical waveform comparison of the two pulses to isolate the degree of distortion, phase shifts, and amplitude differences which may exist. Bode plots can be used to study magnitude and phase when the crash test pulse is extended so it can be represented as a periodic function as shown in Figure 20. Average or mean-square distortion can also be determined analytically.

Left f(t) and g(t) be two signals which are to be compared. They can be expressed in Fourier series as

$$f(t) = \frac{a_0}{2} + a_1\cos\omega_1 t + a_2\cos\omega_2 t + \ldots + a_N\cos\omega_N t$$

$$+ b_1\sin\omega_1 t + b_2\sin\omega_2 t + \ldots + b_N\sin\omega_N t$$

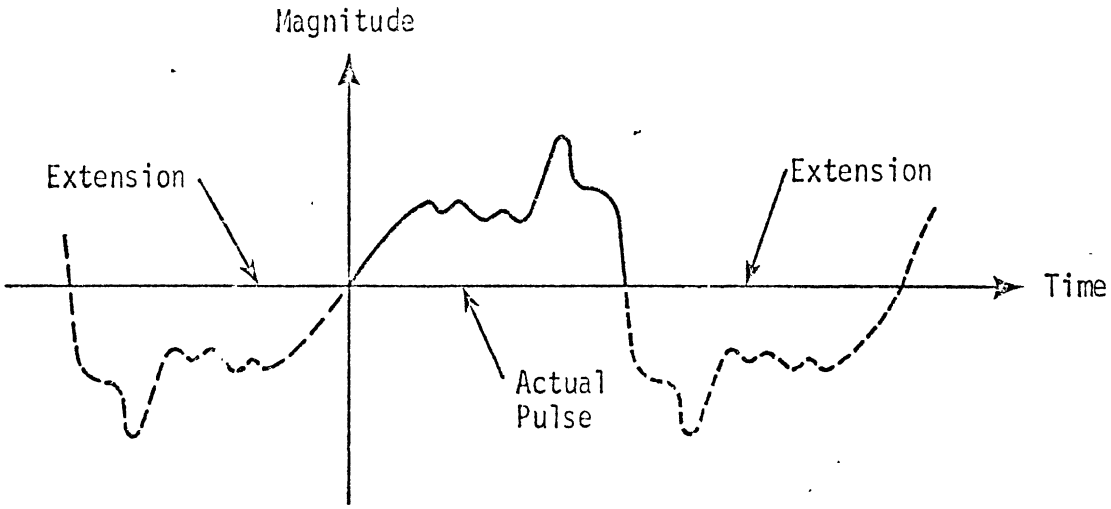

Figure 20. Expansion of Crash Test Pulse to a Periodic Form

$$g(t) = \frac{A_o}{2} + A_1\cos\omega_1 t + A_2\cos\omega_2 t + \ldots + A_N\cos\omega_N t$$

$$+ B_1\sin\omega_1 t + B_2\sin\omega_2 t + \ldots + B_N\sin\omega_N t$$

where N is the highest harmonic included in the analysis. If f(t) and g(t) consist of discrete sets of data points, then N depends on the number of data points. If f(t) and g(t) are continuous, then it should be selected based on expected frequency content. The coefficients a_o, a_1,...,a_N,b ,...,etc., can be computed based either on discrete or continuous data sets as discussed by many authors (See Hildebrand, Reference 16 for a typical reference). The errors inherent in truncation can also be computed and studied which should be a standard procedure in signal comparisons using this technique.

The functions f(t) and g(t) can be rewritten as

$$f(t) = \frac{a_o}{2} + C_1\sin(\omega_1 t+\phi_1) + C_2\sin(\omega_2 t+\phi_2)t$$

$$\ldots + C_N\sin(\omega_N t+\phi_N)$$

$$g(t) = \frac{A_o}{2} + D_1\sin(\omega_1 t+\Phi_1) + D_2\sin(\omega_2 t+\Phi_2)t$$

$$\ldots + D_N\sin(\omega_N t+\Phi_N)$$

where

$$C_i = \sqrt{a_i^2 + b_i^2} \qquad \phi_i = \tan^{-1}\frac{a_i}{b_i}$$

$$D_i = \sqrt{A_i^2 + B_i^2} \qquad \Phi_i = \tan^{-1}\frac{A_i}{B_i}$$

Plots of amplitude ratios and phase shifts (Bode plots) can then be prepared to compare basic properties of the two signals. Schematics of these plots are shown in Figure 21.

Another technique for the analytical comparison of two waveforms is through the measure of distortion. Again let f(t) and g(t) be two functions to be compared. In this case they are defined for $0 \le t \le T$ and are zero for $t > T$.

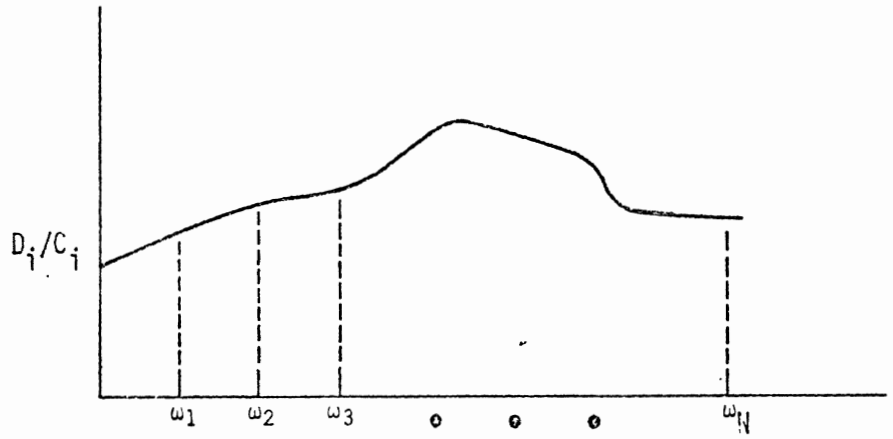

Amplitude Ratio Plot

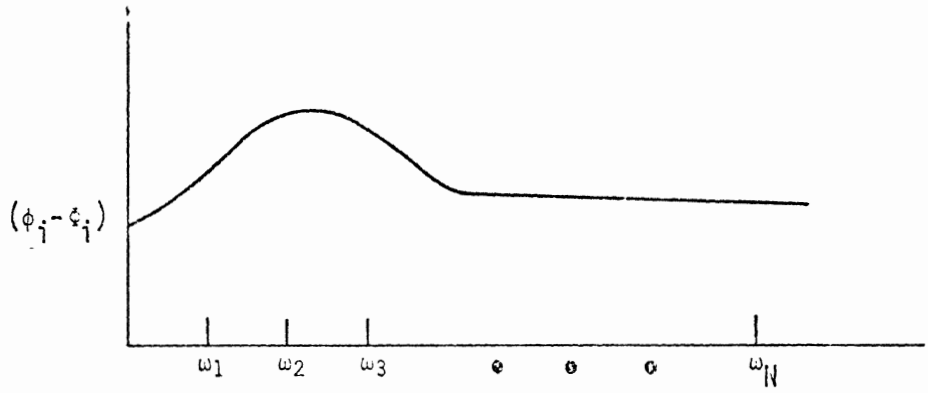

Phase Shift Plot

Figure 21. Schematic Amplitude Ratio and Phase Shift Plots.

In the case of discrete data as might be produced using analytical procedures or read from a continuous data trace the percent average distortion is defined as

$$D_A = \frac{\sum_{n=0}^{N} |f(n\Delta t)-g(n\Delta t)|}{\sum_{n=0}^{N} |f(n\Delta t)|} \times 100$$

where N + 1 is the number of data points and Δt is the time increment. For continuous functions,

$$D_A = \frac{\int_0^T |f(t)-g(t)|dt}{\int_0^T |f(t)|dt} \times 100$$

To accentuate the comparison in terms of mean squares, the following relations can be used for discrete data sets.

$$D_{MS} = \frac{\sum_{n=0}^{N} [f(n\Delta t)^2-g(n\Delta t)^2]}{\sum_{n=0}^{N} [f(n\Delta t)]^2} \times 100$$

For continuous data,

$$D_{MS} = \frac{\int_0^T [f(t)-g(t)]^2 dt}{\int_0^T [f(t)]^2 dt} \times 100$$

The techniques just presented are intended to demonstrate some of the relatively simple tools which are available for analytical waveform comparison. Several of the potential applications of these procedures are: 1. development of an objective procedure for comparisons of tests representing the same physical event; 2. development of an objective procedure for validating the predictions of mathematical models and correlating the predictions with test results; and 3. defining range of performance criteria for the control of state variables in impact tests.

4.3 EXAMPLE COMPARISONS OF FILTER PERFORMANCE

In order to demonstrate physically how different filters affect an input signal, a small computer program was written to operate on the pulse

$$P = C_1 \sin(\omega_1 t+\phi_1)+C_2\sin(\omega_2 t+\phi_2) + C_3\sin(\omega_3 t+\phi_3) + C_4\sin(\omega_4 t+\phi_4)$$

Input data for the program are initial and filtered amplitudes (C_1,..., C_4), frequencies (ω_1,...,ω_4), phase shift (ϕ_1,...,ϕ_4), and time. Output from the program were tabular listings and Calcomp plots of amplitude versus time for the filtered pulse. The examples were selected to illustrate: 1. the range of filter performance allowed under SAE J211a; 2. the effect of filter hardware on an input signal; 3. the effects generated by different types of filters on the same signal; 4. the effects of phase shift; and, 5. the effects of series filtering.

The baseline test pulse shown in Figure 22 is represented by the formula

$$P = 25\sin(5t)+25\sin(15t)+12.5\sin(50t)+12.5\sin(500t)$$

This pulse contains many features of crash deceleration pulses found in the literature. The fundamental frequency is 5 hertz. The resulting sine wave rises to an amplitude of 25G's at 50ms and is reduced to zero at 100ms. A third harmonic component (15 hertz) is superimposed which suppresses the middle of the 5 hertz pulse yielding a signal with two peaks reminiscent of crash pulses. The 50 and 500 hertz pulses sample the frequency spectrum in ranges often yielding major components of the crash pulse. Amplitude is reduced to 12.5G's for these components.

Figure 23 shows the results when the SAE J211a filter limits (Class 60 filter) are applied to the baseline pulse. It should be noted that the upper bound on the Class 60 filter has little effect even on the 500 hertz pulse because of the gradual rolloff. A substantial drop in average amplitude can be noted when the lower limit is applied as represented by the dotted line on Figure 23.

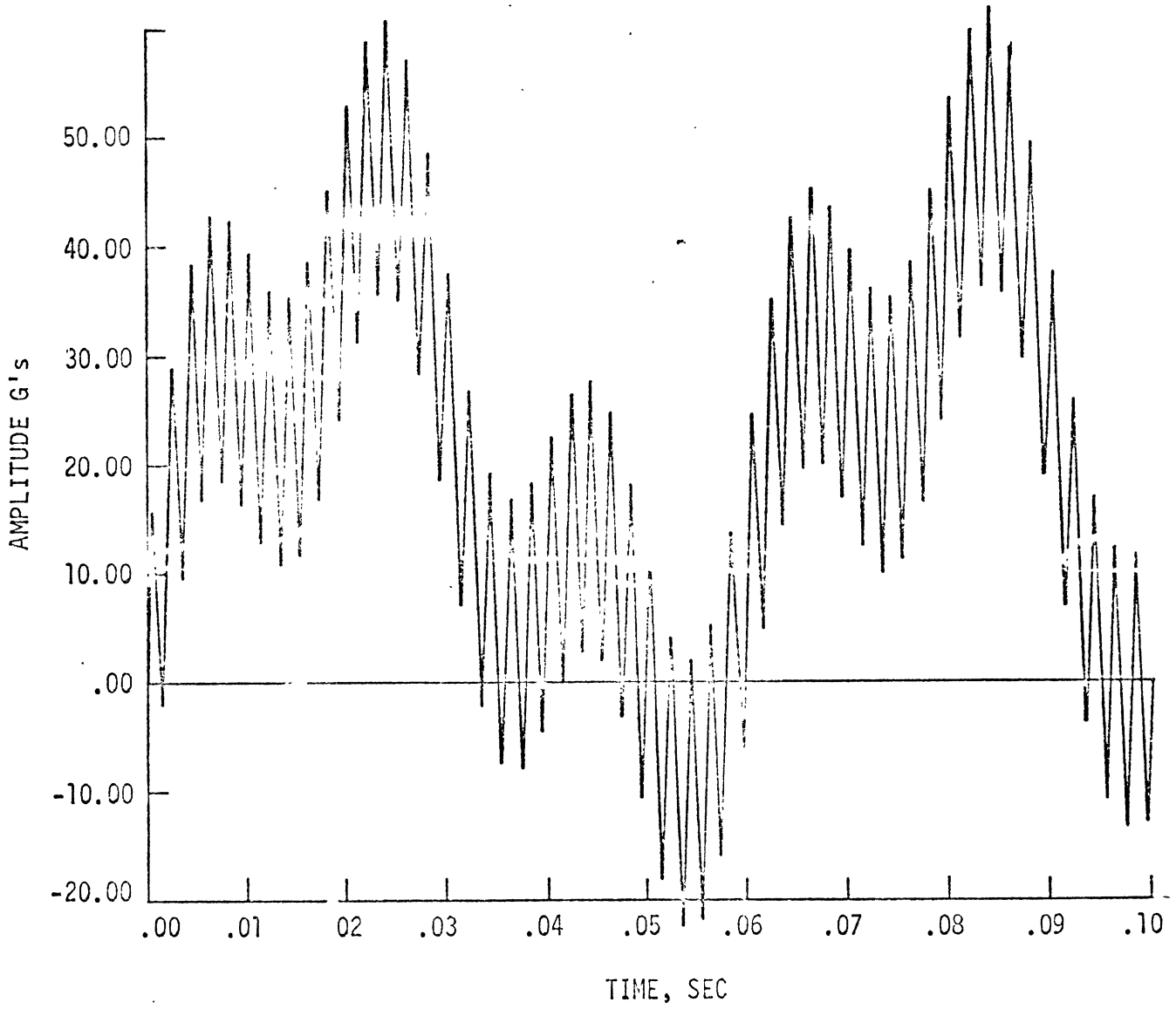

Figure 22. Baseline Example Test Pulse

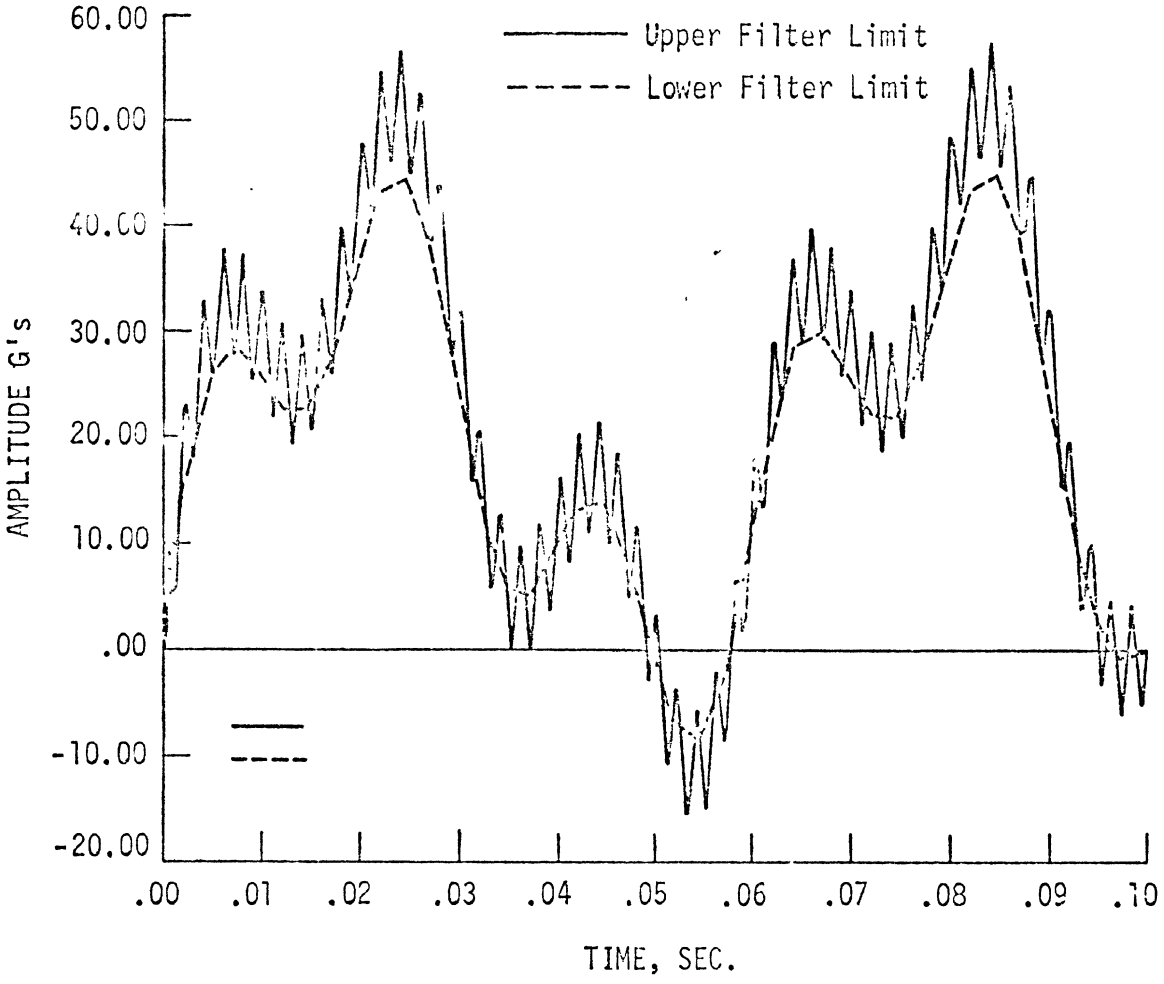

Figure 23. Upper and Lower SAE J211a Filter Limits Applied to Baseline Pulse.

Figure 24 shows the effect of a 3-pole Bessel filter with a 60 hertz cutoff frequency on the baseline pulse. The amplitude and phase response of this filter are shown in Figure 4. The effective reduction of the high frequency component and the nearly linear phase shift of the pulse can be noted. The phase shift must be known accurately if data from accelerometers subject to the variety of filters inherent in any electronic data acquisition system are to be time correlated with high speed motion picture data. The phase shift in this example is about 7ms.

Figure 25 compares the filtering of the 60 hertz Bessel filter described above with that of a 3-pole Butterworth filter with a 60 hertz cutoff. These two types of filters are in common use at crash test facilities. The characteristics of the Butterworth filter are shown in Figure 3. THe Butterworth filter has a sharper rolloff but its phase shift properties are not as linear as the Bessel filter. The differences are easily observed in Figure 25 in that the phase shifts are different for the two filters and the 50 hertz oscillation is suppressed more in the Bessel filter than the Butterworth even though 60 hertz has been selected as the cutoff value.

Figure 26 and 27 evaluate the effect of phase shift on filter performance. Figure 26 shows the performance of the 60 hertz Bessel filter with its nearly linear phase shift as a dotted line. The solid line on the curve represents the same changes in amplitude of the four sine components of the baseline pulse but with zero phase shift. It should be noted that some filter hardware is built with zero phase shift and also that many digital computer processes yield zero phase shift. The shape of the pulse is affected by the presence or lack of a phase shift as is shown in Figure 27. That figure superimposes the two curves to illustrate this major effect.

The application of filters in series can lead to different versions of the same test data. A hypothetical case where this may occur is in the playback of test data. First, an "unfiltered" signal is recorded on tape.

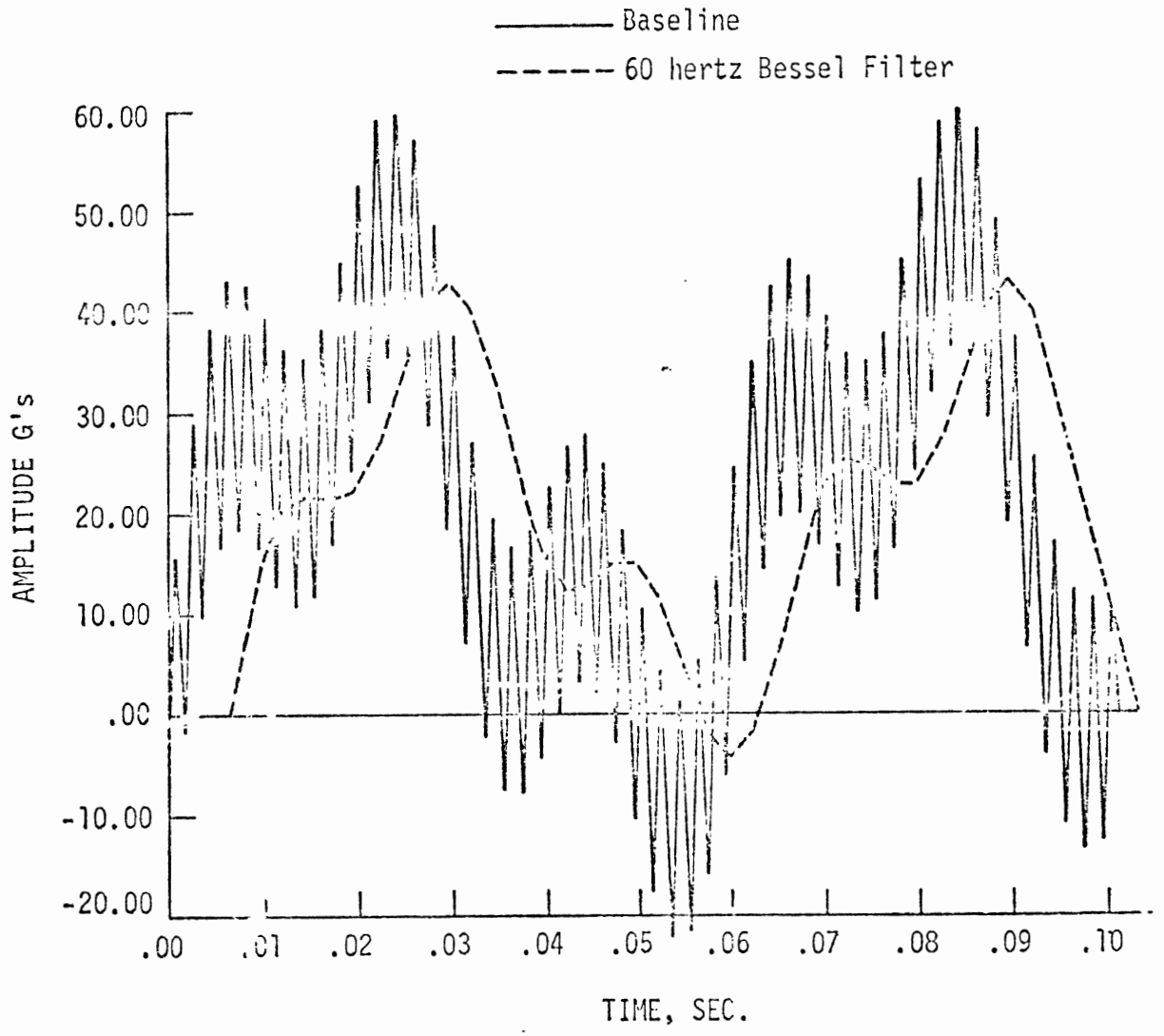

Figure 24. Effect of Bessel 60 hertz Filter on Baseline Signal.

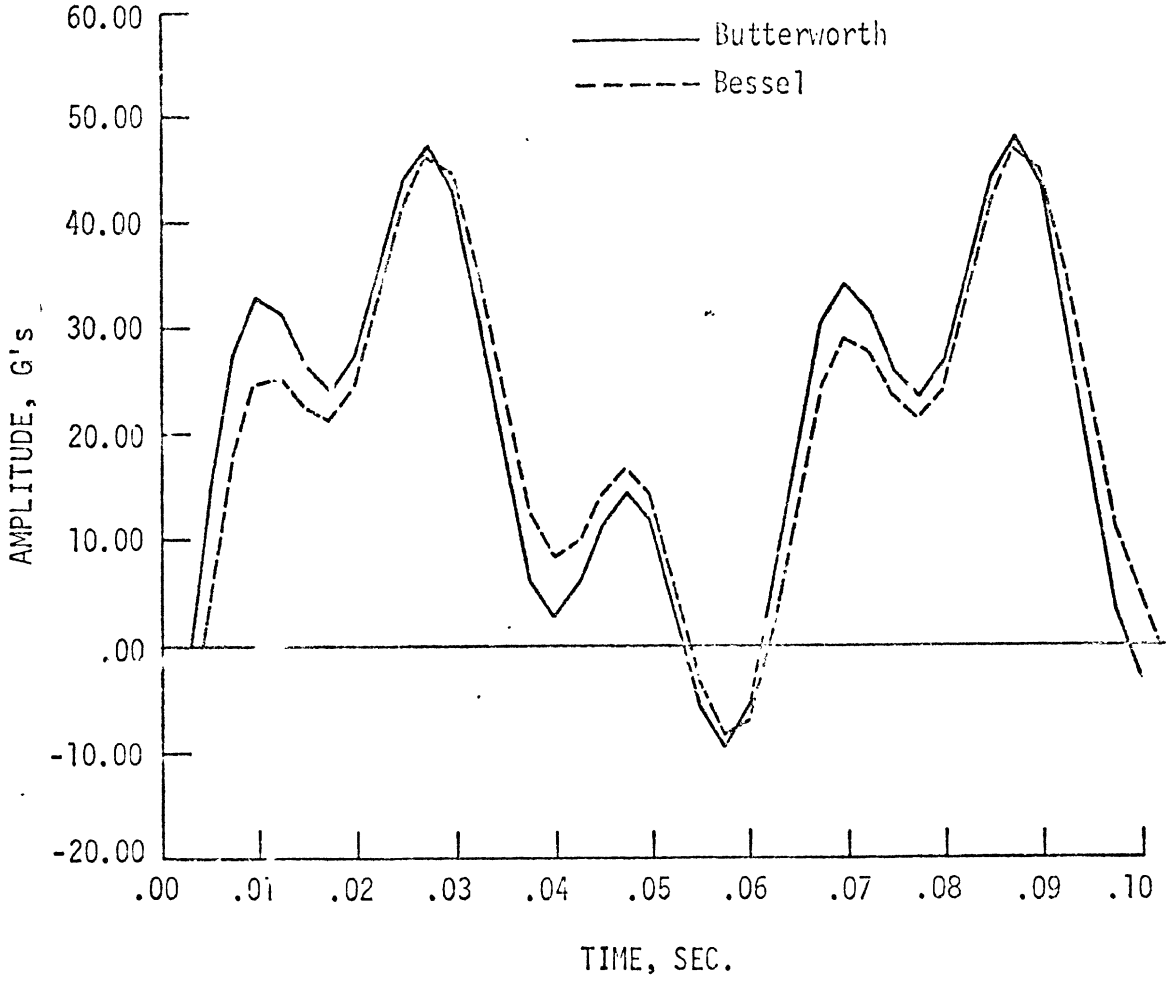

Figure 25. Effect of Bessel and Butterworth 100 hertz Filters on Baseline Signal.

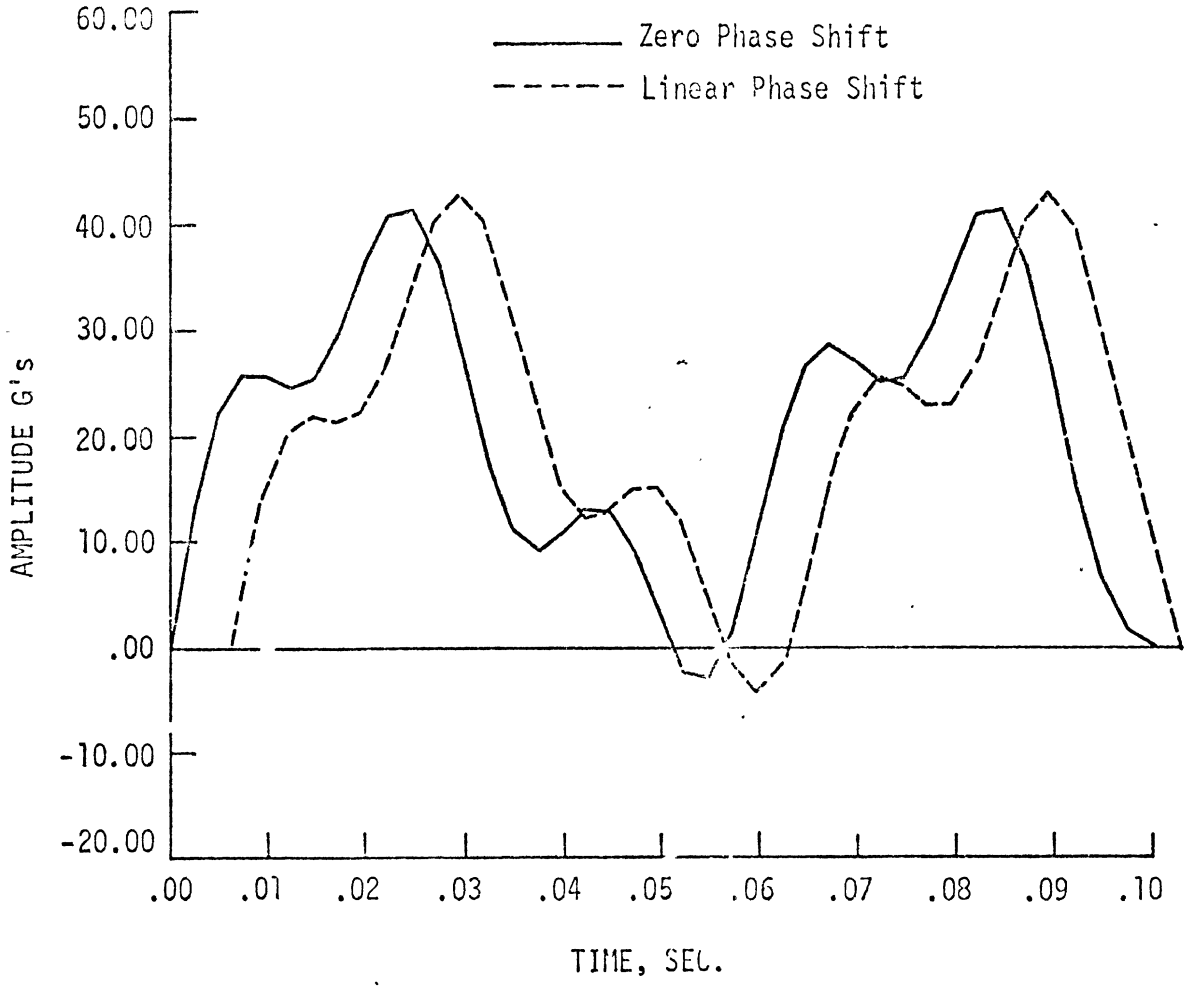

Figure 26. Comparison of Bessel 60 hertz Filters with Linear and Zero Phase Shift.

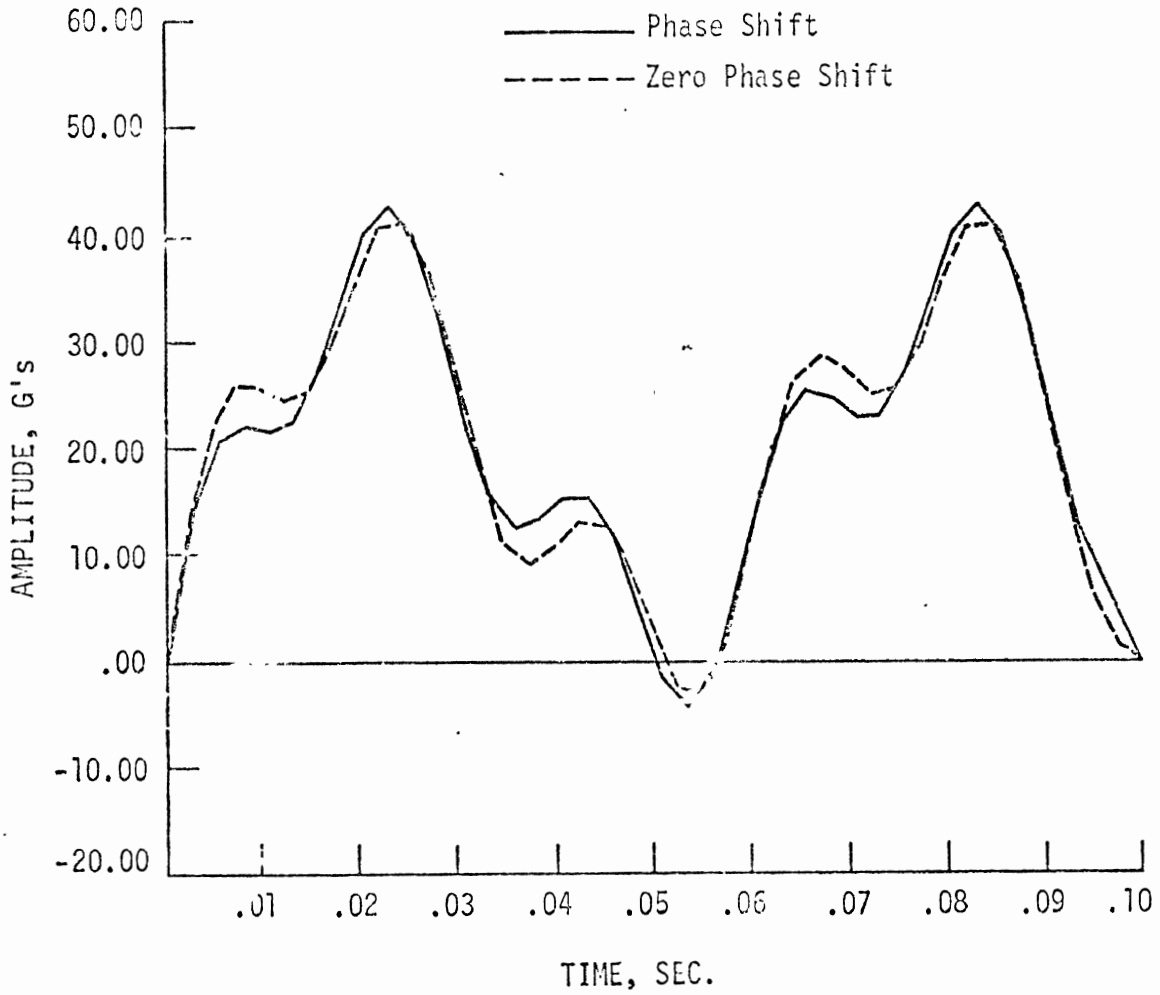

Figure 27. Superposition of Bessel 60 hertz Filters with and without Phase Shift to Show the Effect on Wave Shape.

Second, it is played through a filter into a light beam oscillograph where a quickly-obtained record can be reviewed (and often published subsequently in the open literature). Third, it is played through the filter to a computer for digitizing and any one of many procedures for data analysis. It is doubtful, however, if the digital procedures yield the same record or filter the signal in the same manner as the galvanometers in the oscillograph. Figures 28 and 29 show the effects of series filtering with a Bessel 60 hertz filter. The increased phase shift and the slight amplitude reduction are apparent in the solid line of Figure 28 and in the superposition of the waves in Figure 29.

Some conclusions can be drawn on the basis of these simple examples. The first conclusion is that clear understanding must be demonstrated on the part of crash test engineers and data analysts of the amplitude and phase characteristics of the individual filters in the data acquisition and analysis system. The second conclusion is that specifications more complete than SAE J211a, which does not include requirements on phase shift, should be developed to provide test data of sufficient clarity for comparison with the predictions of mathematical crashworthiness models.

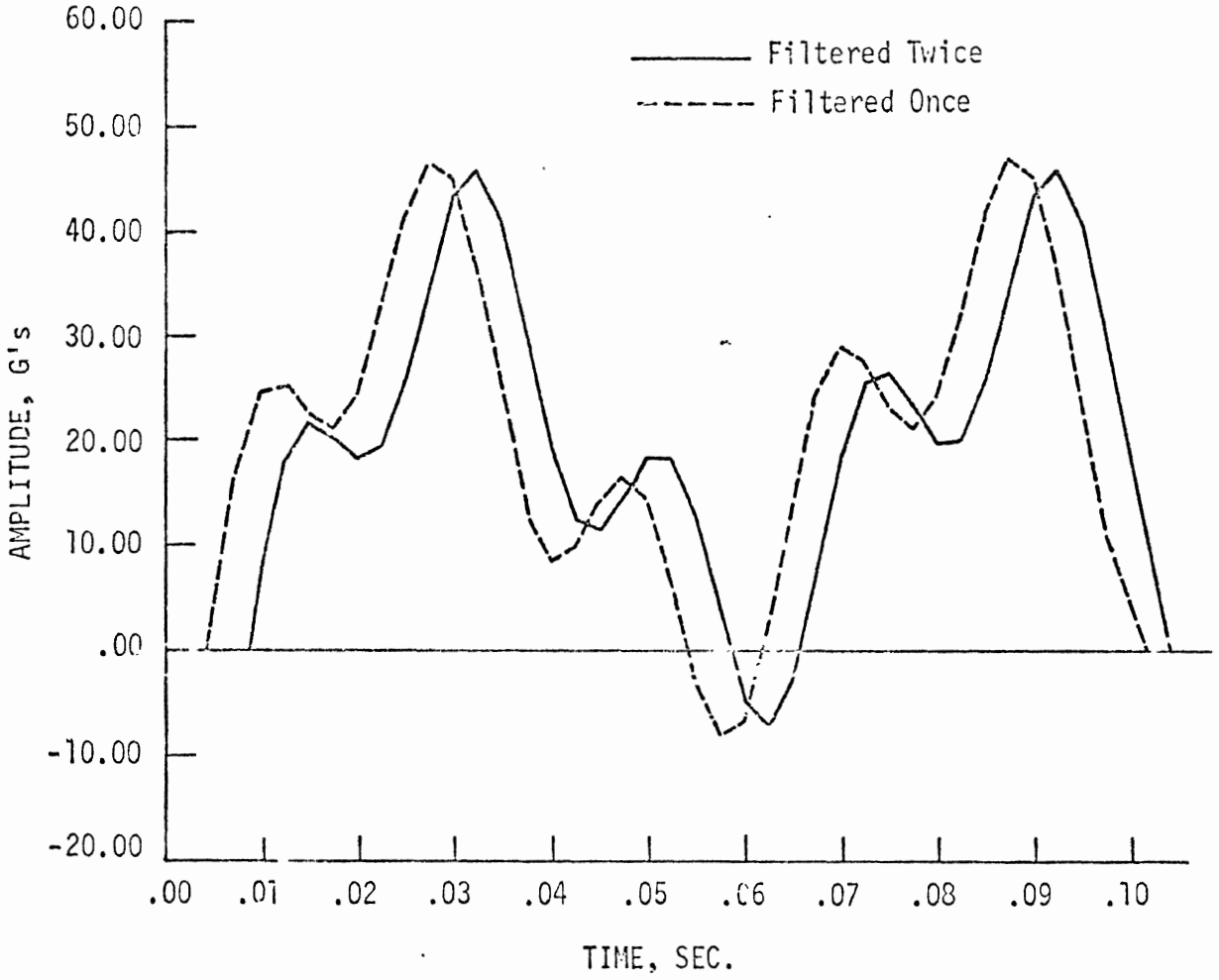

Figure 28. Effect on Baseline Pulse of One and Two Applications of a Bessel 100 hertz Filter.

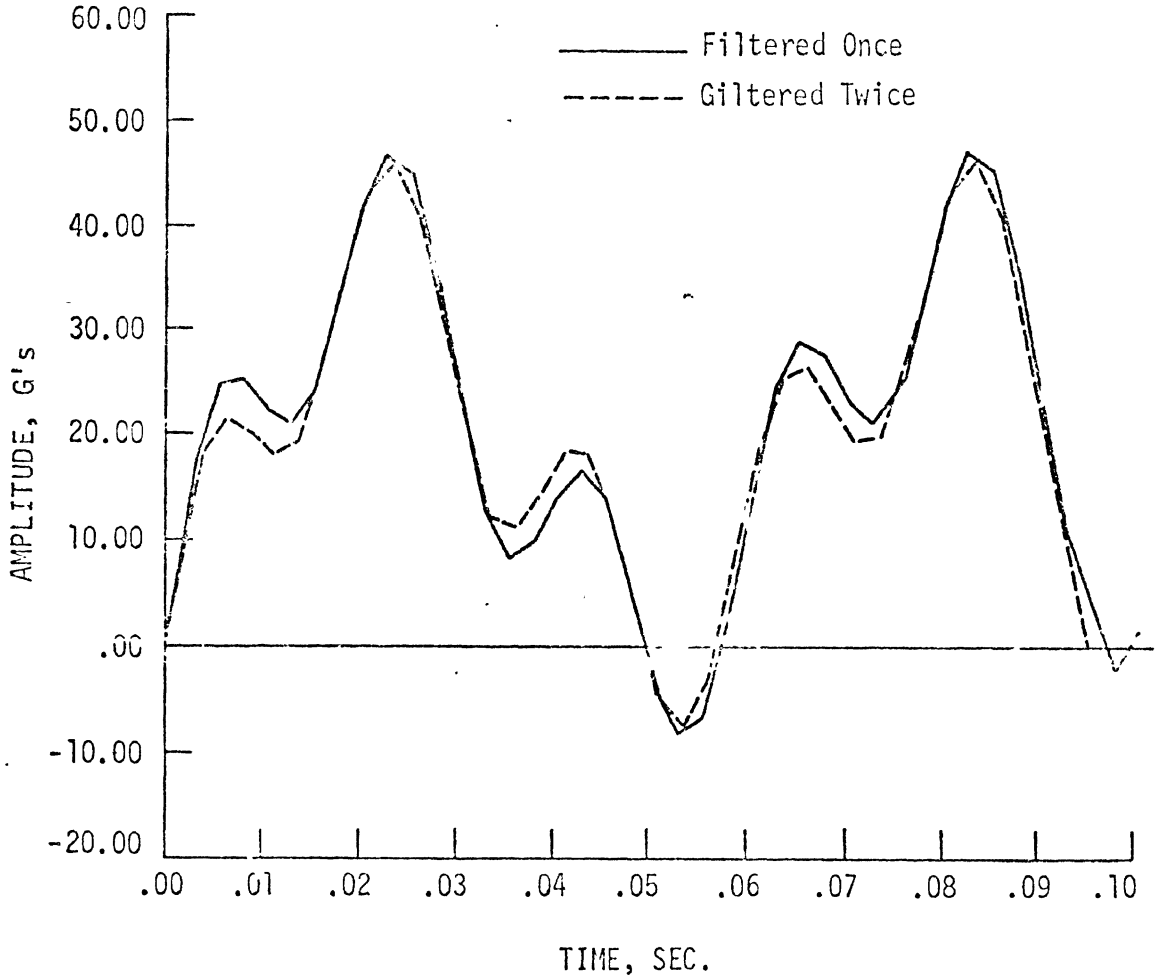

Figure 29. Superposition of One and Two Applications of a Bessel 100 hertz Filter to the Baseline Pulse.

4.4 SUMMARY AND RECOMMENDATIONS

It has been stated that a variety of the problems which seem to be occurring in the conduct of "reproducible crashworthiness experiments" and the development of "verified computer simulations" seem to be related to the understanding of electronic and digital filtering. The study which has just been presented was designed to take a preliminary look at these problems from four points of view: 1. identification of the characteristics of digital and electronic filtering procedures; 2. available and potential means for comparing waveforms to study test reproducibility, mathematical model verifiability, and filter performance; 3. development of simple examples of filter performance using a waveform having similarities with a crash pulse; and, 4. demonstration of the extent of the role of filters in crashworthiness analyses and experiments.

Four recommendations can be made to NHTSA for the follow-up of this work:

1. Develop a catalog of specifications for analytical procedures such as integration and differentiation as well as for all types of electronic and transducer hardware used in crashworthiness tests.
2. Because filters are in series in an analysis or an experiment, a filter system specification should be developed which includes the effects of all filters in the analysis or the experiment. The functions of a specification of this type would be to: a. assign filtering limits to analytical and experimental procedures; and b. ease the task of determining the possible level of agreement which should be expected between an experiment and mathematical prediction.
3. Existing filter specifications such as SAE J211a should be updated and expanded to include the effects of phase shift and distortion.

4. Analytical techniques should be developed for waveform comparison in order to more precisely define the degree of distortion, phase shift, and amplitude change. These procedures could be used in developing specifications of the accuracy which must be demonstrated by an analytical model in predicting a physical event.

5.0 SUMMARY OF CONCLUSIONS AND RECOMMENDATIONS

Conclusions reached based on the evaluation of the state of the art of crashworthiness testing can be summarized as follows:

1. Techniques for retrieving structural crash response data from tests span the range of electromechanical motion, velocity, acceleration, and force transducers as well as optical recording techniques.
2. Control of state variables such as impact velocity is highly important and a particular problem in full scale crash tests.
3. The confidence level of a physical simulation technique as a realistic indicator of the crash event can only be estimated roughly at best. Two of the reasons for this are the variety of real world accident situations and the lack of criteria for comparison of data gathered in different tests.
4. Crashworthiness testing is expensive, usually costing a minimum of $1000 for simple substructural component tests.

Recommendations on the relationship of physical testing to mathematical crashworthiness modeling are summarized as follows:

1. Guidelines for verification experiments should be developed which define a realistic band of expected agreement between experimental results and model predictions based on the accuracy of model input data as well as filter properties of the systems producing both the experimental and the computer-generated data.

2. Crashworthiness model computer programs should include user-oriented preprocessor subprograms for aiding in the preparation of input data and post-processor sub-programs to present output in a form compatible with experimental data.

3. Techniques should be developed for estimating the overall properties (the [illegible]) of a system of filters in series to aid in quantifying the verifiability of a model before the fact and the level of agreement between model predictions and experimental results after the fact.
4. A body of data on the force-deformation properties of vehicles and their components should be compiled as an aid to crashworthiness modelers and model users.
5. Research should be conducted to upgrade optical techniques for three-dimensional position measurement and the associated computer data-processing software.
6. Research should be initiated to develop new techniques of force measurement within structures.
7. Research should be initiated to develop techniques for verification of advanced finite element models.

In conducting this study the importance of filtering both experimental and computer-generated data became apparent and resulted in four additional recommendations.

1. Develop a catalog of specifications for analytical procedures such as integration and differentiation as well as for all types of electronic and transducer hardware used in crashworthiness tests.
2. Because filters are in series in an analysis or an experiment, a filter system specification should be developed which includes the effects of all filters in the analysis or the experiment. The functions of a specification of this type would be to: a. assign filtering limits to analytical and experimental procedures; and, b. ease the task of determining the possible level of agreement which should be expected between an experiment and a mathematical prediction.

3. Existing filter specifications such as SAE J211a should be updated and expanded to include the effects of phase shift and distortion.
4. Analytical techniques should be developed for waveform comparison in order to numerically define the degree of distortion, phase shift, and amplitude change. These procedures could be used in developing specifications of the accuracy which must be demonstrated by an analytical model in predicting a physical event.

6.0 REFERENCES

1. McIvor, I.K., "Modeling, Simulation and Verification of Impact Dynamics-Vol. 1, Executive Summary," Final Report on NHTSA Contract No. DOT-HS-031-2-481, July 1973.

2. McIvor, I.K., Wineman, A.S., Yang, W.H., and Anderson, W.J., "Modeling, Simulation and Verification of Impact Dynamics - Vol. 2, State of the Art of Crashworthiness Mathematical Modeling," Final Report on NHTSA Contract No. DOT-HS-031-2-481, July 1973.

3. McIvor, I.K., Wineman, A.S., Yang, W.H., Anderson, W.J., and Wang, H.C., "Modeling Simulation and Verification of Impact Dynamcis - Vol. 4, Three Dimensional Plastic Hinge Frame Model," Final Report on NHTSA Contract No. DOT-HS-031-2-481, July 1973.

4. Emori, R.I., "Analytical Approach to Automobile Collisions," SAE Paper No. 680016, Jan. 1968, 9p.

5. IBM, "System/360 Continuous System Modeling Program Users' Manual, Program Number 360A-CX-16X," IBM No. GH20-0367-3, 4th ed., April 1971.

6. Herridge, J.T. and Mitchell, R.K., "Development of a Computer Simulation Program for Collinear Car/Car and Car/Barrier Collisions," NTIS No. DOT-HS-800654, January 1972.

7. Shieh, R.C., "Basic Research in Crashworthiness II-Large Deflection Dynamic Analysis of Plane Elasto-Plastic Frame Structures Including the Cases of Collision into a Pole or Flat Barrier," Cornell Aeronautical Laboratory, Inc. Report No. YB-2987-V-7, August 1972.

8. Young, J.W., "CRASH: A Computer Simulator of Non-Linear Transient Response of Structures, Basis for Car Crash Simulation," NTIS No. DOT-HS-091-125-5, March 1972

9. Melosh, R.J., "Car-Barrier Impact Response of a Computer Simulated Mustang," NTIS No. DOT-HS-091-1-125-A, March 1972.

10. Anders, E.B. et al, "Digital Filers," NASA Contractor Report No. CR-136, 1964, 132p.

11. Kuo, F.F. and Kaiser, J.F., "System Analysis by Digital Computer," John Wiley and Sons, Inc., New York, 1966.

12. Blackman, R.B., "Linear Data-Smoothing and Prediction in Theory and Practice," Addison-Wesley Publishing Company, Inc., Reading, Mass., 1965.

13. Friant, R.J., "Numerical Filters for Data Processing," General Electric Technical Information Series Report No. R58EMH29, June 1958.

14. Robinson, E.A., "Multi-Channel Time Series Analysis with Digital Computer Programs," Holden-Day, 1967.

15. Morrison, N., "Introduction to Sequential Smoothing and Prediction," McGraw-Hill Book Company, New York, 1969.

16. Hildebrand, F.B., "Introduction to Numerical Analysis," McGraw-Hill Book Company, New York, 1956.

17. Robbins, D.H. et al, "Motion Measurement of a Rigid Body in Three Dimensions," Proceedings of the SPIE National Seminar on Optical Instrumentation, Volume 34, 1972.

18. IBM Corporation, "System 360 Scientific Subroutine Package, Version III, Programmers Manual," Edition GH20-0205-4, August 1970.

19. Kay, I.W. and Zobel, E.C., "Simplified Three-Dimensional Photogrammetric Analysis of Moving Bodies," SAE Paper No. 730278, 1973.

20. Bartz, J.A., "A Three-Dimensional Computer Simulation of a Motor Vehicle Crash Victim," Calspan Corp. Report No. VJ-2978-V-2 on U.S. DOT Contract No. FH-11-7592, December 1972.

21. Robbins, D.H., Bennett, R.O., and Bowman, B.M., "HSRI Six-Mass, Three-Dimensional Crash Victim Simulator," Final Report on Grant from MVMA to HSRI, February 1973.

22. Ralston, Wilf, "Mathematical Methods for Digital Computers," Wiley, New York/London, 1960, pp. 95-109.

23. Ralston, "Runge-Kutta Methods with Minimum Error Bounds," MTAC, Vol. 16, ISS.80(1962),pp.431-437.

24. Krylov, V.J., "Approximate Calculation of Integrals," Macmillan, New York/London, 1962,pp.100-111 and 337-340.

25. Zurmühl, R., "Praktische Mathematik für Ingenieure und Physiker," Springer, Berlin/Gottingen/Heidelberg, 1963, pp. 214-221.

26. Burr-Brown Research Corporation," Active Filters," April 1969.

27. "Electronic Engineers Master," United Technical Publications, Inc., Garden City, N.Y., 1972.

28. Dotson, W.P., "Reconstruction Errors in Digital-to-Analog Conversion," Instruments and Control Systems, January 1971, pp. 99-101.

29. Dove, R.C. and Adams, P.H., "Experimental Stress Analysis and Motion Measurement," Charles E. Merrill Books, Columbus, Ohio, 1964.

30. Bouche, R.R., "Accelerometers for Shock and Vibration Measurements," Endevco Technical Paper TP243, 1967.

31. Bouche, R.R., "Instrumentation for Shock and Vibration Measurements," Endevco Technical Paper TP223, 1962.

32. "Honeywell Instrumentation Handbook," Honeywell, Inc., 1970, p. 91.

33. "Galvanometer Users' Handbook," Consolidated Electrodynamics Corporation Bulletin 7300/467.

34. "Instrumentation for Impact Tests - SAE J211," Society of Automotive Engineers, 1972.